CRUSTAL MOTION STUDIES IN THE SOUTHWEST PACIFIC: GEODETIC MEASUREMENTS OF PLATE CONVERGENCE IN TONGA, VANUATU AND THE SOLOMON ISLANDS

A DISSERTATION SUBMITTED TO THE GRADUATE DIVISION OF THE UNIVERSITY OF HAWAI'I IN PARTIAL FULFILLMENT OF THE REQUIREMENTS FOR THE DEGREE OF

DOCTOR OF PHILOSOPHY

IN

GEOLOGY & GEOPHYSICS

DECEMBER 2003

By
David A. Phillips

Dissertation Committee:

Michael G. Bevis, Chairperson
L. Neil Frazer
Frederick W. Taylor
Donald M. Thomas
Richard J. Wainscoat

Dedication

I dedicate this work to my parents, Ila and Gary Phillips, and to my first geology teachers, Gary Goodwin and Robert Bell. My father and Mr. Bell both passed away during the course of this dissertation.

Acknowledgements

Acknowledgements related to specific research projects are included at the end of their respective chapters. However, the successful outcome of this dissertation as a whole was made possible through the professional and personal support of many colleagues, friends and family members whom I would like to recognize here.

I would especially like to thank my wife, Francine Coloma, for her love, encouragement and total support through the years it took to complete this work. Moreover, as a scientist at the USGS Hawaiian Volcano Observatory, she contributed greatly to the technical aspects of this dissertation as well.

My dissertation committee consisted of some of the most brilliant and genuinely good people I know. I would like to thank my committee chairperson, Michael Bevis, for his vision, unbridled enthusiasm and constant support. Mike's work in the South Pacific is the foundation for many of the ideas presented in this dissertation and I am proud to have had him as my Ph.D. advisor. My research, especially in the Solomon Islands, is directly related to work that Fred Taylor has been engaged in for many years. Fred and I have spent many collective months in the field together, from Antarctica to the South Pacific, and he has helped me to maintain my course in terms of research and life in general. Don Thomas has been a friend and counselor since my undergraduate years at UH Hilo. It seems that whenever I have a major life

decision to make, Don is the first person I call! The vast majority of my graduate courses in geophysics were taught by Neil Frazer. Neil has enlightened and inspired me in countless ways, both in academics and in the ways of the world. Richard Wainscoat graciously joined my committee at a relatively late hour. He has been generous with his time even thought the subject of plate tectonics does not often arise in his own field of astronomy.

Dana Caccamise has been a good friend and co-conspirator since our days together at UH Hilo. As fate would have it, he has also been my office mate for most of our days together at UH Manoa. Dana contributed greatly to the success of this dissertation through his ideas and technical skills. Fellow members of the Pacific GPS Facility, whom I also consider good friends, include James Foster, Eric Kendrick, Hao Zhou and Ben Brooks. James and Eric were the source of invaluable assistance with my data processing.

I would also like to thank the fine citizens of the Geology and Geophysics Department, the Hawaii Institute of Geophysics and Planetology, and the School of Ocean and Earth Science and Technology . Certain individuals deserving of special recognition include Leona Anthony, Janet Becker, Grace Furuya, Andrew Goodliffe, Yasushi Harada, Loren Kroenke, Brian Taylor, Paul Wessel, and the entire RCF staff. Besides being a great department chair, Paul is also one of the developers of the

Generic Mapping Tool software which I used to generate nearly all the figures in this dissertation.

Being international in nature, my research benefited greatly from the support and friendship of countless individuals around the world. My research in Vanuatu benefited greatly from the hard work and kindess of Stephane Calmant, Pierre Lebellegard, Bernard Pelletier and Jean-Michel Bore. Individuals in Vanuatu who contributed to this work include Douglas Charley, , Charles Pakoa , Moses Kalsale Williams and Jean-Claude Willy. In the Solomon Islands, I would like to especially thank Idris Lane, Allison Papabatu and Stanley Basi. Paserio Samisoni and Eroni Vari are collaborators and good friends from Fiji. Toelau Iulio facilated work in Samoa. Tevita Malolo, Francis Vatu and Fetu'u Vea facilitated work in Tonga. John Beavan, Dion Matheson and Roger Williams of the New Zealand Institue of Geological and Nuclear Sciences are collaborators for the research in Tonga-Lau system. I would also like to thank Shinichi Miyazaki of the University of Tokyo's Eartquake Research Institute and Shigeru Matsuzaka and Hiroshi Munekane of the Geographical Survey Institute in Tsukuba, Japan for data and assistance related to the Pacific Superplume GPS network.

Professional and personal guidance during the course of this dissertation was also provided by many people on the Big Island of Hawaii, including Darcy Bevens at UH

Hilo and Michael Lisowski, Asta Miklius, Arnold Okamura Paul Okubo and Maurice Sako at the USGS Hawaiian Volcano Observatory.

This dissertation marks the end of my tenure as a graduate student. My sister Wendy, however, is in the midst of completing her Master's degree. Wendy provided constant moral support thoughout this project and was always there to help me keep things in perspective.

Abstract

The southwest Pacific is one of the most tectonically dynamic regions on Earth. This research focused on crustal motion studies in three regions of active Pacific-Australia plate convergence in the southwest Pacific: Tonga, the New Hebrides (Vanuatu) and the Solomons Islands. In Tonga, new and refined velocity estimates based on more than a decade of Global Positioning System (GPS) measurements and advanced analysis techniques are much more accurate than previously reported values. Convergence rates of 80 to 165 mm/yr at the Tonga trench represent the fastest plate motions observed on Earth. For the first time, rotation of the Fiji platform relative to the Australian plate is observed, and anomalous deformation of the Tonga ridge was also detected. In the New Hebrides, a combined GPS dataset with a total time series of more than ten years led to new and refined velocity estimates throughout the island arc. Impingement of large bathymetric features has led to arc fragmentation, and four distinct tectonic segments are identified. The central New Hebrides arc segment is being shoved eastward relative to the rest of the arc as convergence is partitioned between the forearc (Australian plate) and the backarc (North Fiji Basin) boundaries due to impingement of the d'Entrecasteaux Ridge and associated Bougainville seamount. The southern New Hebrides arc converges with the Australian plate more rapidly than predicted due to backarc extension. The first measurements of convergence in the northern and southernmost arc segments were also made. In the Solomon Islands, a four-year GPS time series was used to generate the first geodetic

estimates of crustal velocity in the New Georgia Group, with 57-84 mm/yr of Australia-Solomon motion and 19-39 mm/yr of Pacific-Solomon motion being observed. These velocities are 20-40% lower than predicted Australia-Pacific velocities. Two-dimensional dislocation models suggest that most of this discrepancy can be attributed to locking of the San Cristobal trench and elastic strain accumulation in the forearc. Anomalous motion at Simbo island is also observed.

Table of Contents

List of Tables

List of Figures

Chapter 1. Introduction

The southwest Pacific is one of the most tectonically dynamic regions on Earth. It is the zone of active collision between the Pacific and Australian plates and includes some of the most dramatic examples of subduction, spreading and transform phenomena on the planet. Early geophysical studies of the southwest Pacific resulted in some of the first models of plate tectonic theory (e.g., Isacks et al., 1968; Karig, 1970) and the region continues to be one of the richest sources of discovery and debate in modern geophysics (e.g., Bevis et al., 1995; Hamburger and Isacks, 1987; Okal and Kirby, 1998; Pelletier et al., 1998; Taylor et al., 1996; Zellmer et al, 2001). The goal of my research was to make precise geodetic measurements in key areas of the southwest Pacific in order to observe crustal motions associated with local and regional processes related to plate convergence. The course of my research involved designing and testing field instrumentation and data recovery systems, conducting field work at numerous sites in more than a dozen countries, analyzing the data using specialized software, and interpreting the data using numerical models.

1.1. Study Area

The active Australia-Pacific (A-P) plate boundary stretches from New Zealand to Papua New Guinea along a complex system of subduction zones, transforms and spreading systems (Figure 1.1). One of the most notable features of the A-P plate

boundary is the change in subduction polarity that occurs within the system: the Pacific plate subducts westward beneath the Australian plate along the Tonga trench while the Australian plate subducts northeastward beneath the Pacific plate along the New Hebrides and San Cristobal trenches. The North Fiji Basin, a broad region of extension, separates these two opposite facing subduction systems (Figure 1.2). This study focuses on three specific areas of the A-P plate boundary: the Tonga-Lau system, the New Hebrides system and the Solomon Islands system.

The Pacific plate undergoes westward subduction at the Tonga trench at mean rates of 150 to 250 mm/yr (results from this study). These extremely rapid subduction rates are faster than any other convergent system and are in fact the fastest tectonic motions yet observed anywhere on Earth. Indeed, there are very few places in the world where large areas of the lithosphere could undergo more than a meter of aseismic displacement in the time required to complete this dissertation. Such rapid convergence is primarily due to the relatively weak coupling that occurs between the colliding plates, a situation that allows for nearly "aseismic" convergence at shallow depths. However, the number and magnitude of seismic events related to subduction at the Tonga trench increases significantly with depth and ultimately this system becomes the greatest source of seismic energy release on the planet (Oliver and Isacks, 1967).

Figure 1.1. Map of study area including major tectonic features.

Solid lines represent active tectonic features. Dotted lines indicate inactive features. After Pelletier et al. (1998). NST = North Solomon Trench; SCT = San Cristobal Trench; NHT = New Hebrides Trench; TT = Tonga Trench; KT = Kermadec Trench; OJP = Ontong Java Plateau; SS = Solomon Sea plate; WB = Woodlark Basin; NH = New Hebrides arc; LR = Loyalty Ridge; NC = New Caledonia; NFB = North Fiji Basin; VTL = Vitiaz Trench Lineament; CKL = Conway-Kandavu Lineament; FP = Fiji Platform; LB = Lau Basin; N = Niuafo'ou microplate; T = Tonga ridge microplate; SR = Samoa Ridge.

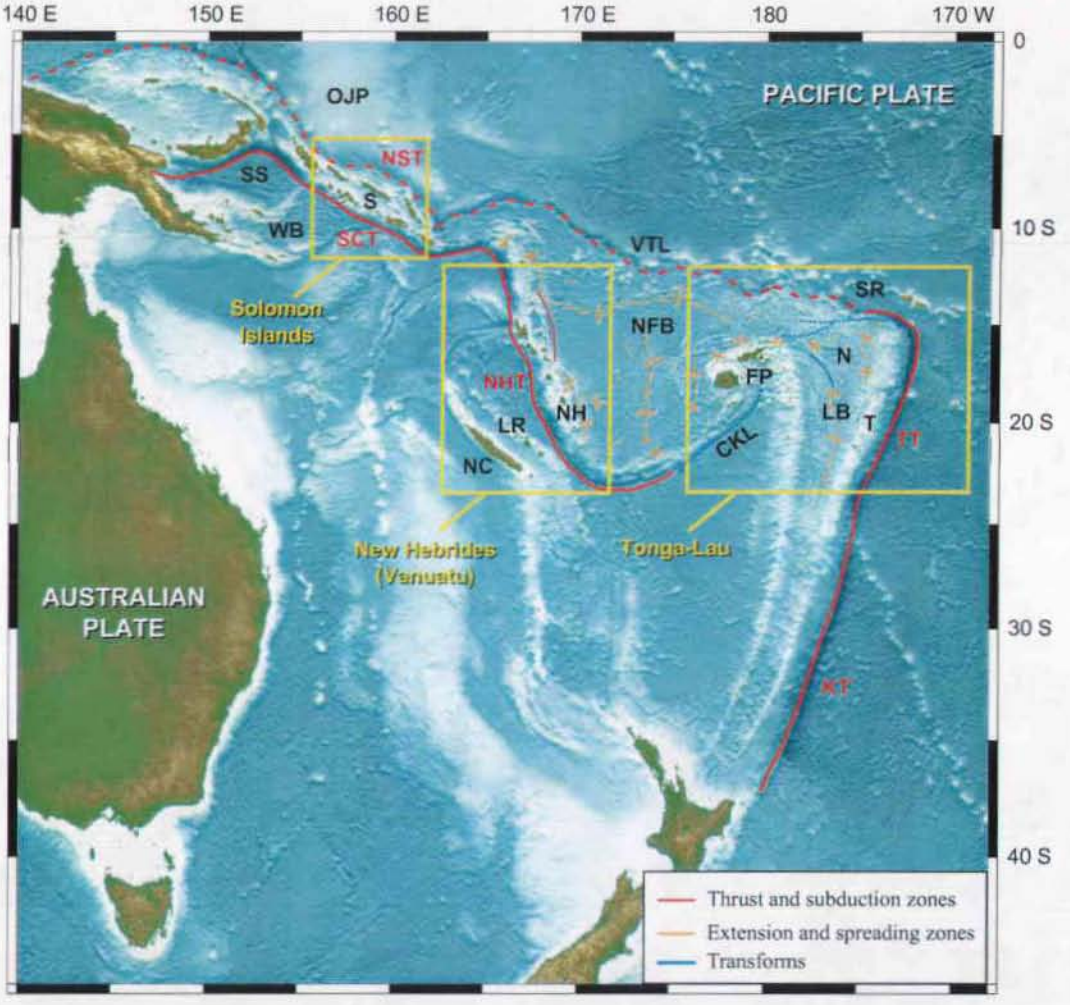
140 E
150 E
160 E
170 E
180
170 W
0
10 S
20 S
30 S
40 S
OJP
PACIFIC PLATE
NST
SS
S
WB
SCT
VTL
SR
Solomon Islands
NFB
N
FP
NHT
NH
LB
T
LR
CKL
TT
NC
New Hebrides (Venuatu)
Tonga-Lau
AUSTRALIAN PLATE
KT
Thrust and subduction zones
Extension and spreading zones
Transforms

Figure 1.2. Plate tectonic map of the Tonga-New Hebrides region.

Solid lines represent active features. Dotted lines indicate inactive features. Numbers represent rates of motion in cm/yr. After Pelletier et al. (1998). NHT = New Hebrides trench; TT = Tonga trench, VTL = Vitiaz trench lineament; WNFB = West North Fiji Basin; NH = New Hebrides arc; TP = Torres Plateau; DR = D'Entrecasteaux Ridge; NBAT and SBAT = resp. North and South New Hebrides Back Arc Troughs; CBAC/BATB = Central New Hebrides Back-Arc Compressional zone / Back-Arc Thrust Belt; HHR = Hazel-Holmes Ridge; LR = Loyalty Ridge; NC = New Caledonia ridge; CKL = Conway-Kandavu lineament; WSR = West Spreading Ridges of the North Fiji Basin; ELSC, CLSC, NWLSC and NELSC = resp. East, Central, North-West and North-East Lau Spreading Centers; PR = Peggy Ridge; FP = Fiji Platform; TR = Tonga Ridge; SR = Samoa Ridge; SC = San Cristobal

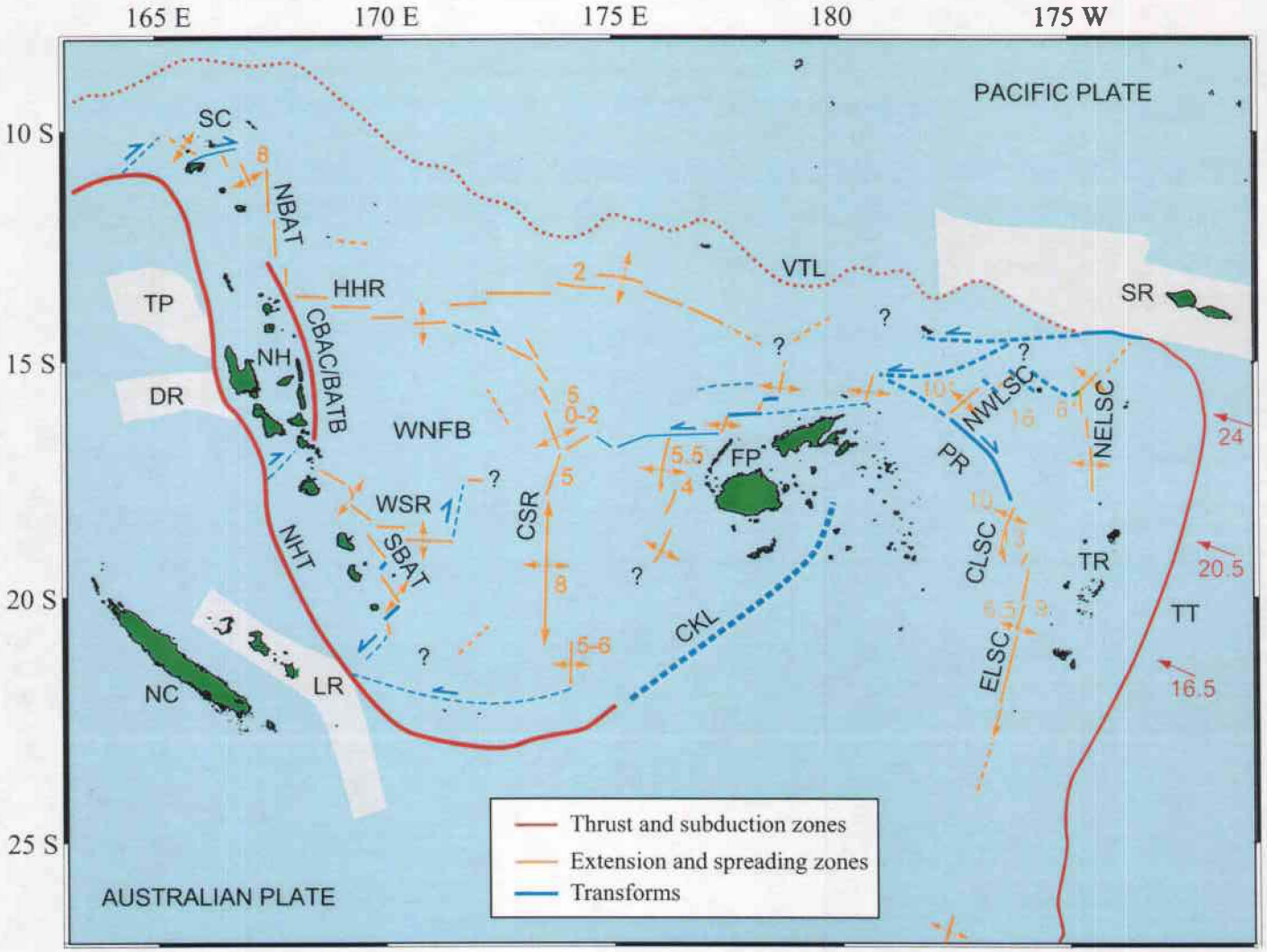
165 E
170 E
175 E
180
175 W
10 S
15 S
20 S
25 S
PACIFIC PLATE
AUSTRALIAN PLATE
SC
NBAT
HHR
VTL
TP
DR
NH
CBAC/BATB
WNFB
WSR
SBAT
NHT
CSR
FP
PR
NWLSC
NELSC
SR
CLSC
ELSC
TR
TT
CKL
LR
NC
24
20.5
16.5
Thrust and subduction zones
Extension and spreading zones
Transforms

A very different situation is observed in the New Hebrides (Vanuatu) and Solomon Islands systems. Unlike Tonga-Lau, these systems experience strong interplate coupling and convergence rates vary from 30 to 125 mm/yr (results from this study). Large, shallow earthquakes are also more common. The downgoing Australian plate features very rugged topography, including numerous ridges and plateaus of significant size. When such features enter the trench, they resist subduction. The process of subduction resistance is not only important at local scales, where transverse and back-arc faults and anomalous zones of deformation can develop, but also at the regional scale, where subduction resistance can ultimately lead to arc polarity reversal. Indeed, it is widely accepted that present day subduction of the Australian plate along the Greater Melanesian arc system is due to a subduction polarity reversal that occurred at approximately 10 Ma in response to impingement of the Ontong-Java plateau on the Pacific plate (Yan and Kroenke, 1993). In the New Hebrides, subduction is currently resisted by the d'Entrecasteaux and Loyalty ridges and the West Torres plateau. In the Solomon Islands, subduction is currently resisted by the Simbo and Ghizo ridges of the Woodlark Basin.

1.2. Geodetic Measurements of Crustal Motion

Geodesy is the study of the shape of the Earth and the relationship of points on the Earth's surface. The absolute shape of the Earth and the relationship between points on the Earth's surface, however, is constantly changing due to the effects of plate

tectonics, isostatic adjustments, tidal forces and other phenomena. During the last century, the development of space-borne geodetic techniques such as Satellite Laser Ranging (SLR), Very Long Baseline Interferometry (VLBI) and the Global Positioning System (GPS) made it possible to very precisely measure the shape of the Earth and to observe changes in its shape through time (e.g., Larson et al., 1997; Robaudo and Harrison, 1993; Robbins et al., 1993; Sella et al., 2002; Smith et al., 1990). GPS in particular has become an incredibly versatile technique for studying crustal motions associated with a wide range of phenomena (e.g., Bevis et al., 1995; Owen et al., 1995; Bock et al., 1997; Kendrick et al, 1999; Blewitt et al., 2001). This study uses GPS geodesy as a tool for investigating crustal motions in the southwest Pacific associated with plate convergence in Tonga, the New Hebrides and the Solomon Islands.

Chapter 2. Methods

The observational components of my research were based on methods developed for terrestrial surveys using space geodesy techniques, in this case the Global Positioning System (GPS). The analysis components were based on GPS data processing procedures developed by the crustal motion geodesy community and numerical modeling techniques developed for the study of coseismic and interseismic elastic strain in the Earth's crust. An overview of these methods is provided in the following sections.

2.1. The Global Positioning System

The Global Positioning System (GPS) was developed by the United States Department of Defense for navigational and other strategic applications. Since the time of the first prototype satellite launch in 1978, however, GPS has become the basis for countless non-military applications and the term "GPS" has become a household word. From guiding missiles to tracking patients with Alzheimer's disease, GPS has become a staple technology in today's world. The GPS observation and analysis techniques used for this study, however, are significantly more complex than the techniques required to relocate a favorite fishing spot and a brief overview of the system and its signal structure is in order.

The Global Positioning System consists of three segments: the Space Segment, the Control Segment, and the User Segment (Misra and Enge, 2001). The Space Segment consists of twenty-four satellites orbiting the Earth at an altitude of approximately 20,000 km and arranged in six orbital planes with inclinations of 55° relative to Earth's equator. The orbital period of each satellite is approximately 12 hours. The Control Segment consists of a network of ground based tracking stations maintained by the U.S. Air Force that is responsible for monitoring and maintaining the status of the Space Segment. The User Segment consists of GPS receivers and the people who use them.

Each satellite broadcasts phase modulated binary data over two L-band carrier frequencies. There are three primary signal components: carrier, code and navigation data. The carrier frequencies are referred to as L1 (f = 1575.42 MHz, λ = 19 cm) and L2 (f = 1227.60 MHz, λ = 24 cm). Ranging code data include the coarse/acquisition (C/A) code and the precision or encrypted (P or Y) code. The P (or Y) code is not available to non-military GPS receivers. Navigation data include satellite status, ephemeris, clock bias parameters, and almanac information.

The GPS signal is subject to intentional degradation from such processes as Anti-Spoofing (AS) an Selective Availability (SA). Anti-Spoofing involves the encryption of the P code into the Y code and has been activated since 1994. The only practical concern that AS presented to this project was that certain GPS receivers

manufactured before 1994 were unable to recognize the signal without a firmware upgrade. Selective Availability involves a deliberate five-fold increase in positioning error but SA has not been implemented since 2000. Fortunately, even when SA was activated it was of no practical concern to this study because geodetic observations rely primarily on carrier (phase) data rather than code data. One aspect of the GPS signal that did have to be addressed during this study was the GPS End of Week (EOW) rollover event. GPS time as recorded by the system and broadcast in the navigation message began on 5 January 1980 and is limited to a cycle of 1024 weeks. Week 1024 ended on 21 August 1999. To prepare for this event, it was necessary to upgrade the receiver firmware and download software version at each and every GPS site in my network.

There are two basic approaches to GPS positioning: code phase measurements and carrier phase measurements. The code phase, or "pseudorange", technique is based on the apparent transit time of the GPS signal from the satellite to the receiver. A GPS receiver uses the code data broadcast by a satellite to measure the time it takes for the signal to travel from the satellite to the receiver. Assuming the signal propagated at a speed close to that of light, and applying the standard distance = rate * time equation, the receiver calculates the approximate distance (the pseudorange) to that satellite. When the pseudoranges to at least four satellites are determined, the receiver can "triangulate" its position on the Earth. Accuracy of the pseudorange technique using the C/A code is typically on the order of five meters when SA is not

activated. While useful for navigation, the positioning accuracy provided by the pseudorange technique is clearly not adequate for geodetic measurements.

Carrier phase measurements are much more precise than code phase measurements and can provide millimeter level positioning. This is the technique employed for my research. The carrier phase measurement is the difference between the phases of the carrier signal from the satellite and a reproduction of the carrier signal generated by the receiver at the instant of the measurement. While the phase of the received signal at any point in time can be related to the phase at the satellite at the time of transmission, and thus related to the transit time and distance between the satellite and receiver, the carrier phase measurement is an indirect, or ambiguous, measurement. The only inherent measurement is the fractional difference between the observed and reproduced cycles, while the integer number of whole cycles between the signals cannot be measured. To derive precise positioning from the carrier phase measurements, sophisticated post-processing must be performed on a computer using specialized data analysis software such as GAMIT, as described below.

2.2. Data Collection

Data collection represents a significant component of my research. Most of the data presented in this dissertation were collected directly by the author. The following

sections describe the instrumentation, observation strategies, and data recovery methods employed.

2.2.1. Instrumentation

All GPS data were collected using geodetic receivers capable of recording precise carrier phase and pseudorange measurements at both the L1 and L2 frequencies. Most data were collected using Ashtech Z-XII receivers coupled with Ashtech Dorne-Margolin choke-ring antennas. Most pre-existing data from 1990 and 1992 were collected using Trimble 4000 receivers with geodetic antennas while some more recent observations were made using Ashtech Micro-Z receivers and choke-ring antennas. Some continuous GPS sites maintained by the International GPS Service (IGS) were equipped with Rouge SNR-8 or SNR-8000 receivers. The make and model of the receiver/antenna combination used for each GPS observation was entered into the setup files of the GPS data processing software for proper analysis.

Whenever possible, roving GPS surveys were conducted using Tech-2000 geodetic antenna masts instead of traditional tripod/tribrach arrangements. The Tech-2000 mast was developed by M. Bevis, F. W. Taylor and E. Wheeler specifically to facilitate precise roving surveys. The primary advantages of the Tech-2000 mast include 1) a fixed antenna height, 2) enhanced stability during the survey and 3) enhanced portability when traveling to the site. When it was not possible to use a

Tech-2000 mast, a traditional survey tripod equipped with a fixed or rotating optics tribrach was employed.

Continuous GPS sites in Samoa, Vanuatu and the Solomon Islands were also equipped with Paroscientific MET3 meteorological sensors. Computer and communications equipment is described below in the data recovery section.

2.2.2. Rover GPS Data

The roving, or campaign, approach to GPS surveys is the most typical and traditional way of collecting geodetic GPS data. A rover GPS site consists of a permanent monument (i.e., survey benchmark) affixed to the ground. Most of the rover sites in my network utilize the Bevis pin monument. During a roving survey, the GPS antenna was precisely centered and leveled above the monument's reference point using a TECH-2000 mast or tripod/tribrach. When the survey was concluded, the antenna and receiver were removed from the site and only the permanent monument remained. The monument was then re-measured at some later time, typically after one or more years. The end result is a time series of discrete measurements at each rover site. The longer the time series and the greater the number of observations, the greater the quality of the resulting estimate of the monument's position though time. A typical rover GPS survey in the southwest Pacific is shown in Figure 2.1.

Figure 2.1. Roving GPS survey in the southwest Pacific.

The GPS antenna is centered and leveled over the rover monument using a Tech 2000 mast. The monument is a small stainless steel pin permanently installed in solid bedrock (not visible in photo but located at the base of the antenna mast). A typical roving survey lasted 48 hours or longer.

For crustal motions studies, the premise of the roving survey is that any observed motion of the monument over time in fact represents motion of the surrounding substrate. In the southwest Pacific, it was common to install only a single monument on a given island and to interpret motion of that monument through time as motion of the entire island through time. Obviously, the importance of monument stability can not be overemphasized. Rover sites were therefore established using the following criteria: 1) monument was installed in solid substrate that is obviously solid rock connected to basement material, i.e. substrate could not be a buried boulder or a building or other artificial structure, 2) monument was installed in a location that had a good sky view to prevent obstruction of the GPS satellites during the survey, 3) monument was installed away from potential multipath sources such as flat metal surfaces, flat-sided buildings, fences, etc. and 4) monument was installed in a location where the chance of vandalism during and between surveys was minimized as much as possible.

The duration of each roving survey was dependent on the campaign strategy being utilized and the amount of time available to the surveyor. The GPS surveys conducted in 1990 and 1992 were massive campaign efforts that required occupation times of one week or more at each rover site; moreover, rover sites had to be occupied simultaneously to allow sufficient common epoch observations within the regional GPS network for successful analysis. A significantly more efficient approach to roving surveys, however, is to conduct them in concert with a regional

network of continuous GPS stations that provides common epoch observations along with other benefits. This strategy is referred to as the Multi-modal Occupation Strategy (MOST) for GPS surveys (Bevis et al, 1997) and this was the approach employed throughout my research. In fact, in any region where I installed or expanded roving GPS sites, my first step was to install a regional continuous GPS site. Using the MOST strategy, the duration of a typical roving surveys was on the order of 48 hours or more. Regardless of the total survey duration, data are stored as 24-hour files (relative to Greenwich Mean Time). Roving surveys typically used an epoch sampling rate of thirty seconds.

If the survey was conducted using a Tech-2000 mast, the vertical offset between the monument reference point and the antenna reference point was a known value: either 0.6574, 1.1574, or 1.6574 meters depending on the number of mast sections used. If the survey was conducted using a tripod/tribrach, the offset between the monument reference point and the antenna reference point was carefully measured and recorded.

2.2.3. Continuous GPS Data

Installation of a continuous GPS (CGPS) network in the southwest Pacific to support this and other research projects began in 1996. A typical CGPS site is shown in Figure 2.2. The regional CGPS network used for this research is shown in Figure 2.3.

Figure 2.2. Continuous GPS site in the southwest Pacific.

The GPS antenna, covered by a protective radome, is mounted to a permanent monument that is buried 1-2 meters deep in solid substrate. The GPS receiver and download computer are housed in a nearby shelter.

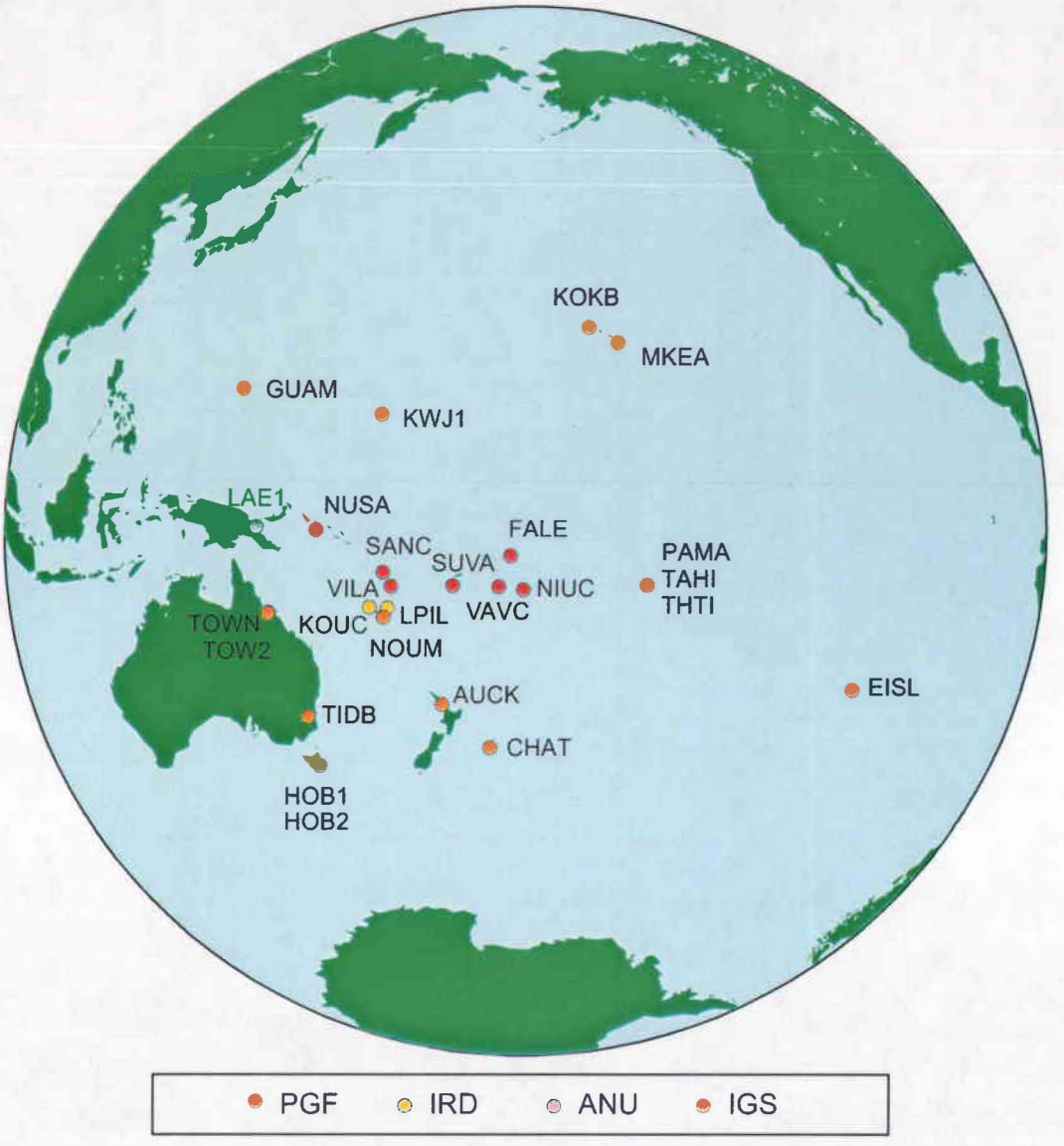

Figure 2.3. Southwest Pacific continuous GPS (CGPS) network.

This regional CGPS network was installed to provide the reference framework for the MOST approach and to allow continuous observation of crustal motions through time. Each CGPS site established during this study is equipped with an Ashtech Z-XII dual frequency receiver and choke-ring antenna. Data are recorded in 24-hour files with an epoch sampling rate of thirty seconds.

As with roving survey measurements, CGPS measurements are interpreted as representing crustal motion behavior through time. And again, monument stability is of paramount importance. In addition to the site criteria required for a rover monument above, the following additional requirements must also be met: 1) site requires facilities for a constant power source such as mains AC or solar panels, and 2) site requires communications facilities for data downloads, such as a telephone-model line or internet connections. In general, airports were good locations for CGPS sites because airports inherently feature a good sky view, tend to have reliable power and communication facilities, and are relatively secure. Because of their high visibility, CGPS sites are more susceptible to vandalism than rover monuments so even greater care was required in site selection. Examples of vandalism during the course of this research included stolen car batteries that were being used as a power source for the CGPS, stolen solar panels, a damaged antenna radome (from rocks being thrown at the site), and cut power/antenna cables. Communications facilities often proved to be problematic as well; in Samoa, for example, the phone-modem connection would stop working during rainy weather. At most CGPS sites,

monumentation consisted of large diameter (e.g., 4-inch) water pipe that was installed in solid substrate using cement. Monument depth was typically on the order of one to two meters and was determined primarily by the substrate properties. Softer material, for example, required a deeper monument foundation.

2.2.4. Data Recovery and Storage

Ultimately, the final destination for all data files was the data archive at the Pacific GPS Facility (PGF) at the University of Hawaii at Manoa. Recovery of roving GPS data simply involved downloading the data files from the receiver and storing them on some kind of medium such as Zip discs or flash cards. As most of the data were recorded using Ashtech Z-XII receivers, the most common data download protocol was Ashtech's DOS-based CGREMOTE software.

CGPS data recovery, however, was often a greater challenge. All CGPS sites were equipped with a dedicated PC download computer running DOS, Windows 98 or Windows 2000. In most cases, this download computer was a Dell Latitude XPi series laptop. Some CGPS sites were equipped with telephone-modem lines that allowed data to be downloaded remotely. To accomplish this, a modem such the U.S. Robotics Courier was connected to the GPS receiver's communications port while a second modem was connected to a PC computer equipped with CGREMOTE software. At many CGPS sites, however, modem connections were not possible or

practical and the data had to be downloaded manually by a designated local site steward. Although several attempts were made throughout the course of this project, internet communications with any CGPS site were not possible due to lack of local infrastructure and/or prohibitive operation costs.

Whether the data were downloaded by modem or by direct connection, a copy of the data files was subsequently stored on site by a local site steward and a copy was sent to the PGF for analysis. Although primitive, the most cost-effective and reliable way of transferring data files from the southwest Pacific to Hawaii was to send the data on Zip discs via post mail. This often resulted in a recovery latency of several months. Because I did not require near real time data flow for this research, however, this latency was inconvenient but seldom problematic. For the CGPS sites in Vanuatu and New Caledonia, the raw data files were sent to French colleagues in Noumea and subsequently delivered to the PGF via FTP transfer. Similarly, raw data files from CGPS sites in Tonga, Samoa and Niue were sent to colleagues at the Institute of Geological and Nuclear Sciences in New Zealand and subsequently transferred to the PGF by FTP. Once the data files arrived at the PGF, they were archived in the main online data repository. Multiple hard copies of the data files were also archived on optical media such as CD and DVD.

2.3. Data Analysis

Data analysis consisted of two basic stages. Stage 1 involved a distributed data processing scheme in which regional network solutions were produced using the software package GAMIT (King and Bock, 2002) and subsequently combined with global network solutions using the software package GLOBK (Herring, 2002) to produce a solution that included an estimate of the geometrical figure or "polyhedron" consisting of all regional and global GPS station included in the daily analysis. In Stage 2, the raw time series was cleaned, filtered and stacked using a series of MATLAB routines collectively referred to as VSTACK. The end result was a velocity estimate for each GPS station in the regional network which could be transformed into a regionally defined reference frame corresponding to a "rigid" tectonic plate. Qualitative descriptions of these analysis procedures are provided in the following sections. For more detailed and quantitative descriptions, the reader is referred to Feigl et al. (1993), Zhang (1997), Bock (1997), and Kendrick et al. (2001).

2.3.1. Analysis Stage 1: Daily Network Solutions

Stage 1 of my data analysis focused of the generation of daily network solutions and a "raw" time series using the GAMIT and GLOBK software packages. GAMIT and GLOBK are a comprehensive suite of programs developed at the Massachusetts Institute of Technology (MIT), Scripps Institution of Oceanography, and Harvard

University for analyzing GPS measurements primarily to study crustal deformation. GAMIT/GLOBK runs under the UNIX operating system. This stage of my analysis was performed using the data processing array at the Pacific GPS Facility which consisted of approximately thirty computers dedicated to GAMIT/GLOBK processing applications.

Daily solutions for each GPS site in my regional (SWP) network were produced using GAMIT, versions 10.03 and 10.06. GAMIT uses the GPS broadcast carrier phase and pseudorange observables to estimate three-dimensional relative positions of ground stations and satellite orbits, atmospheric zenith delays, and earth orientation parameters (King and Bock, 2002). GAMIT requires a plethora of *a priori* information regarding these parameters. Precise satellite orbit, earth orientation and global reference station coordinate *a priori* information was obtained from the Scripps Orbit and Permanent Array Center (SOPAC). *A priori* parameters specific to stations in my regional network were determined from field log sheets and preliminary processing. The final GAMIT product from my analysis was a daily regional network solution for each and every day that sufficient data were available. Each daily solution contains loosely constrained estimates of station coordinate, satellite orbit and Earth orientation parameters along with their corresponding covariance matrices. It should be emphasized that the solution parameters are only loosely constrained and that station coordinates are not strongly tied to any particular reference frame.

Note that my GAMIT analysis only produces daily solutions for my regional, i.e. southwest Pacific, network. To obtain daily global solutions, I employed a distributed processing scheme in which my regional daily solutions were combined with global daily solutions produced by SOPAC using the global International GPS Service (IGS) network in a free-network adjustment using GLOBK (Herring, 2002). This adjustment takes full account of the covariance matrices associated with both the regional and global solution sets. Each combined daily solution is a polyhedron of all global and regional GPS stations. Again, it is emphasized that this solution is only weakly constrained to any particular reference frame.

The primary reason for applying this distributed processing approach was to enhance the overall processing efficiency. A typical daily solution for the SWP network, consisting of ten to twenty sites on any given day, would require approximately one hour of processing time to obtain a GAMIT solution. Producing my own global network solution in addition to my regional network solution would have required either a separate processing run or the inclusion of the global IGS network data along with my regional network data. Either approach would have required significantly longer processing times as well as the added burden of maintaining adjustment records for all sites in the global network. In contrast, the subsequent merge of my regional solution with the SOPAC global solution using GLOBK typically only required an additional five to ten minutes of processing time. Oral (1994) and Zhang

(1996) showed that this distributed approach provides results that are statistically equivalent to a simultaneous adjustment.

2.3.2. Analysis Stage 2: Time Series Generation and Velocity Estimates

The second stage of my analysis used the raw daily solutions generated by GAMIT/GLOBK to produce a time series of station parameters that ultimately yielded a precise velocity estimate for each station in my regional network. Moreover, each velocity estimate could be easily transformed into a regionally defined reference frame corresponding to tectonic plates.

Each daily network solution produced by GAMIT/GLOBK included an estimate of the geometrical figure or "polyhedron" comprised of all global and regional GPS sites included in that day's analysis. In its final stages, the GAMIT/GLOBK analysis places only very weak constraints on the coordinates of the GPS stations and the solution at this stage can be referred to as a "free network solution" that is not strongly tied to any particular reference frame (Heflin et al., 1992; Blewitt, 1998). That is, a given daily polyhedron is strongly constrained in size and shape but not in position or orientation. The primary advantage of free network solutions, as opposed to fiducial network solutions for example, is that they are not significantly influenced by *a priori* information of the individual GPS stations, such as coordinates and relative positions. This is critical because even small errors in *a priori* coordinates

that are used to impose a reference frame on a polyhedron can lead to distortions in the estimated shape of the polyhedron.

A free network solution time series of sufficient length can show how the internal geometry of a network polyhedron changes through time. In the case of my regional network, changes in the internal geometry represent crustal motions. Of course, such changes can also result from computational errors or monument instability; having a long time series from any given station will help distinguish "true" tectonic motions from environmental and artificial signals.

I used the software package VSTACK to perform inner coordinate position and velocity estimation. VSTACK is a suite of MATLAB modules developed by M. Bevis and described in Kendrick et al. (2001). First, a desired subset of regional stations was extracted from the combined daily solutions produced by GAMIT/ GLOBK. (Since the end result of the Stage 1 analysis was a merged regional and global solution set, one may be curious as to why I re-extracted and stacked only my regional subset of GPS stations during the VSTACK analysis rather than making use of the entire global network. The primary reason is that Bock et al. (1997) and Kendrick et al. (1999) among others have reported that global stacking admits significant amounts of spatially coherent noise into a regional time series. Therefore, to obtain the highest resolution possible within my regional network, I stacked only the GPS sites occurring within the SWP network.)

Next, I would use the STACK module to clean the data in 30 day segments. The polyhedra were aligned as closely as possible (onto each other) without accounting for the minimal changes in shape that occur in 30 days. It was possible to identify a bad solution for a given station on a given day because it would not line up properly. At the end of this process I would have 30 days of edited and nicely aligned polyhedra. Note that the inner geometry of the polyhedra is not affected by the stacking process which changes only the orientation and location of each polyhedron (not its shape or size). The only important change in the basic daily solution coming from GLOBK is elimination of discrepant station-days. Finally, I would gather all the edited 30 day "gathers" into one very long time series corresponding to the total network time series.

Next, I used the VSTACK module to apply daily six-parameter transformations to align the polyhedra onto a suite of constant velocity trajectories (unless I incorporated breaks for earthquakes). Now both position and velocity were estimated in some arbitrary reface frame.

The last step was to impose a reference system using the RTVEL module. Typically I would realize a fixed-plate frame. It would have been possible to transform the solutions into a well defined global reference frame such as ITRF-2000 (Altamimi et al., 2002) but for regional investigations such as those described here, it is more useful to transform the results into a reference frame that corresponds to a "rigid"

tectonic plate. For all study areas, I invoked reference frames corresponding to the Australian and Pacific plates as described below and in the following chapters.

A Pacific-fixed reference frame was generated by minimizing motions at the following CGPS stations known to be situated on the Pacific plate: FALE, NIUC, KOKB, KWJ1, THTI and MKEA. Site velocities in this Pacific-fixed frame are reported in Table 2.1 and are shown graphically in Figure 2.4. Velocities of sites located on the Pacific plate are on the order of 0-2 mm/yr, indicating that this plate has indeed been fixed. Velocities of sites located on the Australian plate range from 50-93 mm/yr, increasing with distance from the Australia-Pacific Euler pole (61.04° S, 184.19° E, after Beavan et al, 2002). Also reported in Table 2.1 are predicted site velocities based on the Australia-Pacific Euler vector (61.04° S, 184.19° E, 1.078 deg/Myr, after Beavan et al, 2002).

An Australian-fixed reference frame was generated by minimizing motions at the following CGPS stations known to be situated on the Australian plate: KOUC, LPIL, TOW2, HOB2 and TIDB. Site velocities in this Australian-fixed frame are reported in Table 2.2 and are shown graphically in Figure 2.5. Velocities of sites located on the Australian plate are on the order of 0-1 mm/yr, indicating that this plate has indeed been fixed. Velocities of sites located on the Pacific plate range from 35-121 mm/yr, increasing with distance from the Australia-Pacific Euler pole (61.04° S, 184.19° E, after Beavan et al, 2002). Also reported in Table 2.2 are predicted site

velocities based on the Australia-Pacific Euler vector (61.04° S, 184.19° E, 1.078 deg/Myr, after Beavan et al, 2002).

Table 2.1. Regional CGPS velocities in a Pacific-fixed reference frame.

Predicted site velocities are based on the Australia-Pacific Euler vector 61.04° S, 184.19° E, 1.078 deg/Myr, after Beavan et al, 2002.

Site	Lon	Lat	Time Span (yrs)	GPS Hor.Vel. (mm/yr)	GPS Azimuth (deg)	Pred. Hor.Vel. (mm/yr)	Pred. Azimuth (deg)
				Pacific Plate Sites			
CHAT	-176.57	-43.96	5.8	2.0 ± 0.1	29.3° ± 1.3°	0	--
FALE	-172.00	-13.83	5.7	0.4 ± 0.1	-110.5° ± 6.6°	0	--
KOKB	-159.66	22.13	5.8	1.7 ± 0.1	-165.2° ± 3.3°	0	--
KWJ1	167.73	8.72	5.5	1.4 ± 0.1	87.5° ± 2.4°	0	--
MKEA	-155.46	19.80	5.8	1.3 ± 0.1	-142.2° ± 3.2°	0	--
NIUC	-169.93	-19.06	5.6	0.8 ± 0.0	16.0° ± 4.5°	0	--
THTI	-149.61	-17.58	4.4	0.8 ± 0.2	-66.1° ± 7.3°	0	--
				Australian Plate Sites			
AUCK	174.83	-36.60	5.8	50.3 ± 0.0	78.8° ± 0.1°	51.3	79.4°
HOB2	147.44	-42.80	5.8	59.3 ± 0.1	51.5° ± 0.1°	57.4	52.8°
KOUC	164.29	-20.56	5.7	82.1 ± 0.0	75.6° ± 0.0°	81.7	76.0°
LPIL	167.26	-20.92	5.8	80.1 ± 0.0	77.5°± 0.0°	80.2	77.8°
NOUM	166.41	-22.27	4.9	79.0 ± 0.1	76.4° ± 0.0°	78.4	76.9°
TIDB	148.98	-35.40	5.8	68.9 ± 0.1	59.3° ± 0.0°	67.3	60.2°
TOW2	147.06	-19.27	5.6	93.2 ± 0.1	67.6° ± 0.0°	91.0	67.3°

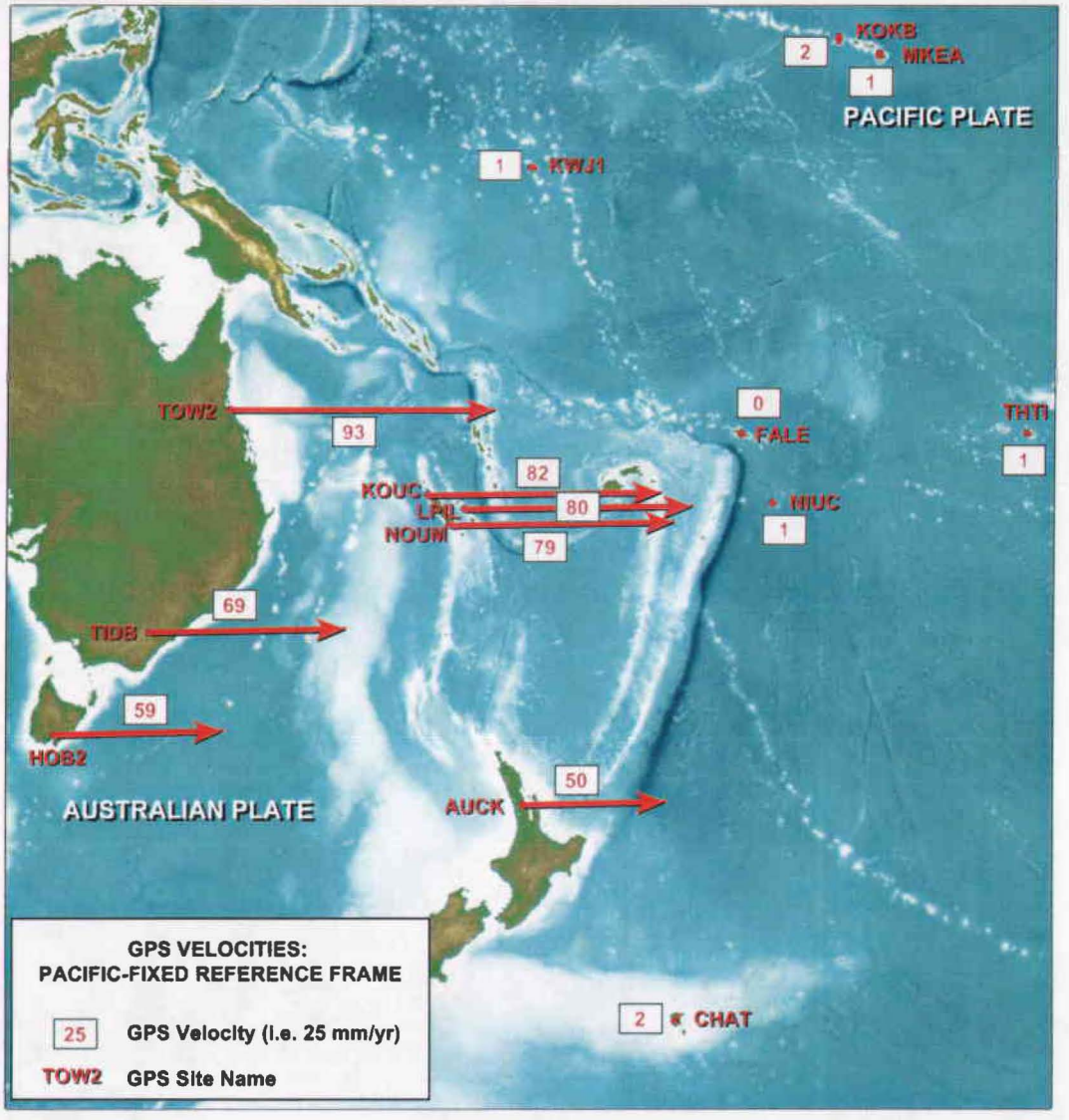

Figure 2.4. Southwest Pacific GPS velocities in a Pacific-fixed reference frame.

Table 2.2. Regional CGPS velocities in an Australia-fixed reference frame.

Predicted site velocities are based on the Australia-Pacific Euler vector 61.04° S, 184.19° E, 1.078 deg/Myr, after Beavan et al, 2002.

Site	Lon	Lat	Time Span (yrs)	GPS Hor.Vel. (mm/yr)	GPS Azimuth (deg)	Pred. Hor.Vel. (mm/yr)	Pred. Azimuth (deg)
				Pacific Plate Sites			
CHAT	-176.57	-43.96	5.82	34.5 ± 0.0	-88.9° ± 0.1°	35.6	-91.2
FALE	-172.00	-13.83	5.71	89.8 ± 0.1	-87.9° ± 0.0°	88.3	-87.5
KOKB	-159.66	22.13	5.81	121.3 ± 0.1	-83.6° ± 0.0°	119.3	-82.2
KWJ1	167.73	8.72	5.55	113.4 ± 0.1	-98.8° ± 0.0°	113.4	-98.3
MKEA	-155.46	19.80	5.81	121.5 ± 0.1	-81.3° ± 0.0°	119.0	-80.2
NIUC	-169.93	-19.06	5.64	81.6 ± 0.1	-85.6° ± 0.0°	80.7	-85.8
THTI	-149.61	-17.58	4.40	90.5 ± 0.2	-73.2° ± 0.1°	88.3	-73.1
				Australian Plate Sites			
AUCK	174.83	-36.60	5.82	1.4 ± 0.0	-102.3° ± 1.9°	0	--
HOB2	147.44	-42.80	5.78	0.9 ± 0.1	24.7° ± 4.1°	0	--
KOUC	164.29	-20.56	5.74	0.7 ± 0.0	-120.6° ± 3.0°	0	--
LPIL	167.26	-20.92	5.82	1.1 ± 0.0	-111.1° ± 1.8°	0	--
NOUM	166.41	-22.27	4.88	0.4 ± 0.1	-102.9° ± 8.4°	0	--
TIDB	148.98	-35.40	5.82	0.6 ± 0.1	31.5° ± 5.6°	0	--
TOW2	147.06	-19.27	5.60	1.3 ± 0.1	123.3° ± 2.6°	0	--

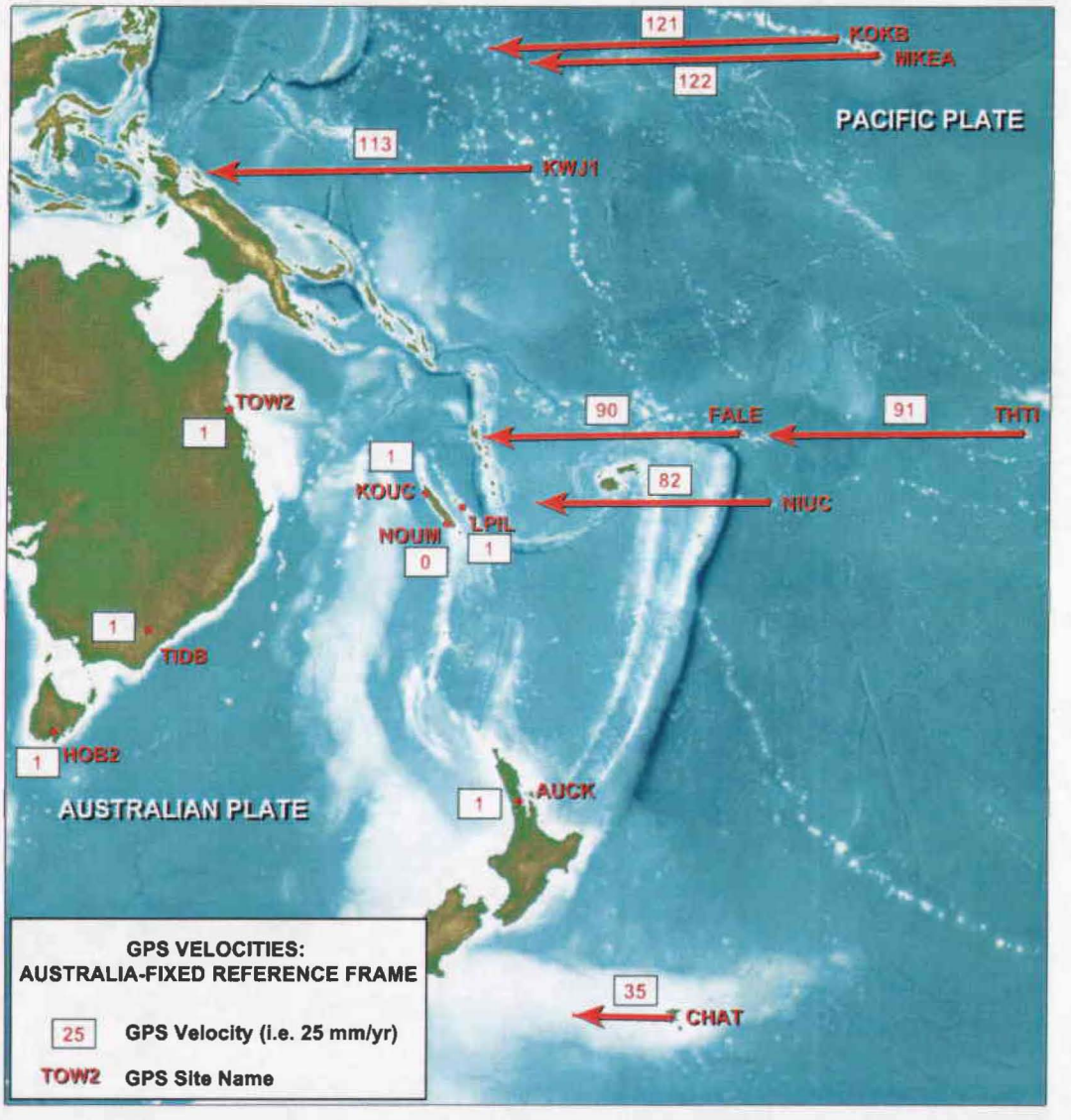

Figure 2.5. Southwest Pacific GPS velocities in an Australia-fixed reference frame.

Chapter 3. Refined Estimates of Crustal Motion in the Tonga-Lau System

David A. Phillips (SOEST, University of Hawaii at Manoa)

Michael G. Bevis (The Ohio State University)

John Beavan (IGNS, New Zealand)

Tevita Malolo (Lands and Survey, Kingdom of Tonga)

Paserio Samisoni (Lands and Survey, Fiji Islands)

Toelau Iulio (Lands and Survey, Samoa)

3.1. Abstract

We used a ten-year GPS time series to analyze crustal motions in the Tonga-Lau system. While velocity estimates presented here are much more accurate than those reported by Bevis et al. (1995), our new solutions in fact vary only slightly from those initial estimates. At 151 to 247 mm/yr, the convergence rate between the Tonga ridge and the Pacific plate remains the highest yet observed on Earth. Our measurements of rapid extension in the Lau Basin, from 80 to 165 mm/yr, are in good agreement with opening rates determined from marine geophysical data and it is likely that these rates have been sustained for at least the past 780,000 years (Zellmer and Taylor, 2001). For the first time we observe anticlockwise rotation of the Fiji

platform relative to the Australian plate. We also observe anomalous deformation of the Tonga ridge forearc between 16°S and 18°S.

3.2. Introduction

The Tonga-Lau subduction system is situated in the southwest Pacific where the Pacific plate subducts westward at the Tonga trench (Figures 1.2, 3.1). This system is remarkable for having the highest rates of subduction and back-arc spreading on earth (Bevis et al., 1995) as well as the highest levels of deep mantle seismicity on earth (Oliver and Isacks, 1967). Geophysical and geodetic data indicate that the Pacific plate undergoes convergence at rates of ~160 mm/yr near 21°S to more than 240 mm/yr at 16°S and that these rates have been sustained for at least 780,000 years (Zellmer and Taylor, 2001). These rather extreme crustal velocities represent the sum of Australia-Pacific convergence and Lau Basin opening.

The Lau Basin is a complex, extensional back-arc system that terminates just south of 24°S, near where the Louisville ridge intersects the Tonga trench. The rate of extension in the Lau Basin effectively increases northward from 24°S to at least 16°S and has produced a V-shaped basin that separates the volcanically active Tofua arc on the Tonga ridge in the east from the inactive Lau ridge on the Australian plate in the west. This asymmetric extension has resulted in rigid clockwise rotation of the

Figure 3.1. Perspective view of the Tonga-Lau system.

The Pacific plate subducts westward at the Tonga trench while extension occurs in the Lau Basin. The Tonga-Lau system has the highest rates of subduction and backarc spreading yet observed on Earth, as well as the planet's highest levels of deep mantle seismicity. View from the southeast.

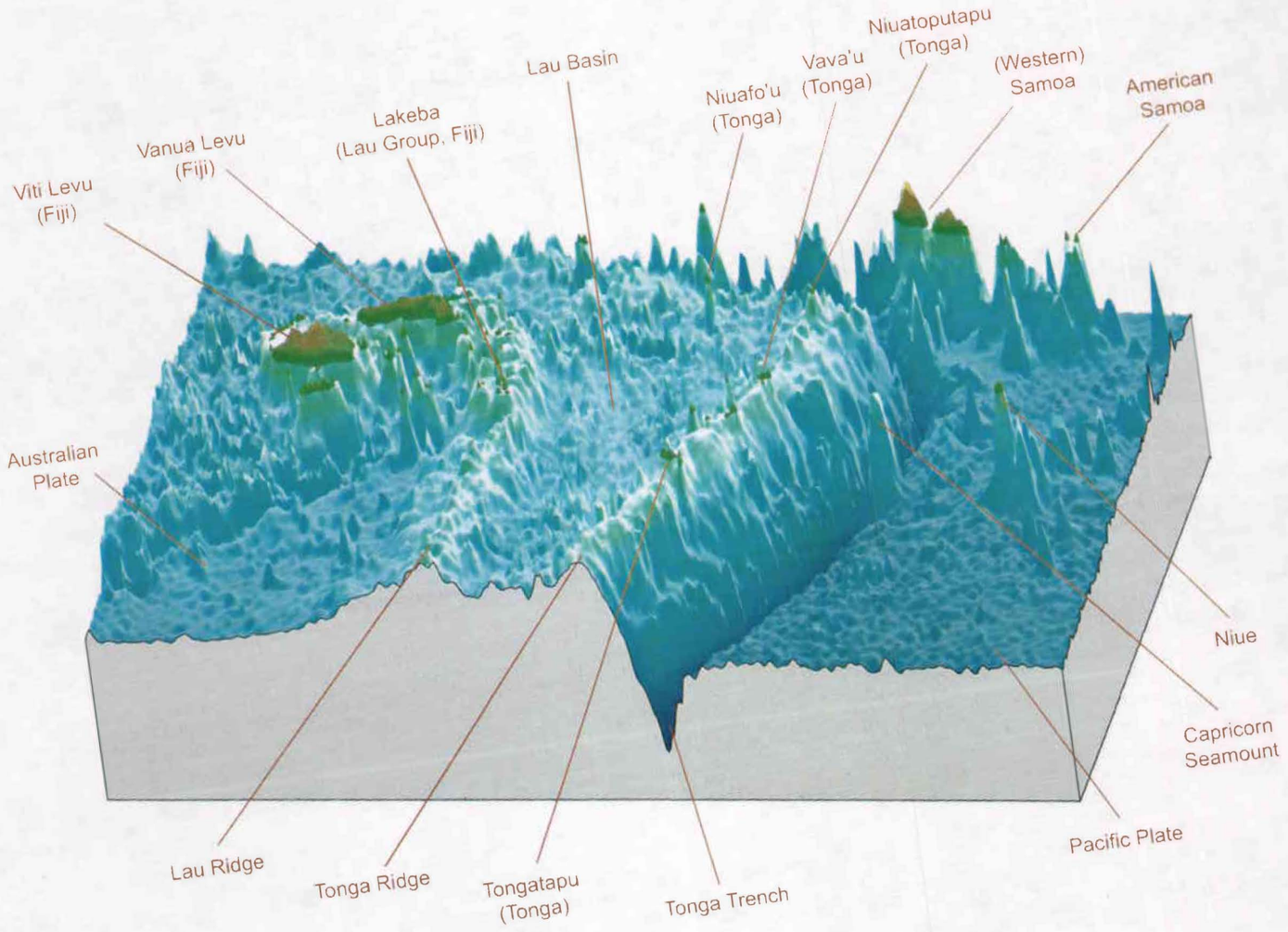
Viti Levu
(Fiji)
Vanua Levu
(Fiji)
Lakeba
(Lau Group, Fiji)
Lau Basin
Niuafo'u
(Tonga)
Vava'u
(Tonga)
Niuatoputapu
(Tonga)
(Western)
Samoa
American
Samoa
Australian
Plate
Niue
Capricorn
Seamount
Pacific Plate
Lau Ridge
Tonga Ridge
Tongatapu
(Tonga)
Tonga Trench

Tonga ridge about a pole located near the southern extent of the basin in a manner that has been described as a "windscreen wiper" effect.

The mode of extension in the Lau Basin has been the topic of considerable debate. Some studies concluded that diffuse and transient extension predominates (e.g., Hamburger and Isacks, 1988) while others concluded that extension occurs along organized networks of spreading centers and transforms (e.g., Chase, 1971; Taylor et al., 1996). Most recent studies indicate that the latter situation is most likely, and numerous active spreading centers and transforms have been identified in the Lau Basin (e.g., Pelletier et al., 1998). Initially, a discrepancy existed between rates of opening observed by GPS measurements and rates determined from seafloor geophysical studies, with the GPS estimates being significantly higher, and it was proposed that the rate of opening in the Lau Basin had recently increased (Taylor et al., 1996). However, this discrepancy was resolved when Zellmer and Taylor (2001) developed a three-plate kinematic model for the Lau Basin, in which extension is partitioned between the Australian plate, the Tonga ridge microplate, and the recently identified Niuafo'ou microplate (Figure 3.2), and confirmed that rates obtained from seafloor geophysics data matched the present day geodetic rates.

Figure 3.2. Three-plate kinematic model for the Tonga-Lau system.

After Zellmer and Taylor (2001). Measured rates of opening in the Lau Basin determined from marine geophysical surveys are given in mm/yr within boxes (box colors correspond to colors of tectonic features). Gray areas indicate regions of positively magnetized crust. A 1500-m bathymetric contour outlines the Lau and Tonga ridges and surrounds the islands (solid black) in the region. A = Australian plate; T = Tonga ridge microplate; N = Niuafo'ou microplate; CLSC, ELSC and NWLSC, = resp. Central, East and North West Lau Spreading Centers; FRSC = Fonualei Rift and Spreading System; FSC = Futuna Spreading Center; LETZ = Lau Extensional Transform Zone, PR = Peggy Ridge; MTJ = Mangatolu Triple Junction. GPS velocities for the Tonga forearc are from Bevis (1997).

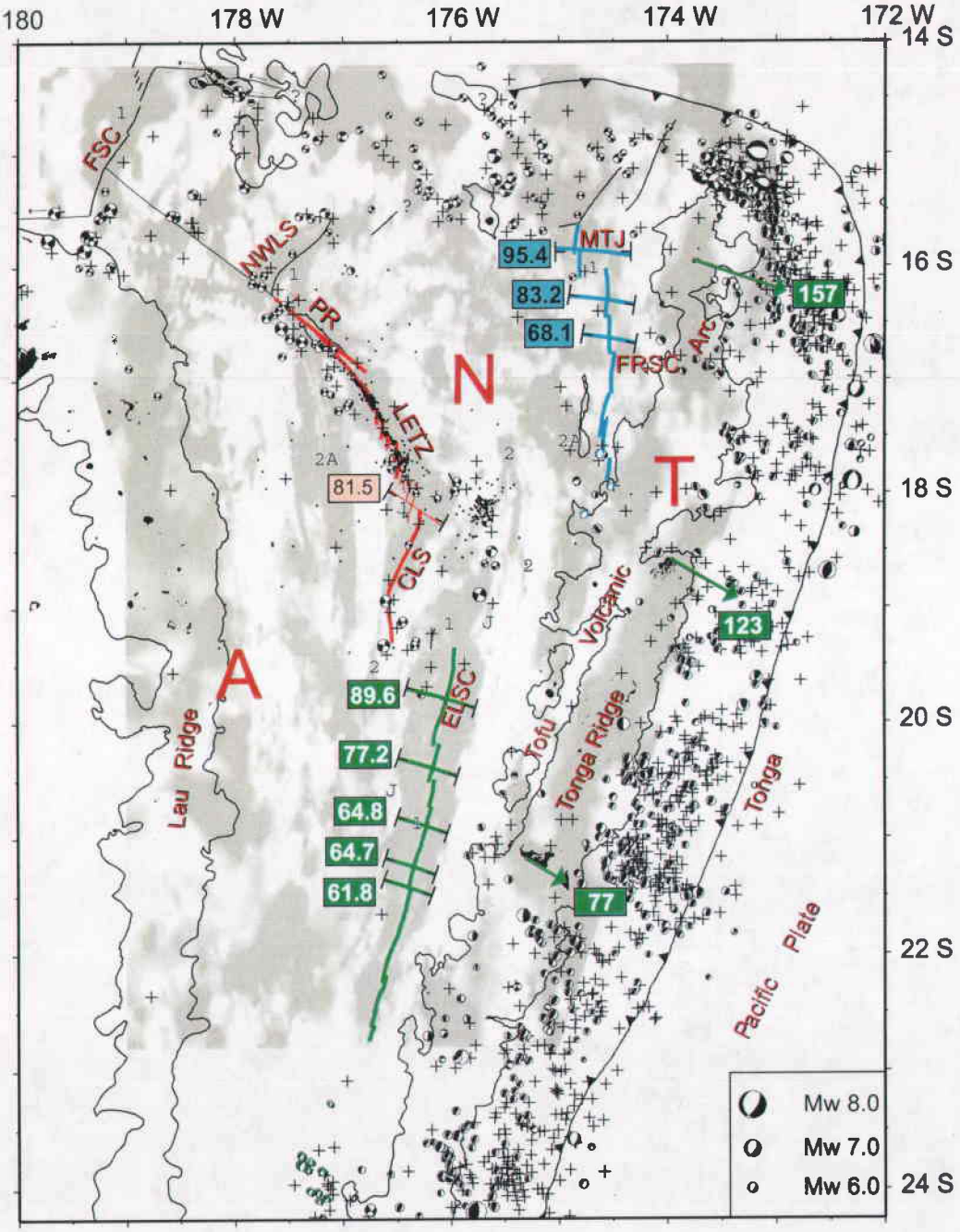
180
178 W
176 W
174 W
172 W
14 S
16 S
18 S
20 S
22 S
24 S
FSC
NWLS
PR
LETZ
CLS
ELSC
MTJ
FRSC
Arc
Volcanic
Tofu
Tonga Ridge
Tonga
Lau Ridge
Pacific Plate
N
T
A
95.4
83.2
68.1
81.5
89.6
77.2
64.8
64.7
61.8
157
123
77
Mw 8.0
Mw 7.0
Mw 6.0

3.3. Data

Initial crustal motion estimates reported by Bevis et al. (1995) were determined from a two year time series of GPS data collected in 1990 and 1992. Crustal motions reported here were determined from a ten year time series that includes data from the original 1992 campaign as well as continuous GPS site and campaign (rover) data collected between 1996 and 2002. Beyond the obvious benefits of having a much longer time series, our current results are also superior to previous estimates due to numerous technical advancements since the original study, including completion of the GPS satellite constellation, improvements in GPS user instrumentation, and superior processing methods. It was estimated that approximately 75% of the formal errors associated with the initial estimates were due to limitations of the 1990 dataset (Bevis et al., 1995) and we did not include the 1990 dataset in this analysis due to its inherently lower quality.

In 1996 we began installing a network of continuous GPS (CGPS) stations throughout the southwest Pacific, including sites in Tonga (VAVC), Fiji (SUVA), Niue (NIUC), Samoa (FALE), New Caledonia (KOUC) and the Loyalty Islands (LPIL). All of our CGPS sites are equipped with Ashtech Z-XII dual-frequency GPS receivers and Dorne-Margolin choke-ring antennas. The CGPS site at Vava'u in Tonga (VAVC) had to be removed in 2000 because of construction at the Vava'u airport but a new CGPS site (VAVS) was subsequently established in Nukulofa

several kilometers away. Data from VAVS are not reported here due to the shortness of its time series and because of possible displacement of this site during a cyclone in 2001. Additional CGPS data were obtained from sites operated by the International GPS Service (IGS), the Institut de Recherches pour le Developpement (IRD), and the Australian National University (ANU). CGPS sites used in this analysis were shown in Figure 2.3.

This CGPS network allowed us to collect data using the methods of the Multi-modal Occupation Strategy (MOST) for GPS surveys (Bevis et al., 1997) rather than mounting resource intensive and logistically difficult campaigns like the ones conducted in 1990 and 1992. As a result, all nine original campaign sites (LLAU, NIUE, NTPT, RARO, TGPU, VANU, VAVA, VITI, and WSAM) were re-occupied as "rover" sites between 1996 and 2002. Additional roving data from sites TGPU, VANU and VITI were collected by local survey agencies as part of the annual Asia Pacific Regional Geodetic Project (APRGP) campaigns organized by the Australian Surveying and Land Information Group (AUSLIG) between 1998 and 2001. Most data were collected using Ashtech Z-XII receivers and Dorne-Margolin choke-ring antennas although Ashtech Micro-Z, Trimble SSE and SSI, and Leica 299 and 9500 receivers (all dual frequency) were used for some surveys.

3.3.1. Data Analysis

GPS data were analyzed using GAMIT, GLOBK, and VSTACK processing routines (King and Bock, 2002; Herring, 2002; Kendrick et al., 2001) using the methods described in Chapter 2. The resulting velocity field was used to establish geodetic reference frames corresponding to the Pacific and Australian plates.

3.3.2. Pacific-Fixed Reference Frame

A Pacific-fixed reference frame was generated by minimizing the motions of stations known to be situated on the Pacific plate. Site velocities in this Pacific-fixed frame are reported in Table 3.1. In this reference frame, velocities at sites located on the "fixed" Pacific plate are on the order of 0-2 mm/yr while site velocities on the Tonga ridge increase northward from 151 mm/yr at Tongatapu (TGPU) to 247 mm/yr at Niuatoputapu (NTPT). Pacific-fixed velocities are shown in Figure 3.3.

3.3.3. Australia-Fixed Reference Frame

An Australian-fixed reference frame was generated by minimizing the motions of stations known to be situated on the Australian plate. Australian-fixed velocities are reported in Table 3.2. Velocities at sites located on the Australian plate are on the order of 0-1 mm/yr while site velocities on the Tonga ridge increase northward from 80 mm/yr at Tongatapu (TGPU) to 165 mm/yr at Niuatoputapu (NTPT). Site velocities in the Fiji islands range from 2 mm/yr at Lekeba on the Lau Ridge (LLAU)

Table 3.1. Tonga-Lau GPS site velocities in a Pacific-fixed reference frame.

(*) indicates continuous GPS site.

COUNTRY	LOCATION	SITE	HOR. VEL.(mm/yr)	AZIMUTH
		Pacific Plate Sites (Fixed)		
Cook Islands	Rarotonga	RARO	0.2 ± 0.4	--
Hawaii	Koke'e	KOKB *	0.4 ± 0.2	--
Hawaii	Mauna Kea	MKEA*	0.4 ± 0.2	--
Marshall Is.	Kwajalein	KWJ1*	1.6 ± 0.3	--
Niue	Niue	NIUC*	2.0 ± 0.2	--
Niue	Niue	NIUE	1.2 ± 1.1	--
Samoa	Faleolo	FALE*	1.9 ± 0.2	--
Samoa	Faleolo	WSAM	1.2 ± 0.5	--
		Tonga-Lau Sites		
Fiji	Lakeba	LLAU	78.9 ± 0.9	87.5° ± 1.1°
Fiji	Vanua Levu	VANU	74.3 ± 1.2	87.1° ± 0.7°
Fiji	Suva	SUVA*	74.6 ± 0.1	87.8° ± 0.1°
Fiji	Viti Levu	VITI	74.4 ± 0.9	90.4° ± 0.6°
Tonga	Tongatapu	TGPU	150.5 ± 0.3	105.7° ± 0.1°
Tonga	Vava'u	VAVA	199.8 ± 0.4	107.5° ± 0.1°
Tonga	Vava'u	VAVC*	199.2 ± 0.2	107.9° ± 0.1°
Tonga	Niuatoputapu	NTPT	247.0 ± 0.6	102.1° ± 0.2°

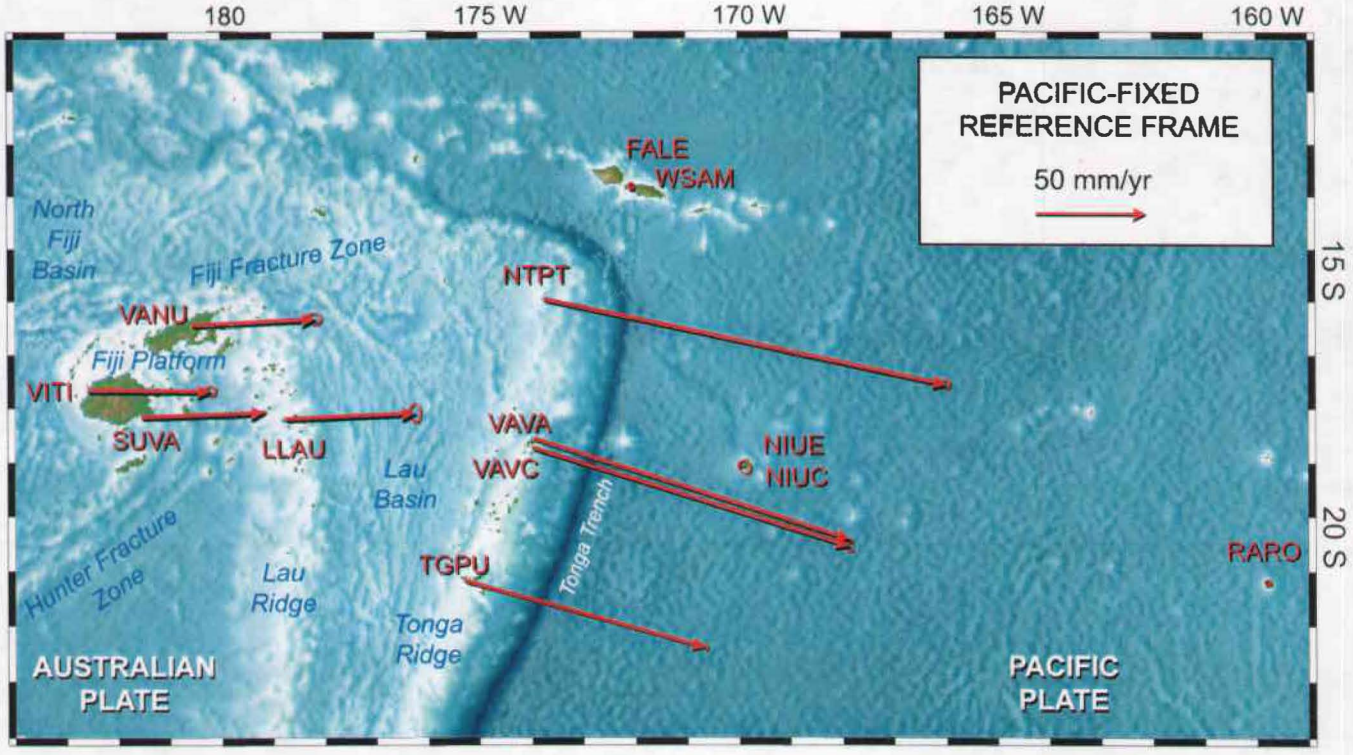

Figure 3.3. GPS velocities in a Pacific-fixed reference frame.

Table 3.2. Tonga-Lau GPS site velocities in an Australia-fixed reference frame.

(*) indicates continuous GPS site.

COUNTRY	LOCATION	SITE	HOR. VEL.(mm/yr)	AZIMUTH
		Australian Plate Sites (Fixed)		
Australia	Tidbinbilla	TIDB*	1.0 ± 0.1	--
Loyalty Is.	Lifou	LFOU	2.3 ± 0.8	--
Loyalty Is.	Lifou	LPIL*	1.5 ± 0.1	--
N. Caledonia	Koumac	KOUC*	1.1 ± 0.1	--
N. Caledonia	Koumac	KOUM	2.2 ± 0.7	--
N. Caledonia	Tindu	TIND	2.0 ± 0.5	--
Tasmania	Hobart	HOB2*	0.6 ± 0.3	--
		Pacific Plate Sites		
Cook Is.	Rarotonga	RARO	78.8 ± 0.5	-77.6° ± 0.3°
Niue	Niue	NIUC*	81.9 ± 0.2	-85.8° ± 0.1°
Niue	Niue	NIUE	78.7 ± 1.0	-85.7° ± 0.8°
Samoa	Faleolo	FALE*	89.3 ± 0.2	-87.9° ± 0.1°
Samoa	Faleolo	WSAM	88.7 ± 0.5	-87.0° ± 0.3°
		Tonga-Lau Sites		
Fiji	Lakeba	LLAU	2.2 ± 0.9	-77.9° ± 39.0°
Fiji	Suva	SUVA*	7.3 ± 0.1	-115.2° ± 1.1°
Fiji	Vanua Levu	VANU	9.5 ± 1.2	-96.9° ± 5.3°
Fiji	Viti Levu	VITI	10.7 ± 0.9	-135.1° ± 4.5°
Tonga	Tongatapu	TGPU	79.6 ± 0.3	120.3° ± 0.2°
Tonga	Vava'u	VAVA	124.6 ± 0.4	117.7° ± 0.2°
Tonga	Vava'u	VAVC*	124.2 ± 0.2	118.4° ± 0.1°
Tonga	Niuatoputapu	NTPT	164.8 ± 0.6	107.5° ± 0.3°

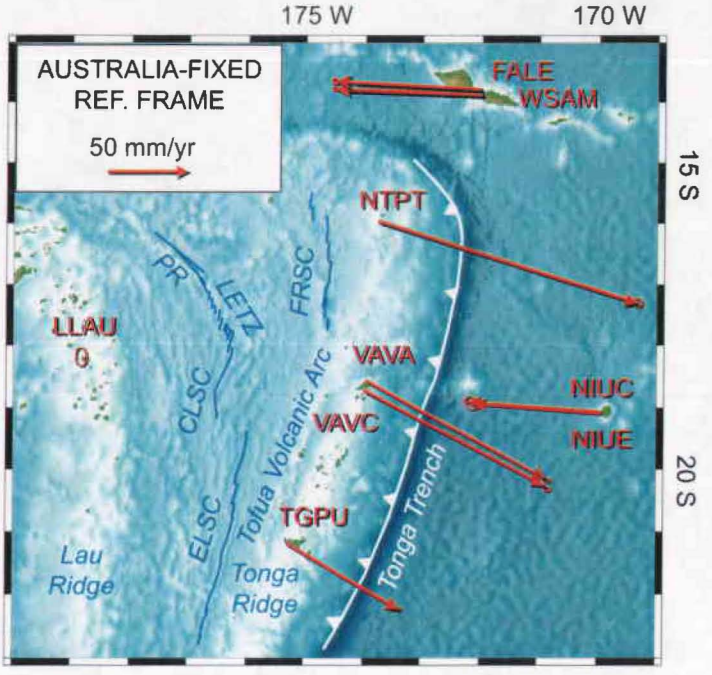

Figure 3.4. GPS velocities in an Australia-fixed reference frame.

GPS site on the Lau ridge (LLAU) shows no significant motion relative to the Australian plate. Sites on the Pacific plate show Australia-Pacific convergence. Sites on the Tonga ridge show opening of the Lau Basin. Tectonic features after Zellmer and Taylor (2001). ELSC = East Lau Spreading Ridge; CLSC = Central Lau Spreading Center; LETZ = Lau Extensional Transform Zone; PR = Peggy Ridge; FRSC = Fonualei Rift and Spreading Center.

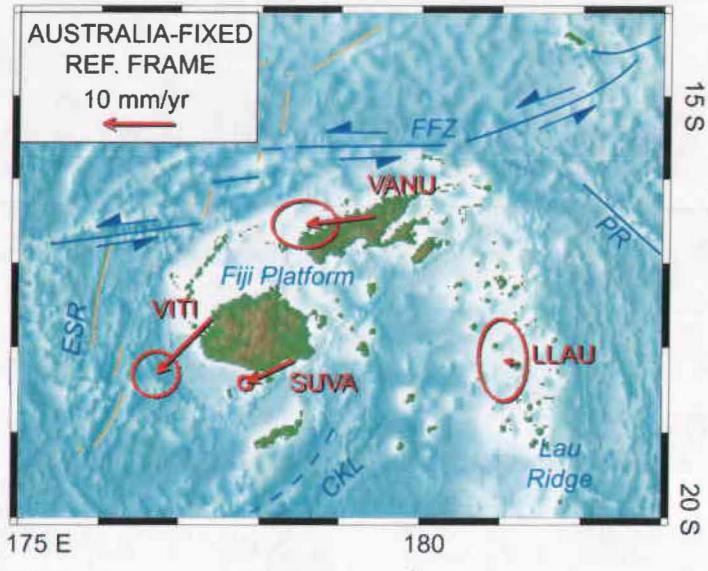

Figure 3.5. Rotation of the Fiji platform in an Australia-fixed reference frame.

Tectonic features after Pelletier et al. (1998): FFZ, Fiji fracture zone; ESR, east spreading ridge; CKL, Conway-Kandavu lineament; PR, Peggy ridge.

to 11 mm/yr at western Viti Levu (VITI). Australia-fixed velocities for Tonga-Lau are plotted in Figure 3.4. Australia-fixed velocities for the Fiji platform are shown in figure 3.5.

3.3.4. Tonga-Fixed Reference Frame

While a spatially limited network consisting of four sites can not be used to realize a true geodetic reference frame, we did fix a subset of sites on the Tonga ridge in order to examine the possibility of differential motion within the ridge itself. Sites at Tongatapu (TGPU) and Vava'u (VAVA and VAVC) were stable relative to each other with resulting velocities of 0 to 1 mm/yr. However, with a velocity of 14 mm/yr along an azimuth of 25°, the site at Niuatoputapu (NTPT) shows significant motion relative to the other sites on the Tonga ridge. The velocity of NTPT relative to other sites in Tonga is provided in Table 3.3 and is shown in Figure 3.6.

3.4. Discussion

Our new estimates of crustal velocity in the Tonga-Lau system are significantly improved over previous estimates. In general our results for most island stations vary only slightly from those previously reported but our improved velocity resolution allows us to refine previous interpretations. Our formal error estimates are supported by comparisons between velocities determined at nearly coincident campaign and

Table 3.3. Tonga-Lau GPS site velocities in a Tonga-fixed reference frame.

The GPS velocity at Niuatoputapu (NTPT) cannot be constrained relative to other sites on the Tonga ridge. (*) indicates continuous GPS site.

COUNTRY	LOCATION	SITE	HOR. VEL.(mm/yr)	AZIMUTH
Tonga	Tongatapu	TGPU	0.5 ± 0.3	--
Tonga	Vava'u	VAVA	1.3 ± 0.4	--
Tonga	Vava'u	VAVC*	0.9 ± 0.2	--
Tonga	Niuatoputapu	NTPT	13.7 ± 0.7	24.6° ± 2.8°

CGPS stations at several locations including Tonga (VAVA/VAVC), Samoa (WSAM/FALE) and Niue (NIUE/NIUC).

3.4.1. Rapid Convergence at the Tonga Trench

A significantly longer data time series and improved analysis techniques have only served to refine the initial conclusion by Bevis et al. (1995) that the Pacific plate undergoes extremely rapid convergence at the Tonga trench. Indeed, our latest estimates confirm that present day convergence rates at the Tonga arc remain the highest rates yet observed on Earth. In a Pacific-fixed reference frame our current velocity at Niuatoputapu (NTPT), at 247 mm/yr, is slightly faster than the previous estimate of 240 mm/yr. Velocity measurements at Vava'u (VAVA) and Tongatapu (TGPU), now at 200 and 151 mm/yr respectively, are slightly slower than previously reported estimates of 205 and 164 mm/yr.

Figure 3.6. Differential motion within the Tonga ridge.

Tectonic features after Zellmer and Taylor (2001): FRSC = Fonualei Rift and Spreading Center; MTJ = Mangatolu Triple Junction. High resolution bathymetry courtesy of A. Goodliffe and B. Taylor.

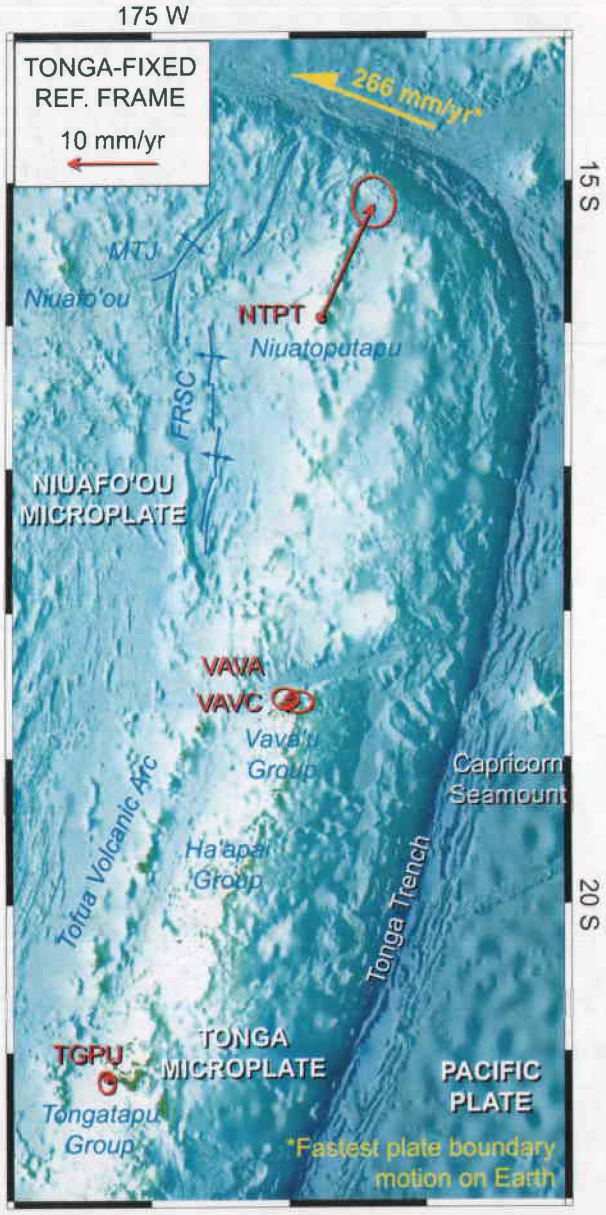
175 W
TONGA-FIXED
REF. FRAME
10 mm/yr
266 mm/yr*
15 S
MTJ
Niuafo'ou
NTPT
Niuatoputapu
FRSC
NIUAFO'OU
MICROPLATE
VAVA
VAVC
Vava'u
Group
Capricorn
Seamount
Tofua Volcanic Arc
Ha'apai
Group
Tonga Trench
20 S
TONGA
MICROPLATE
TGPU
Tongatapu
Group
PACIFIC
PLATE
*Fastest plate boundary
motion on Earth

3.4.2. Rapid Extension in the Lau Basin

The observed velocity field in the Australia-fixed reference frame clearly shows the effects of active extension in the Lau Basin. Our new Australia-fixed velocity for Niuatoputapu (NTPT), at 165 mm/yr, is 5 mm/yr faster than the previous estimate while our new velocities for Vava'u (VAVA) and Tongatapu (TGPU), at 125 and 80 mm/yr respectively, are slower than the original estimates of 130 and 91 mm/yr. Our GPS velocity estimates are in good agreement with velocity estimates determined from seafloor geophysical data for a three plate kinematic model of the Lau Basin consisting of the Australian plate, the Tonga microplate, and the recently described Niuafo'ou plate (Zellmer and Taylor, 2001).

3.4.3. Rotation of the Fiji Platform

A new observation is that the Fiji platform, which moves with the Australian plate to a first approximation, shows gradual anticlockwise rotation relative to the Australian plate. Initial geodetic measurements detected little or no motion at GPS sites on the Fiji platform relative to the Australian plate (Bevis et al., 1995). Our new velocity at Lakeba (LLAU) on the Lau Ridge still shows no significant motion relative to the Australian plate. However, our velocities for sites at Vanua Levu (VANU) and Viti Levu (VITI and SUVA) show motions of up to 11 mm/yr trending east-southeast (Fig. 3.5). Anticlockwise rotation of the Fiji platform between 10 Ma and 3 Ma has

been identified on the basis of paleomagnetism and kinematic analysis of dikes and faults (e.g., Begg and Gray, 2002; Taylor et al., 2000) but these studies reported that such rotation terminated at about 3 Ma. Present day rotation may be due to elastic strain accumulation associated with the Fiji Fracture Zone and the East Spreading Center of the North Fiji basin, tectonic features recently described in detail by Pelletier et al. (2001).

3.4.4. Intra-Arc Deformation at Niuatoputapu

We also observe for the first time what appears to be intra-arc deformation within the Tonga ridge, as the site at Niuatoputapu (NTPT) is moving away from the other sites in the Tonga islands. Intra-arc deformation is not unusual, and in fact would not be at all surprising in the planet's most rapidly converging forearc. However, the magnitude and direction of the observed motion at NTPT is unusual. Elastic strain accumulation in the forearc could produce a deformation signal of this magnitude but the azimuth would be nearly ninety degrees to the azimuth observed. This suggests that the displacement at NTPT is not likely due to elastic strain effects. Another possibility is that this perturbation could be due to coseismic displacement(s) that affected the GPS time series. However, the GPS time series between 1996 and 2002 does not contain any obvious "jumps", nor does the Harvard CMT catalog contain any significant shallow seismic events near this region during the observation period. It is possible that the Tonga arc may be fragmented between the islands of Vava'u

and Niuatoputapu although an active structure separating these two parts of the forearc has yet to be identified.

Due to the complex and poorly understood dynamics of the northernmost Lau Basin, it is not unreasonable to suggest that a previously unrecognized microplate may be present. The western boundary of such a microplate would likely occur along the Northeast Lau Spreading Center while the northern and eastern boundaries would occur along the Pacific plate boundary. However, no unusual zones of seismicity have been recognized between Tongatapu and Vava'u so the southern boundary of such a microplate can not presently be constrained.

3.5. Conclusions

We have used a ten-year GPS time series to analyze crustal motions in the Tonga-Lau system. While our new velocities differ only slightly from the initial estimates of Bevis et al. (1995), the new estimates are much improved in terms of accuracy and error constraints. While velocities at most sites on the Tonga ridge are slightly lower than the initial estimates, subduction of the Pacific plate at the Tonga trench still produces the highest convergence rates yet observed on Earth. It remains likely that this very rapid subduction of the Pacific plate contributes to the tremendous mantle seismicity associated with this subduction system. Rapid extension occurs in the Lau Basin and our GPS measurements are in good agreement with regional kinematic

models based on marine geophysical data and previous geodetic measurements. For the first time we observe anticlockwise rotation of the Fiji platform relative to the Australian plate. We also observe anomalous deformation of the Tonga ridge forearc between 16°S and 18.5°S. This deformation does not appear to be caused by elastic strain accumulation or coseismic displacement and it is possible that Niuatoputapu is situated on a previously unrecognized microplate.

3.6. Acknowledgements

We would like to thank the citizens of Tonga, Fiji, Niue, Samoa and the Cook Islands for their hospitality. Data collection in Tonga was facilitated by Francis Vatu and Fetu'u Vea. Data collection in Fiji was facilitated by Eroni Vari, Andrick Lau and Mesake Vakalala. Data collection in the Cook Islands was facilitated by Bruce Manuela and Mark Vaikai. Field work in Samoa was facilitated by Peter Rogers. Dion Matheson, Roger Williams and Laura Wallace from IGNS assisted with data collection in Tonga, Niue and Samoa. Data analysis at the Pacific GPS Facility was facilitated by Eric Kendrick and James Foster.

Chapter 4. Crustal Motion Studies in the New Hebrides Island Arc

David A. Phillips (SOEST, University of Hawaii at Manoa)

Stephane Calmant, Bernard Pelletier and Pierre Lebellegard (Laboratoire de Geophysique, Centre IRD, Noumea, New Caledonia, France)

Michael G. Bevis (The Ohio State University)

Frederick W. Taylor (Institute for Geophysics, University of Texas at Austin)

4.1. Abstract

Initial GPS measurements reported by Taylor et al. (1995) showed that convergence rates in the southern part of the New Hebrides arc were higher than Australia-Pacific motion predicted by NUVEL-1A while convergence in the central arc was much lower than predicted. This abrupt change in along strike convergence was attributed to accelerated velocities in the south due to rapid backarc extension in the North Fiji Basin and fragmentation of the central arc due to impingement of the d'Entrecasteaux Ridge and associated Bougainville seamount, large bathymetric features on the downgoing Australian plate. The present study provides new and refined estimates of convergence in the New Hebrides arc using a ten year GPS time series and a

significantly expanded GPS network. Based on our new measurements, the New Hebrides arc consists of four tectonically distinct provinces. Observed convergence at the northern segment, which includes the Torres and Banks islands, is ~70 mm/yr oriented ~N260°. Convergence at the central segment, which includes all the islands surrounding the Aoba basin, is ~30-40 mm/yr oriented ~N245° at the forearc and ~55 mm/yr oriented ~N255° at the backarc. Convergence at the southern segment, which includes the Sheppard islands, Efate, Tanna and Aneytum, is ~60-120 mm/yr oriented ~N230° to ~N250°. Convergence at the southernmost segment, which includes the islets of Matthew and Hunter, is ~45 mm/yr oriented ~N190°. The existence and characteristics of these arc segments is directly related to the impingement of bathymetric features on the downgoing plate. In particular, convergence at the central New Hebrides is partitioned between the forearc (Australian plate) and the backarc (North Fiji basin) as subduction of the d'Entrecasteaux Ridge system produces strong, shallow interplate coupling at the trench and displaces the central block eastward into the North Fiji Basin. We have simulated this process with an elastic model in which interplate slip ceases for an extended period of time on the shallow end of the interplate thrust zone.

4.2. Introduction

The New Hebrides island arc is part of the Greater Melanesian arc system and is situated between latitudes 166-172°E and longitudes 13-23° S (Figure 1.1, 1.2).

The Australian plate undergoes eastward subduction at the New Hebrides trench (NHT), which forms the western margin of the New Hebrides (NH) arc (Figure 4.1). Numerous large bathymetric features are present on the downgoing Australian plate, including the Torres Plateau, the d'Entrecasteaux Ridge system, and the Loyalty Ridge system. The arc's eastern margin consists of a series of extensional (in the north and south) and compressional (in the central) systems that separate the arc from the North Fiji basin (NFB), a back arc basin resulting from complex spreading (Figure 1.2).

Plate motions at the NH arc have previously been estimated using four different sources of data: 1) global plate models such as NUVEL-1A (DeMets et al., 1990; 1994) and regional GPS analyses (Beavan et al., 2002); 2) the geometry of microplate spreading centers and fault systems in the North Fiji Basin (Louat et al., 1989; Auzende et al., 1995; Pelletier et al., 1998); 3) convergence rates for the Australian plate based on vertical and horizontal motions of reefs as they crossed the NHT outer rise (Dubois et al., 1977; Taylor et al., 1994); and 4) direct GPS measurements across the NH arc (Taylor et al., 1995; Calmant et al., 1995; 1997). Each approach addresses a different time scale and provides different insights on NH tectonic history.

Figure 4.1. Perspective view of the New Hebrides arc.

The Australian plate subducts eastward along the New Hebrides trench. The central arc is being backshoved by the d'Entrecasteaux Ridge system. Viewed from the southwest.

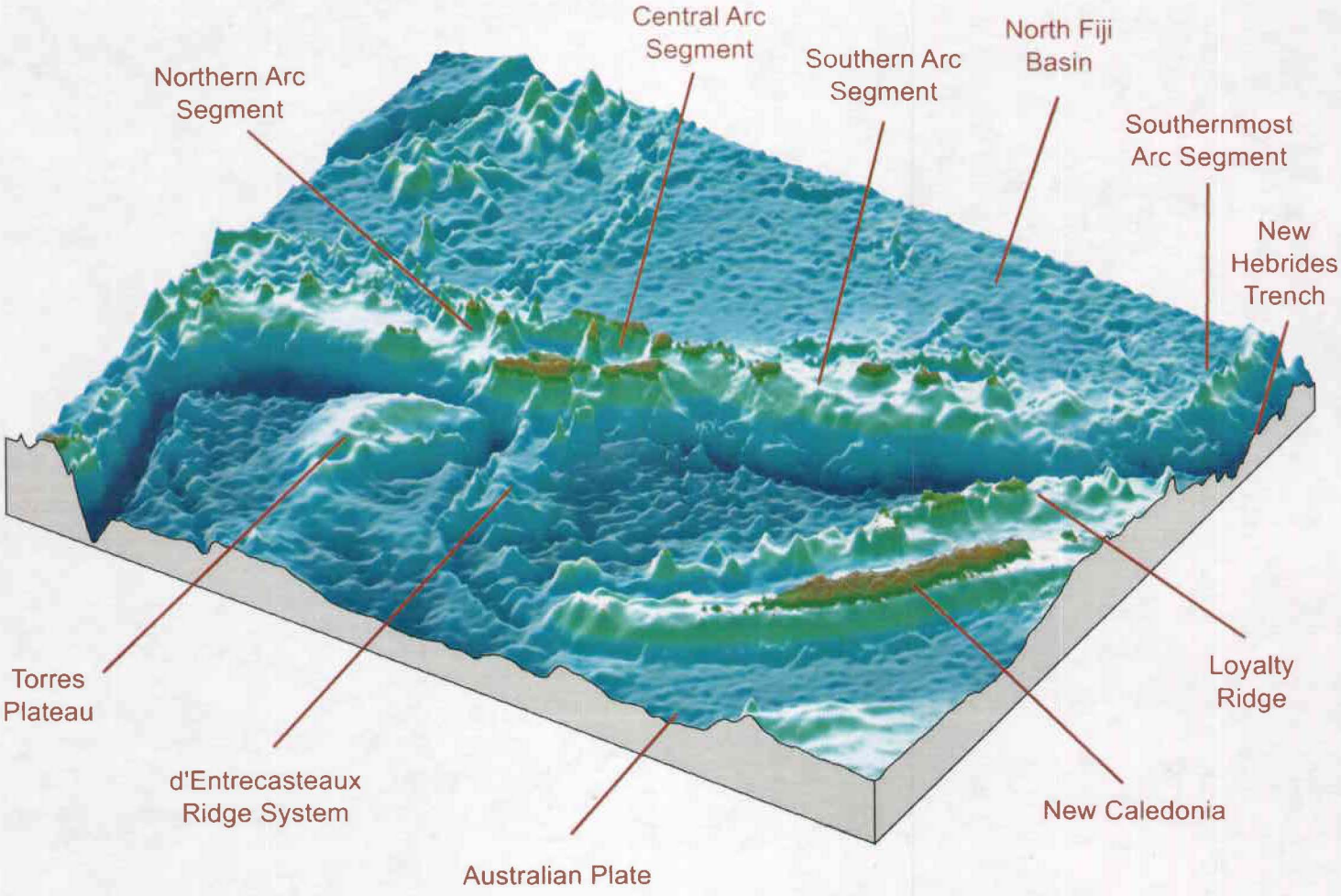
Central Arc Segment
North Fiji Basin
Northern Arc Segment
Southern Arc Segment
Southernmost Arc Segment
New Hebrides Trench
Torres Plateau
d'Entrecasteaux Ridge System
Australian Plate
Loyalty Ridge
New Caledonia

Relative motion between the Australian and Pacific plates is accommodated along the east-west trending Fiji Fracture Zone transform fault system passing north of Viti Levu, Fiji (Figure 3.5). GPS measurements show that the Fiji platform, to first approximation, moves with the Australian plate (Chapter 3). Therefore, the Late Quaternary plate convergence rate of the Australian plate at the NH arc is approximated by the Australian-Pacific (A/P) relative plate motion (Demets 1990; 1994; Louat et al., 1989; Pelletier et al., 1998; Beavan et al., 2002) and by the rate of motion of the NH arc relative to the North Fiji Basin due to back-arc reverse faulting (Taylor et al., 1995; Pelletier et al., 1998; 2000). That is, in addition to A/P relative motion, the NH arc must also accommodate seafloor spreading within the North Fiji Basin so that the actual convergence rate should be equivalent to the predicted regional A/P rate plus a contribution from back-arc opening. Predicted A/P convergence in the NH arc, based on the Euler vector of Beavan et al. (2002), ranges from 82 mm/yr at Tanna in the southern part of the arc to 88 mm/yr at Santo in the central NH (CNH).

Taylor et al. (1994) used corals drilled from the Bougainville Guyot during Ocean Drilling Project (ODP) Leg 134 (Site 831) to determine a convergence rate of 130 ±20 mm/yr at the CNH. Farther south at 21–23° S Dubois et al. (1977) calculated a similar mean convergence rate of 124 ±15 mm/yr since 0.2 Ma based on the rates of reef uplift on the Loyalty Islands as they ride up the trench outer rise.

Previously reported GPS measurements in the NH show modern convergence rates of 103 ±5 and 118 ±10 mm/yr at Efate and Tanna, respectively, consistent with the Late Quaternary rates determined from coral reefs (Taylor et al., 1995). However, at the CNH, GPS measured much slower convergence rates of only ~40 mm/yr. This is less than half the rate predicted by NUVEL-1A and regional plate models. Previous elastic modeling of the CNH GPS data suggested that no more than 10–20 mm/yr of the convergence rate deficit at CNH could be attributed to horizontal elastic strain within the arc (Taylor et al., 1995). The slow CNH convergence indicated that the whole CNH arc segment was moving eastward at a rate of 40–60 mm/yr relative to the rest of the arc and that this motion was accommodated in the back arc area by reverse faulting. This interpretation is supported by focal mechanisms for earthquakes along active strike-slip fault zones separating the CNH from the rest of the arc and thrusting focal mechanisms at the boundary between the CNH and NFB. The most recent examples of this eastward motion of the CNH are a strike-slip type M_S=7.5 earthquake just south of Malakula in 1994 and an M_S=7.5 event just east of Ambrym in 1999 that has a thrust focal mechanism dipping ~30° to the west (Regnier et al., in press; Pelletier et al., 2000). These events demonstrate significant modern eastward displacement of the CNH arc segment relative to the North Fiji Basin along back-arc reverse faults.

The d'Entrecasteaux Ridge (DR) system intersects the NH arc between southern Malakula and northern Espiritu Santo and is a major recognized factor in the unusual

tectonic evolution, structure, and morphology of the CNH including backthrusting of the 250 km-long CNH arc segment (Figure 4.2) (Taylor et al., 1980; Collot et al., 1985; Greene et al., 1994; Fisher, 1986; Fisher et al., 1986; 1991a; 1991b; Taylor et al., 1995; Calmant et al., 1997; Pelletier et al., 1998; Meffre and Crawford, 2001). The DR system trends nearly east-west, is about 100 km wide, and consists of two parallel linear features: a more-or-less continuous northern d'Entrecasteaux Ridge and a southern d'Entrecasteaux seamount chain. The northern ridge is about 40 km wide and rises 3 km higher than the adjacent seafloor immediately to the north (Monzier et al., 1984). The seamounts include the living reef-capped Sabine Bank about 50 km west of the plate boundary and the drowned reef-capped Bougainville Guyot (BG), which indents the edge of the arc by about 10 km (Collot et al., 1985; Fisher et al., 1991b; Greene et al., 1994; Taylor et al., 1994). The upper part of the southeast flank of the BG slopes on the order of 25°, typical of an atoll fore-reef slope. At its base, the BG is about 50 km in diameter and its lower flanks slope ~5°. Including its lower slopes, BG has an area of ~2500 km^2 and its summit plateau is roughly 400 km^2. The northern part of the CNH has begun to be underthrust by the distal flank of the Torres Plateau. This feature appears to be a recent arrival at the CNH arc but it may contribute to interplate coupling and deformation along the northern part of the CNH.

We assume that the DR system extends with the Australian plate beneath the CNH and that the subducted DR had bathymetric relief similar to the part that we can see in bathymetry. A DR seamount probably has arrived at the CNH every few hundred

Figure 4.2. Perspective view of the central New Hebrides arc.

The anomalous morphology and reduced convergence rates at the forearc in this region result from impingement of the d'Entrecasteaux Ridge and associated Bougainville Guyot. Viewed from the southwest.

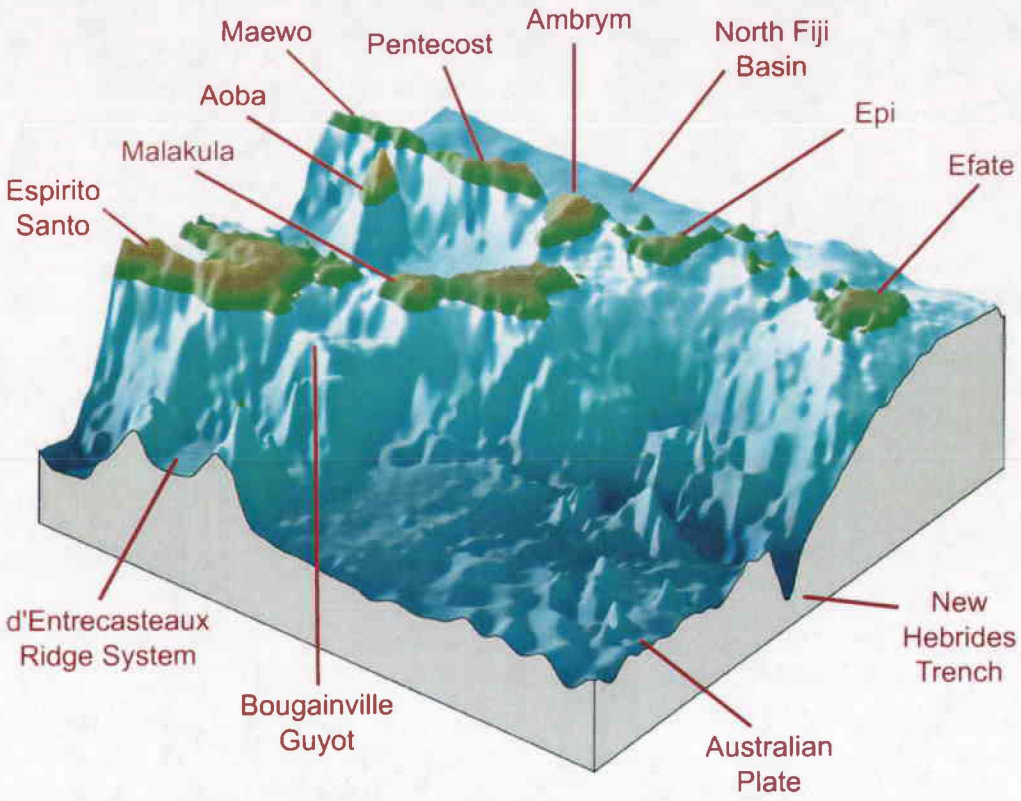
Maewo
Pentecost
Ambrym
North Fiji Basin
Aoba
Epi
Malakula
Efate
Espirito Santo
d'Entrecasteaux Ridge System
New Hebrides Trench
Bougainville Guyot
Australian Plate

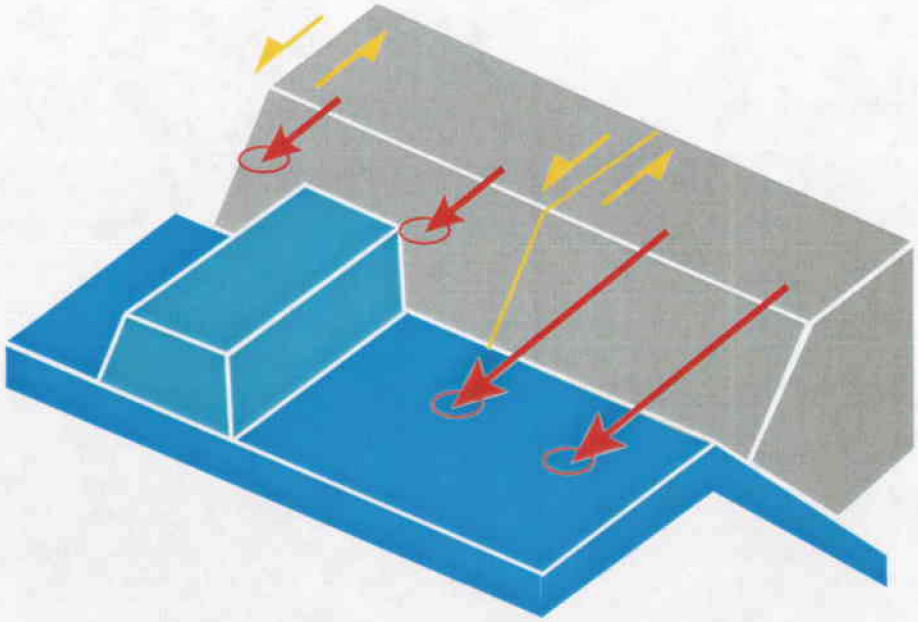

thousand years, given the 50 km spacing between BG and Sabine Bank and the mean convergence rate of ~130–155 mm/yr (*e.g.*,,. Collot and Fisher, 1991). The tectonic effects of impinging seamounts should occur as distinct events in contrast to ridges which are continuous features. Ridges may impose major adjustments only once, perhaps by erosion of a "tunnel" or "draping" of the forearc over the downgoing DR.

Rates and directions of plate convergence between the NH arc and Australian plate control interactions between the Australian plate and DR at the CNH. Our focus here is on the horizontal deformations taking place at the CNH, which we have measured using GPS. A comprehensive treatment of the vertical tectonic motions in the CNH associated with subduction of the DR system, as well as the broader implications of rapid forearc uplift and subsidence due to impinging bathymetric features, will be presented in Taylor et al. (in press).

4.3. Data

Initial crustal motion estimates reported by Taylor et al. (1995) were determined from a two year time series of GPS data collected during survey campaigns in 1990 and 1992. Crustal motions reported here were determined using a ten year time series that included the original 1992 campaign data, additional campaign GPS data collected since 1993, and continuous GPS data collected since 1996. In addition to a much longer time series, many more GPS sites were used for this analysis.

In 1996 we began installing a network of continuous GPS (CGPS) stations throughout the southwest Pacific. Two CGPS sites were installed in the New Hebrides arc: one near Port Vila on Efate (VILA) and one at southeast Santo (SANC). This regional CGPS network also included sites in New Caledonia (KOUC) and the Loyalty Islands (LPIL). All of these CGPS sites are equipped with Ashtech Z-XII dual-frequency GPS receivers and Dorne-Margolin choke-ring antennas. Additional CGPS data were obtained from sites operated by the International GPS Service (IGS), the Institut de Recherches pour le Developpement (IRD), and the Australian National University (ANU). CGPS sites used in this analysis are shown in Figure 2.3.

This CGPS network allowed us to collect data using the methods of the Multi-modal Occupation Strategy (MOST) for GPS surveys (Bevis et al., 1997) rather than mounting resource intensive and logistically difficult campaigns like the ones conducted in 1990 and 1992. As a result, all six campaign sites in the original NH network (EFAT, MAWO, MLKL, PNCT, SNTO, TANN) were re-occupied as "rover" sites between 1996 and 2001. Also in 1996, the University of Hawaii, the University of Texas and IRD established three additional sites on the southern coast of Santo (LISB, RATA, TASM). This rover network, consisting of the six original sites plus the three additional Santo sites, will be referred to as the "core" NH network.

Beginning in 1997, IRD established twenty-six additional rover sites throughout the NH (AMBR, ANIW, AOBA, BIGB, DILB, EMAE, FTNV, HOGB, HUNT, LMBU, LVMP, MALO, MGAL, MTTW, NAMU, NEPI, RNSR, SWBY, TGOA, TNMR, UTAN, VMVS, VOTL, WLRN, WUSI, YTUM). These additional rover sites, together with the NH core network, will be referred to as the "expanded" NH network.

Most roving GPS data were collected using Ashtech Z-XII receivers and Dorne-Margolin choke-ring antennas although Ashtech Micro-Z, Trimble SSE and SSI, and Leica 299 and 9500 receivers (all dual frequency) were used for some surveys. Whenever possible, Tech 2000 antennas masts were used although many surveys were conducted using standard survey tripods and tribrachs.

4.3.1. Data Analysis

Data were analyzed independently by this author and by co-authors at IRD and velocity solutions for two independently processed time series are presented here. We published the IRD solutions, which cover a longer time series and include a greater number of stations, in Calmant et al. (2003).

In determining our velocity solutions, we assumed that each site moved with a constant velocity. However, several significant earthquakes generated coseismic offsets that interrupted the time series of GPS sites throughout the network. Our solutions were adjusted for coseismic steps related to the following earthquakes: the Aneytum event (Mw = 6.9) of January 1994, the Malakula event (Mw = 7.3) of July 1994, the Walpole event (Mw = 7.5) of May 1995, the Ambrym event (Mw = 7.5) of November 1999, and the Santo event (Mw = 6.9) of October 2000. Preliminary results related to the sparsely surveyed Malakula and Walpole events were analyzed by Calmant et al. (1997) and Calmant et al. (2000), respectively. The 26 November 1999 Ambrym earthquake produced meter to centimeter level displacements at all sites in the CNH; Pelletier et al. (2000) reported field observations of ground motions related to this event.

4.3.2. Velocity Solutions for the Core Network, 1992 to 1999

Solutions for the period 1992-1999 were produced by this author using the methods described in Chapter 2. An Australian-fixed reference frame was generated by minimizing the motions of stations known to be situated on the Australian plate. Australian-fixed velocities are reported in Table 4.1. Velocities at sites located on the Australian plate are on the order of 0-1 mm/yr while site velocities in the NH arc vary significantly along the strike of the convergent boundary, from 126 mm/yr at Tanna (TANA) in the southern part of the arc to 34 mm/yr in the CNH (LISB) in the CNH.

4.3.3. Velocity Solutions for the Expanded Network, 1992 to 2001

Solutions for the period 1992-2001 were produced by coauthors at IRD using a different strategy and software package than described in Chapter 2. Details regarding the IRD analysis procedures and results are described in Calmant et al. (2003). Australian-fixed velocities for sites in the core NH network are provided in Table 4.1. Australian-fixed velocities for sites in the expanded NH network are provided in Table 4.2. Velocities at sites located on the Australian plate are on the order of 0-2 mm/yr (RMS discrepancy between ITRF 2000 reported and predicted values) while site velocities in the NH arc vary significantly along the strike of the convergent boundary, from 124 mm/yr at Tanna (TANA) to 27 mm/yr in the CNH (LVMP). Australia-fixed velocities for the NH expanded network throughout the arc for the period 1992-2001 are plotted in Figure 4.3. Australia-fixed velocities for the NH expanded network on Santo for the period 1992-2001 are plotted in Figure 4.4. WNFB-fixed velocities for the expanded NH network were also determined and presented in Calmant et al. (2003) but are not discussed here.

Table 4.1. New Hebrides GPS velocities in an Australian-fixed reference frame: a comparison of three independent solution sources from the core network.

Solution sources: FWT = Taylor et al. (1995); DAP = Phillips, unpublished; (CAL) = Calmant et al., (2003); (A/P) = predicted rate based on the Australia-Pacific Euler vector 61.04° S, 184.19° E, 1.078 deg/Myr, after Beavan et al, 2002; predicted rate is zero for all sites on the Australian plate. (*) indicates continuous GPS site. (**) indicates the GPS time series was interrupted by a coseismic offset; velocity solutions have been adjusted for coseismic steps.

Location	Site	Hor. Vel. (mm/yr)	Azimuth (deg)	Total Time Span	Solution Source
		Australian Plate (Fixed)			
Australia	HOB2*	2 ± 1	--	1994-1999	DAP
		0 ± 1	--	1994-2001	CAL
	TIDB*	1 ± 1	--	1996-1999	DAP
		2 ± 1	--	1996-2001	CAL
	TOW2*	2 ± 1	--	1995-1999	DAP
		1 ± 1	--	1995-2001	CAL
Loyalty Is.	LFOU	6 ± 6	--	1990-1992	FWT
		3 ± 1	--	1992-1999	DAP
		1 ± 1	--	1990-2001	CAL
	LPIL*	1 ± 1	--	1996-1999	DAP
		1 ± 1	--	1996-2001	CAL

Table 4.1 (Continued) NH GPS velocities in an Australian-fixed reference frame.

N. Caledonia	KOUC*	1 ± 1	--	1996-1999	DAP
		0 ± 1	--	1996-2001	CAL
	KOUM	3 ± 4	--	1990-1992	FWT
		1 ± 1	--	1992-1999	DAP
		1 ± 1	--	1992-2001	CAL
	TIND	10 ± 3	--	1990-1992	FWT
		2 ± 1	--	1992-1999	DAP
		3 ± 1	--	1990-1999	CAL
		Central New Hebrides Forearc			
Santo	SNTO	39 ± 4	115 ± 5	1990-1992	FWT
		42 ± 1	259 ± 1	1992-1999**	DAP
		88	258	--	A/P
	SANC*	39 ± 1	242 ± 1	1992-1999**	DAP
		38 ± 1	245 ± 1	1992-2001**	CAL
	RATA	39 ± 1	254 ± 2	1992-1999**	DAP
		39 ± 2	242 ± 4	1992-2001**	CAL
	TASM	34 ± 1	254 ± 1	1992-1999**	DAP
		35 ± 2	238 ± 3	1992-2001**	CAL
	LISB	34 ± 1	253 ± 1	1992-1999**	DAP
		31 ± 2	244 ± 4	1992-2001**	CAL

Table 4.1 (Continued) NH GPS velocities in an Australian-fixed reference frame.

Malakula	MLKL	41 ± 4	240 ± 5	1990-1992	FWT
		47 ± 1	239 ± 1	1992-1999**	DAP
		42 ± 2	248 ± 2	1992-2001**	CAL
		87	259	--	A/P
		Central New Hebrides Backarc			
Maewo	MAWO	41 ± 2	237 ±2	1990-1992	FWT
		60 ± 1	258 ± 1	1992-1999**	DAP
		57 ± 1	253 ± 1	1992-2001**	CAL
		88	259	--	A/P
Pentecost	PNCT	47 ± 4	260 ± 2	1990-1992	FWT
		58 ± 2	258 ± 1	1992-1999**	DAP
		55 ± 2	260 ± 1	1992-2001**	CAL
		88	259	--	A/P
		Southern New Hebrides			
Efate	EFAT	103 ± 5	248 ± 1	1990-1992	FWT
		97 ± 1	249 ± 1	1992-1999**	DAP
		94 ± 1	245 ± 1	1992-2001**	CAL
	VILA*	90 ± 1	246 ± 1	1992-1999**	DAP
		89 ± 1	246 ± 1	1992-2001**	CAL
Tanna	TANA	118 ± 10	247 ± 1	1990-1992	FWT
		126 ± 2	248 ± 1	1992-1999**	DAP
		124 ± 1	249 ± 1	1992-2001**	CAL
		82	259	--	A/P

Table 4.2. New Hebrides GPS velocities in an Australian-fixed reference frame: IRD solutions from the expanded network.

These solutions were determined at IRD and were published in Calmant et al (2003). (*) indicates continuous GPS site. (**) indicates the GPS time series was interrupted by a coseismic offset; velocity solutions have been adjusted for coseismic steps.

Island	Site	Hor. Vel. (mm/yr)	Azimuth (N°W)	No. of Occupations	GPS Time Series
		Northern Segment			
Torres	TORS	64.8 ± 4.8	254 ± 3	4	1997-1999
Banks	MOTA	76.3 ± 3.6	266 ± 2	5	1997-1999
		Central Segment			
Santo	BIGB	37.6 ± 4.4	248 ± 5	6	1997-2000**
	HOGB	42.5 ± 2.0	257 ± 3	10	1997-2001**
	WUSI	29.5 ± 1.3	253 ± 3	6	1997-2001**
	SANC*	37.7 ± 0.5	245 ± 1	CGPS	1996-2001**
	LISB	31.4 ± 1.9	244 ± 4	7	1996-2001**
	RATA	38.5 ± 2.2	242 ± 4	8	1996-2001**
	TASM	34.7 ± 1.5	238 ± 3	10	1996-2001**
Malo	MALO	34.6 ± 5.4	246 ± 7	5	1997-2001**
Aoba	AOBA	40.5 ± 3.4	260 ± 3	6	1997-2000**
Maewo	MAWO	57.2 ± 0.9	253 ± 1	7	1992-2000**
Pentecost	PNCT	55.1 ± 1.6	260 ± 1	7	1992-2000**
Malakula	TNMR	28.3 ± 2.5	249 ± 8	6	1997-2001**
	WLRN	29.1 ± 1.2	258 ± 4	11	1996-2001**
	RNSR	30.8 ± 3.6	256 ± 4	12	1998-2001**
	LVMP	26.6 ± 13.1	263 ± 1	5	1998-2001**
	LMBU	29.8 ± 4.1	257 ± 6	6	1997-2001**
	MLKL	41.8 ± 1.7	248 ± 2	12	1992-2001**

Table 4.2 (Continued) NH GPS velocities in an Australian-fixed reference frame.

	SWBY	28.4 ± 2.5	255 ± 4	9	1996-2000**
	VMVS	17.3 ± 8.8	227 ± 29	3	1999-2001
Ambrym	AMBR	32.4 ± 5.3	239 ± 7	9	1996-2001**
		Southern Segment - Sheppard Area			
Epi	NEPI	57.7 ± 12.2	232 ± 10	7	1997-2000**
	VOTL	71.2 ± 1.9	235 ± 2	5	1996-1999**
	NAMU	69.3 ± 7.3	230 ± 6	2	1999-2001
Tongoa	TGOA	77.8 ± 2.4	250 ± 3	5	1997-1999**
Emae	EMAE	77.5 ± 6.6	243 ± 4	4	1997-1999**
Nguna	UTAN	83.1 ± 1.2	245 ± 1	4	1997-2001
Efate	MGAL	85.5 ± 3.6	247 ± 1	4	1997-2001
	VILA*	89.3 ± 0.3	246 ± 1	CGPS	1996-2001
	EFAT	94.0 ± 1.0	245 ± 1	18	1990-2001**
		Southern Segment			
Erromango	DILB	117.7 ± 1.7	247 ± 1	4	1996-1999
Aniwa	ANIW	116.2 ± 3.3	246 ± 1	3	1997-1999
Tanna	TANA	123.8 ± 1.3	249 ± 1	19	1992-1999**
Aneytum	YTUM	118.0 ± 2.1	248 ± 1	4	1997-1999
		Southernmost Segment			
Matthew	MTTW	48.1 ± 2.4	197 ± 6	11	1992-2000**
Hunter	HUNT	42.3 ± 11.8	177 ± 30	4	1997-2000
		West North Fiji Basin			
Futuna-iti	FTNV	95.7 ± 1.1	259 ± 1	4	1996-1999

Figure 4.3. New Hebrides arc GPS velocities in an Australia-fixed reference frame.

Red arrows indicate GPS site velocities. White arrow near 18°S represents predicted NUVEL-1A convergence vector. These solutions were produced at IRD for the expanded NH network. HHR = Hazel Holme Ridge; A = Australian plate; NHT = New Hebrides Trench; WNFB = Western North Fiji Basin; NNH = Northern NH arc segment; CNH = Central NH arc segment; SNH = Southern NH arc segment; SMNH = Southernmost NH arc segment; DR = D'Entrecasteaux Ridge; TP – Torres Plateau; NBAT = North Back-Arc Trough; SBAT = South Back-Arc Troughs; WSR = West Spreading Ridge; NC = New Caledonia; LR = Loyalty Ridge.

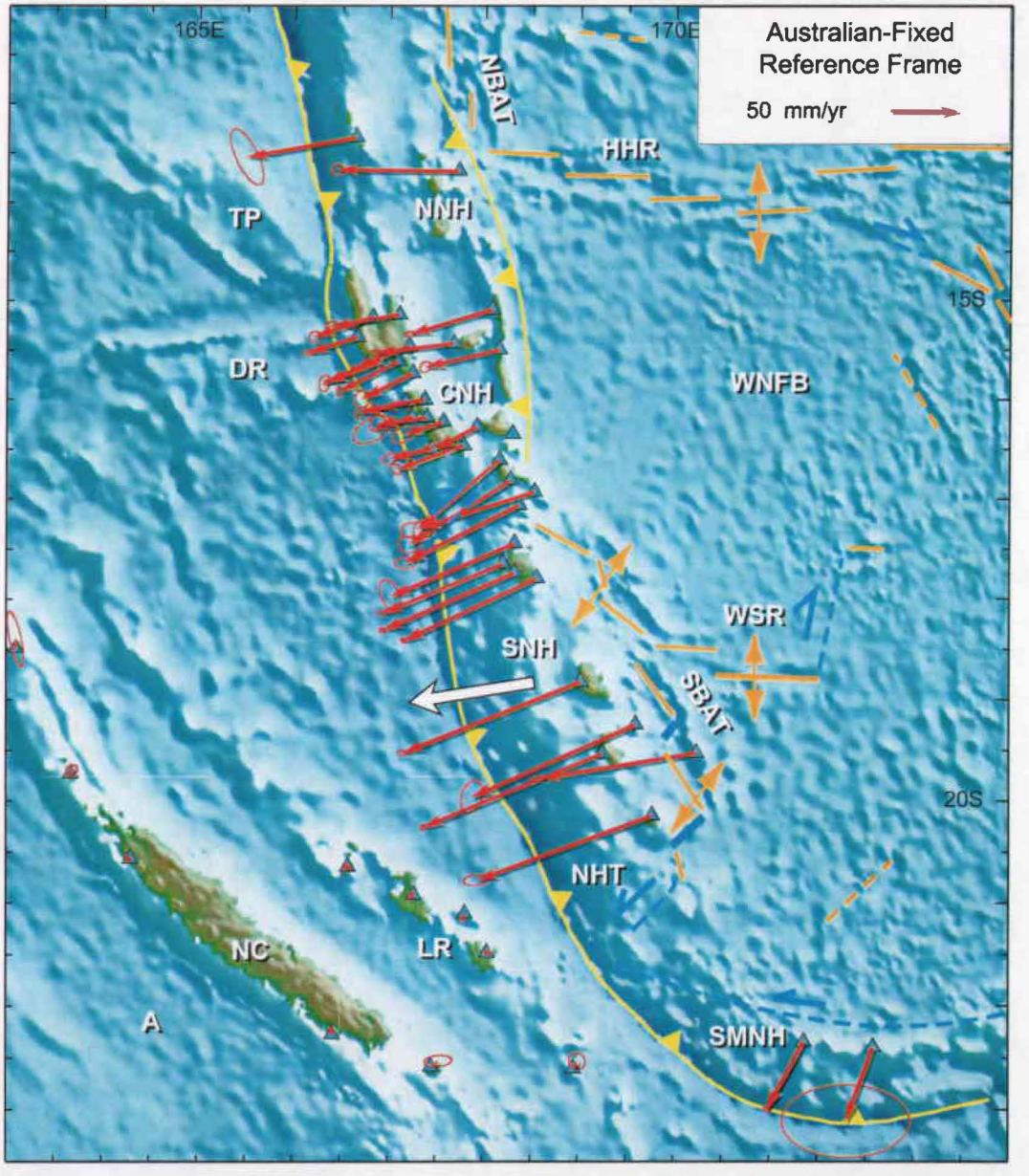
Australian-Fixed
Reference Frame
50 mm/yr
165E
170E
15S
20S
NBAT
HHR
TP
NNH
DR
CNH
WNFB
WSR
SNH
SBAT
NHT
NC
LR
A
SMNH

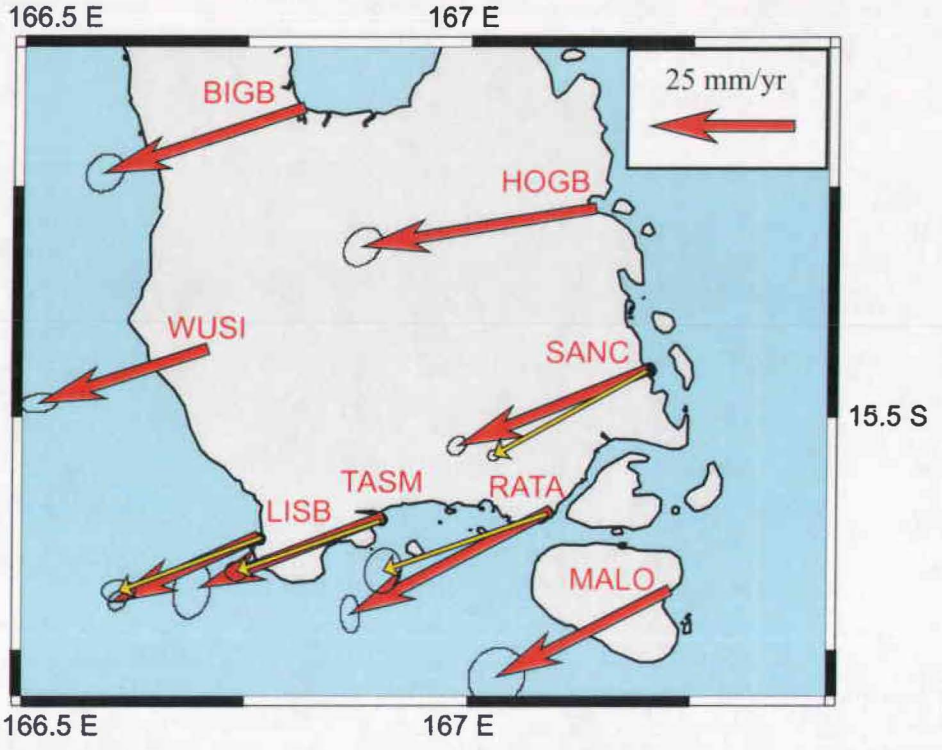

Figure 4.4. Santo GPS velocities in an Australian-fixed reference frame.

Red vectors are from IRD's expanded network solution for the period 1992-2001. Yellow vectors are from the core network solution for the period 1992-1999. Mean convergence on the western coast of Santo is ~30 mm/yr and increases to ~40 mm/yr along the eastern coast of Santo.

4.4. Discussion

While previous geodetic measurements of convergence in the NH arc successfully identified the basic present day tectonic behavior of this system, the much longer time series and greater number of GPS stations provided by the present analysis has led to new observations, considerable refinement of previous observations, and the development of more sophisticated and insightful models.

There is very good agreement among the velocity estimates determined independently by Taylor et al. (1995), this author, and coauthors at IRD. Where discrepancies of more than a few mm/yr do exist between the solutions sets at a given site, it is likely that part of the discrepancy may be due to effects from the many earthquakes that interrupted the NH GPS data time series. While our GPS solutions have been adjusted for coseismic offsets, it is still possible that a site's "long term" velocity may remain only loosely constrained by the available GPS data. Other factors that may contribute to discrepancies include issues related to reference frame generation and the different analysis strategies used. As a general rule, a longer GPS data time series will yield a more reliable solution. Accordingly, the remainder of this discussion focuses on the velocity solutions produced at IRD.

As expected, significant along strike variations in the rate and direction of convergence are observed throughout the NH arc. The highest rate of convergence,

124 mm/yr, is found at Tanna (TANA) in the southern NH while the lowest rate, 28 mm/yr, is found at Malakula (TNMR) in the CNH. Lower rates at sites VMVS (17.3 mm/yr) and LVMP (26.6 mm/yr), also on Malakula, are derived with large uncertainties and need further observations to be confirmed. Along the study area, vectors for predicted A/P convergence vary little. For example, using the A/P Euler vector of Beavan et al. (2002), predicted convergence at Tanna is 82 mm/yr oriented N259 ° while predicted convergence Malakula is 87 mm/yr oriented N259 °. Therefore observed convergence variations are not related to the position of the A/P pole but rather to local tectonic processes.

The most dramatic changes in convergence vectors occur where an aseismic ridge born by the Australian plate is subducting. First, at 15.7 ° S, subduction of the d'Entrecasteaux Ridge system is associated with reduced convergence at all the islands in the CNH. Second, at 22 ° S, the Loyalty ridge enters the trench and collides with the arc. North of this collision area, convergence rates are the highest observed along the arc: 118 mm/yr at Aneytum (YTUM) and 124 mm/yr at Tanna (TANA). South of this collision area, much lower rates are found: 48 mm/yr at Matthew (MTTW) and 42 mm/yr at Hunter (HUNT).

Another point highlighted by this data set is that convergence vectors are nearly always normal to the trench axis and parallel to the slip vector of major thrust-type earthquakes related to the subduction of the Australian plate all along the NH trench.

This is particularly noticeable at the southern virgation of the trench where GPS vectors trend N197° and N177° at Matthew (MTTW) and Hunter (HUNT), respectively, while trending N248° and N249°at Aneytum (YTUM) and Tanna (TANA), respectively.

Based on observed convergence variations, the NH arc can be split into four distinct provinces identified geographically: northern, central, southern, and southernmost. The following sections provide a summary of observations from each of the NH arc segments with a detailed look at the phenomenology of the CNH. It should be noted that discussion of arc kinematics is described more fully in Calmant et al. (2003) while a thorough treatment of the horizontal and vertical deformation of the CNH, including the long term effects of impinging bathymetric features, will be presented in Taylor et al. (in press).

4.4.1. The Northern NH Segment

The northern segment includes the Torres and Banks island groups. Relative to the Australian plate, observed convergence rates in the northern segment are higher than in the CNH but still lower than the predicted A/P value of 91 mm/yr oriented N259° based on the A/P Euler vector of Beavan et al. (2002). The site in the Torres Islands (TORS), the northernmost site in this dataset, shows a convergence rate of 65 mm/yr oriented N254°.relative to the Australian plate. The Banks Islands are active volcanic

edifices associated with subduction along the arc and lie about 100 km east of the NH trench. Mota lies directly south of the junction between the Hazel Holme ridge and the NH platform. The observed convergence rate at Mota island (MOTA), an abandoned volcanic edifice on the eastern side of the Banks Islands, is 76 mm/yr oriented N266°.

4.4.2. The Central NH Segment

In the central segment (CNH), convergence rates are much lower than the predicted A/P vector of 88 mm/yr oriented N259° (Beavan et al., 2002). Observed convergence in the CNH forearc is ~30 mm/yr along the western coasts of Santo and Malakula (e.g., LISB and WLNR) and increases slightly to ~40 mm/yr along the eastern coasts of these islands (e.g., SANC and MLKL). Convergence in the CNH backarc, relative to the Australian plate, is ~56 mm/yr based on measurements at Maewo (MAWO) and Pentecost (PNCT). The observed convergence deficit in the CNH is due to impingement of the d'Entrecasteaux Ridge (DR) system and associated Bougainville Guyot (BG).

The horizontal force applied to the arc by the BG, combined with that of the subducting DR, TP, and their outliers, is so great that a ~250 km-long section of the arc is being displaced eastward. Exactly when eastward motion of the CNH began is not known, but uplift of the backarc islands of Maewo and Pentecost is due to motion

on reverse faults accommodating eastward CNH motion (Collot et al., 1985; Taylor et al., 1995; Pelletier et al., 2000). We find uplifted Holocene reefs on these islands, but not a sequence of Holocene–130 Ka reefs. If the 40–60 mm/yr backthrusting rate had begun by 100 Ka, then there would be 4–6 km of eastward displacement of the CNH. There is no discernible bulge in the back-arc margin and no other convincing evidence of more than slight total displacement. The existing evidence suggests that uplift of the back arc began only in Holocene or latest Pleistocene time. As the BG contact with the arc increased, the proportion of convergence accommodated by eastward backthrusting increased at the expense of underthrusting of the DR. Given the present approximately equal amounts of forearc and back arc convergence, we infer that backthrusting is resisted about as much as subduction. Elastic modeling of the CNH interplate thrust zone is discussed in section XX.

4.4.3. The Southern NH Segment - Sheppard Area to Efate

In the southern segment, which extends from Epi to Aneytum, convergence rates increases southward, equaling then exceeding predicted A/P motion with observed values ranging from ~60 mm/yr at North Epi to ~120 mm/yr at Tanna and Aneytum. The Sheppard area of the southern segment represents a transition zone between the central and southern arc segments. In an Australian-fixed reference frame, GPS velocities in the Sheppard area range from 58 mm/yr at Epi (NEPI) to 94 mm/yr at

Efate (EFAT). The predicted convergence rate for the Sheppard area, based on the A/P Euler vector of Beavan et al. (2002), is 85 mm/yr oriented N259°.

Analysis of GPS velocities in a West North Fiji basin-fixed reference frame and earthquake focal mechanisms, as presented in Calmant et al. (2003), indicates that dextral shear between the central and southern NH arc segments is accommodated within the Sheppard area. Strike-slip type focal mechanism solutions in this region show slip orientations trending from N050° to N090°. The pole-predicted right-lateral strike-slip motion is 51 ± 3 mm/yr oriented N060° ± 5°. This pole-derived orientation and the orientation of earthquake slip vectors are consistent with the strike of a series of submarine canyons revealed in bathymetry data, especially those collected southwest of Epi during the CALVA cruise aboard the N/O l'Atalante (Eissen et al., 1997). These canyons, running N050°, are interpreted as the surface expression of strike-slip faults across the NH platform that currently accommodate or formerly accommodated the shear between the central and southern segments. Moreover, the progressive clockwise rotation of the GPS vectors corresponds to changes in the structural direction of the Efate Trough, which trends NNW-SSE but is prolonged in the north by NW-SE and then WNW-ESE trending scarps where it abuts in the Sheppard Island area. Convergence at the southern tip of the Backarc Thrust Belt, extension at the northern tip of back arc troughs running east of Efate, and the aforementioned dextral strike-slip motion might join in a kind of triple junction around on 17°S, 168.5°E. It is worth noting that the Kuwae submarine volcano lying

at this connection area produced one of the largest historical eruptions in 1420–1430 A.D. (Monzier et al., 1994).

4.4.4. The Southern NH Segment - Erromango to Aneytum

South of Efate, the southern NH segment is characterized by having the highest rates of convergence observed in the NH arc at ~120 mm/yr relative to the Australian plate. This high convergence was recognized previously at Tanna (Taylor et al., 1995; Calmant et al., 1995, 2000). It is regionally confirmed in this extended data set, where values exceeding the A/P vectors by 30–35 mm/yr southwestward are found for all these islands. The predicted convergence rate for this region, based on the A/P Euler vector of Beavan et al. (2002), is 82 mm/yr oriented N259 °. The observed velocity at Futuna-Iti (FTNV), at 95 mm/yr oriented N259°, is not consistent with other velocities in the southern segment and we consider it to be situated in the West North Fiji Basin rather than in the NH arc.

Pelletier et al. (1998) showed that the difference between actual convergence and A/P implies that some extension should occur in the troughs at the rear of the southern NH arc. The Erromango-Futuna Trough is the southern part of this series of troughs that border the NH platform on the east (Figure XX). Based on kinematic analyses and marine geophysical data, as detailed in Calmant et al (2003), it is likely that

backarc extension in this region is driven by rotation of this arc segment rather than being related to some general process of back arc expansion.

4.4.5. The Southernmost NH Segment

For the first time, GPS measurements were made in the southernmost NH segment at sites on Matthew (MTTW) and Hunter (HUNT) islands However, the GPS-derived convergence vectors established at the southern termination of the NH trench are derived with large uncertainties due to a combination of short observations, the use of poorly calibrated Leica GPS antennas, and the occurrence of the Walpole earthquake in May 1995. Relative to the Australian plate, they notably differ in both modulus and orientation from A/P vectors that predict mostly strike-slip motion along this portion of the trench which runs almost parallel to the A/P relative motion. Louat and Pelletier (1989) inferred from the seismicity occurring in this area that some residual N-S convergence might occur between the North and South Fiji Basins. The change in azimuth in the slip vectors, which turn along the strike of the trench and remain normal to the trench, was also invoked in that study to propose that no strike-slip motion is accommodated at the plate boundary and that some kind of transform fault within the overriding plate should accommodate the differential motion between the Tanna and Matthew blocks. Convergence rates of 42 mm/yr at HUNT and 48 mm/yr at MTTW, suggest that convergence between the North and South Fiji Basins is in fact ongoing. Indeed, the GPS convergence vector is even larger than the projection

of the A/P vector in this direction. This platelet is not being accreted to the Australian plate.

4.4.6. Elastic Modeling of the Interplate Thrust Zone at the CNH

In previous studies the CNH subduction zone was modeled assuming the full Australia-Pacific convergence rate of about 100 mm/yr and with a conventional locked interplate thrust zone at depths of 15 to 45 km that intermittently ruptured (Taylor et al., 1980; 1987; 1995). The amount of interplate slip accounted for by historical large thrust events was much less than the convergence rate, so that a significant proportion of aseismic slip was invoked (Taylor et al., 1987; 1990). Our new GPS measurements have shown that the convergence rate is much less than the 100 mm/yr assumed previously so that little if any aseismic slip is required. Our understanding that DR and TP subduction with the added impingement of the BG causes great resistance to underthrusting has led us to propose that the uppermost part of the interplate thrust zone is *permanently* locked. This requires a quite different modeling approach than we used previously.

Historical earthquakes show that the main thrust zone at 15-50 km depth intermittently ruptures and slips on the order of several meters per event. This "stick-slip" behavior of the plate interface leads to a cycle of sustained interseismic strain accumulation in the upper plate and occasional, catastrophic release of elastic strain

energy during the coseismic phase of the earthquake deformation cycle. But for vertical deformation to accumulate over thousands of years, producing long term and significant changes in topography, there must be some (nonelastic) deformation in the upper plate that is not recovered on the interseismic time scale. We propose that this occurs when the upper part of the plate interface (perhaps 0 – 15 km) is locked permanently (or at least for many thousands of years) in response to the 'collision' of inbound topography with the plate boundary. We suggest that further down the plate interface, immediately below this permanently locked zone, is a zone (perhaps 15 – 50 km) that sticks and slips in more conventional fashion. That is, the anomalous segment of the plate boundary associated with impinging topographic features consists of both "stick-stick" and "stick-slip" zones. It is the permanently locked (or stick-stick) zone that leads to the rapid growth of topography in the upper plate, since plastic failure of the upper plate is the mechanism that accommodates plate convergence when part of the plate interface is never allowed to slip.

It may seem strange that we model the deformation associated with the permanently locked zone (PLZ) using an elastic formalism. However, we propose that as plate convergence proceeds, secular straining of the upper plate is essentially an elastic process, but as the PLZ never breaks and the stresses in the upper plate inevitably exceed the yield stress, the failure of this plate occurs by sequences of small earthquakes on many faults located in various parts of the upper plate. That is, the non-elastic deformation of the upper plate is achieved through seismic flow driven by

stresses that accumulate through elastic compression of the upper plate. Accordingly, we postulate that the largest seismic deformations occur in that part of the plate where plate convergence in the presence of a PLZ causes the highest rate of elastic straining. We use secular rate of elastic deformation associated with the PLZ as a proxy for the long-term deformation associated with the growth of topography.

We base our new model on the well-known backslip formalism of Savage (1983). This model assumes that for a typical subduction zone undergoing stick-slip behavior, elastic strain accumulation in the upper plate during the interseismic phase of the earthquake cycle will be very similar to that associated with a dislocation coincident with the locked portion of the plate interface but with the opposite sense of shearing. In effect this back slip represents the perturbation associated with locking of the plate boundary in that it exactly cancels the slip that would occur if the plate boundary freely slipped. We modify this approach by dividing the locked zone into a permanently locked zone (PLZ) and a temporarily locked zone (TLZ), and keeping track of their separate contributions to the displacement of the leading edge of the upper plate. The net deformation is assumed to represent the interseismic displacement field. When the PLZ ruptures the straining it produced would be recovered, so only the surface velocity field associated with backslip on the PLZ is used to estimate the growth of topography. (Again we assume that the straining associated with this displacement is eventually released by small earthquakes on

faults that pervade the upper plate, and this ensures the uplifts associated with locking of the PLZ are not eventually recovered).

We defined the interplate thrust zone profile based on the relocated hypocenters of large interplate thrust events in the CNH (Pascal et al., 1978; Ebel, 1980; Chinn and Isacks, 1983) (Fig. 4.5-A). GPS sites in the CNH are projected onto a profile trending N70° E through southern Santo (Fig. 4.5-B and -C), perpendicular to the arc trend. Epicenters of aftershocks of the August 1965 central New Hebrides interplate thrust sequence indicate that the zone from 15 to 50 km ruptured (e.g., Isacks et al., 1981), consistent with the analysis of maximum depth of New Hebrides rupture zones of Pacheco et al. (1993). We assume a convergence rate of the Australian plate of 70 mm/yr, which requires that approximately 30 - 50 mm/yr of convergence is accommodated by back-arc thrusting (Pelletier et al., 1998; 2001).

We implemented the backslip model of Savage (1983) using the formulas derived by Singh and Rani (1993) for a 2-D elastic deformation (one which is infinitely long in the strike direction). We applied a simpler version of this methodology with stick-slip at 15-50 km and an uncoupled zone at 0-15 km depth in our previous analysis of GPS data for the CNH (Taylor et al., 1995). We have adapted the original code that assumes a planar fault to simulate a more realistic curve of the downgoing Australian plate - New Hebrides arc interface by dividing the fault into many small increments and adding them together. We have held the shallow end of the fault from the

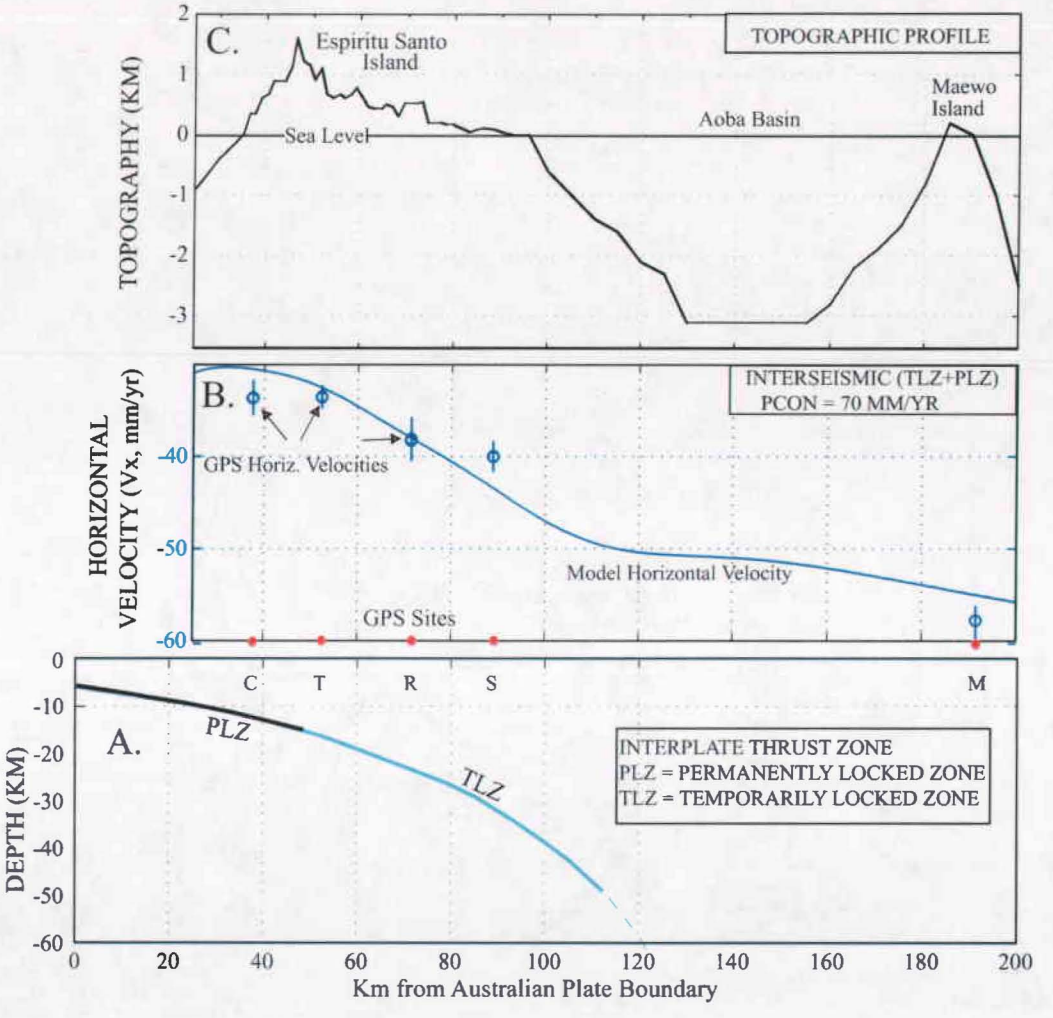

Figure 4.5. Elastic model of the interplate thrust zone at the central New Hebrides

seafloor to 15 km depth locked through interseismic and coseismic cycles on the deeper stick-slip zone (Fig. 4.5-A).

When the elastic model runs, horizontal and vertical elastic strain accumulates in a pattern dictated by an interplate thrust zone that is continuously locked from the sea floor at the plate boundary to a depth of 50 km (Fig. 4.5-A). Interseismic strain produces eastward horizontal motion and subsidence of all of Santo and Malakula (Fig. 4.5-B). Horizontal strain rates are consistent with measured GPS rates at the four GPS core stations from the western to eastern coasts of Santo (LISB, TASM, RATA, SNTO, MAWO). Further details regarding horizontal and vertical tectonic models for the CNH will be presented in Taylor et al. (in press).

4.5. Conclusions

We have produced new and refined estimates of crustal motion in the New Hebrides arc using more than a decade of GPS measurements. In addition to this long time series, much more detailed spatial estimates have resulted from a greatly expanded and densified network of GPS sites. We have confirmed and refined earlier observations of along-strike variations in convergence of the Australian plate at the New Hebrides trench and four distinct segments have been identified. The existence and characteristics of these arc segments is directly related to the impingement of large bathymetric features on the downgoing plate. In particular, convergence at the

CNH is partitioned between the forearc (Australian plate) and the backarc (North Fiji basin) as subduction of the d'Entrecasteaux Ridge system produces strong, shallow interplate coupling at the NHT and displaces the CNH block eastward into the North Fiji Basin. This process was simulated by an elastic model in which interplate slip ceases for an extended period of time on the shallow end of the interplate thrust zone. Clearly, the impingement of large bathymetric features is of fundamental importance to the present, past and future tectonic development of the NH arc.

4.6. Acknowledgements

Velocity solutions and many of the interpretations presented here were published in: Calmant, S., B. Pelletier, P. Lebellegard, M.G. Bevis, F.W. Taylor, D.A. Phillips, New insights on the tectonics along the New Hebrides subduction zone based on GPS results, Journal of Geophysical Research, Vol. 108, No. B6, 2319-2340, 2003. Material in this chapter regarding observations and modeling of vertical tectonics of the New Hebrides will be published in: Taylor, F.W., M.G. Bevis, R. L. Edwards, H. Cheng, S. Gray, G.S. Burr, J.W. Beck, K.B. Cutler, D.A. Phillips, G. Cabioch, P. Mann, Alternating rapid forearc subsidence and uplift caused by impinging bathymetric features: examples from the New Hebrides and Solomon arcs (in prep).

Much of the GPS data used for these analyses were collected by J-M Bore, J-L Laurent, M. Kalsale Williams, J-C Willy, Douglas Charley, and Charles Pakoa. Mr.

Pakoa passed away in early 2003 but his support and kindness will always be remembered. Data analysis at the University of Hawaii was facilitated by Eric Kendrick and James Foster of the Pacific GPS Facility. Finally, we express our gratitude to the citizens of Vanuatu for all their hospitality and assistance.

Chapter 5. Geodetic Measurements of Crustal Motion in the New Georgia Group, Solomon Islands

David A. Phillips (SOEST, University of Hawaii at Manoa)

Frederick W. Taylor (Institute for Geophysics, University of Texas at Austin)

Allison K. Papabatu, Stanley Basi (Ministry of Natural Resources, Solomon Islands)

Michael G. Bevis (The Ohio State University)

5.1. Abstract

Using a four-year GPS time series, we observe crustal motions in the New Georgia Group of the Solomon Islands relative to the Australian and Pacific plates. We find 57-84 mm/yr of Australia-Solomon motion and 19-39 mm/yr of Pacific-Solomon motion. Most of this motion is related to subduction of the Australian plate at the San Cristobal trench (SCT) but our GPS velocities are 20-40% lower than the predicted Australia-Pacific convergence rate. 2-D dislocation models suggest that most of this discrepancy can be attributed to locking of the SCT and elastic strain accumulation in the forearc. It is likely that differential motion between the Solomon arc and the Pacific plate contributes to this difference as well. We also find that Simbo island, thought to be on the Australian plate, is converging with the Australian plate almost as fast as the other GPS sites in the New Georgia Group.

5.2. Introduction

The Solomon Islands are situated in the southwest Pacific and are part of the Greater Melanesian Arc System, along which the Pacific, Australian and Solomon Sea plates collide (Figure 5.1). The Australian and Solomon Sea (SS) plates, separated by the Woodlark Basin spreading center, subduct at the San Cristobal trench (SCT) while the Pacific plate subducts at the North Solomon trench (NST). Late Miocene collision of the Ontong Java Plateau (OJP) at the NST resulted in arc polarity reversal so that currently most Australia-Pacific convergence is accommodated at the SCT. However, because the sectors of the Australian and SS plates approaching the SCT also resist subduction, a small but imprecisely determined proportion of convergence still occurs at the NST (e.g., Phinney et al, 1999).

This area is particularly interesting because it is one of the few places in the world where extremely young lithosphere is currently subducting. The Woodlark Basin undergoes seafloor spreading at ~70 mm/yr (full rate) just offshore of the SCT (ref). This extremely young, hot, buoyant lithosphere underlies a topographically rugged and shallow seafloor that interacts with the Solomon arc lithosphere as it subducts at mean rates of ~100 mm/yr (Beavan et al., 2002).

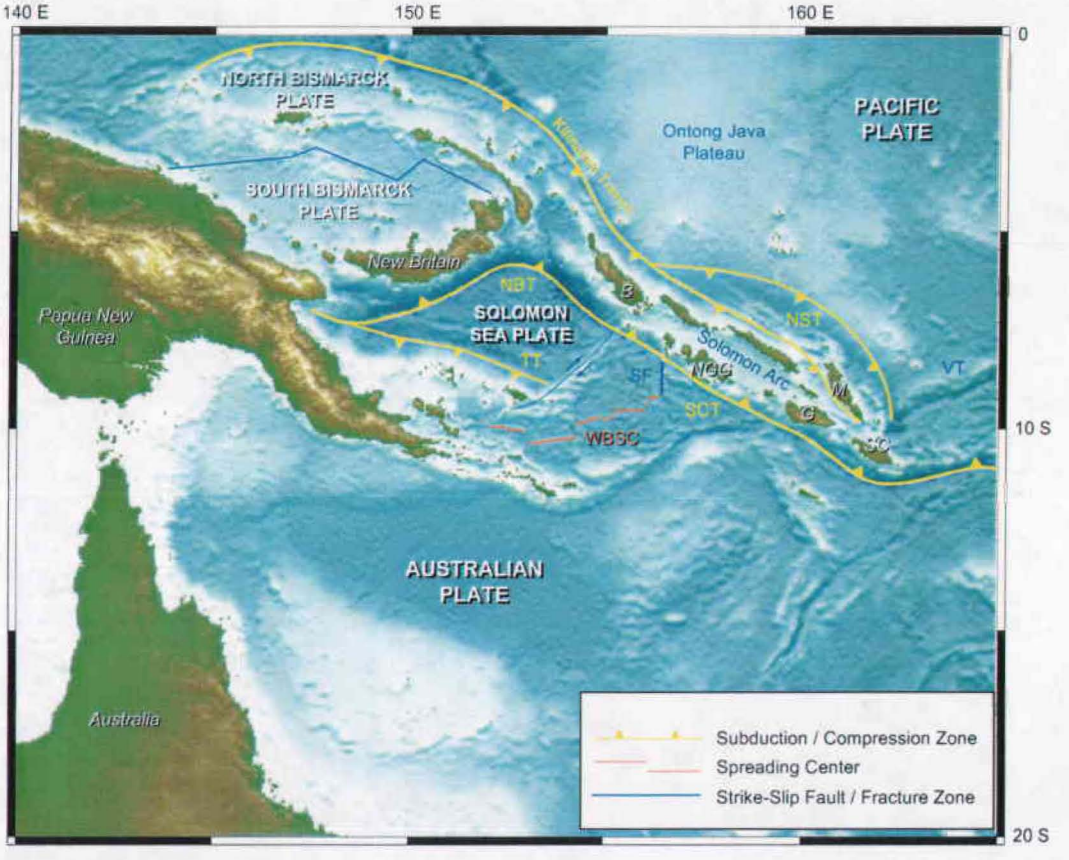

Figure 5.1. Solomon Islands location map and regional tectonic setting

The islands of the New Georgia Group (NGG) are primarily dormant or extinct stratovolcanoes related to subduction of the Pacific plate but which are now involved in forearc tectonics associated with subduction of the Australian plate (Figure 5.2). The southernmost islands of the NGG undergo rapid uplift that may be associated with subduction of topographically prominent features on the downgoing plate. Present day uplift of southern Rendova and Tetepare islands, at rates as high as 8 mm/yr, is likely due to impingement of the Coleman seamount or other bathymetrically prominent features near the eastern end of the Ghizo Ridge (Mann et al, 1998). Similarly, Ranonnga island undergoes uplift at rates as high as 5 mm/yr due to subduction of the Simbo Ridge, a high-standing fracture zone that forms the boundary between the Australian and SS plates.

Interplate coupling at the SCT has been characterized as aseismic based on the near absence of shallow interplate seismicity in the immediate vicinity and the interpretation that the downgoing plate is so young and warm that the interplate thrust zone would not support elastic strain and subsequent rupture (Cooper and Taylor, 1985). However, rapid deformation of the New Georgia forearc suggests the possibility of strong interplate coupling that may allow elastic strain accumulation in this region. As subduction at the NST is opposed by the 35-km thick OJP, the result is that the western Solomon arc is being compressed between two major plates, both of which strongly resist underthrusting.

Figure 5.2. Perspective view of the New Georgia Group.

The Australian plate and Woodlark Basin crust subduct at the San Cristobal Trench. The Simbo ridge, Ghizo ridge, Kana Keoki seamount and Coleman seamount resist subduction. View from the southeast.

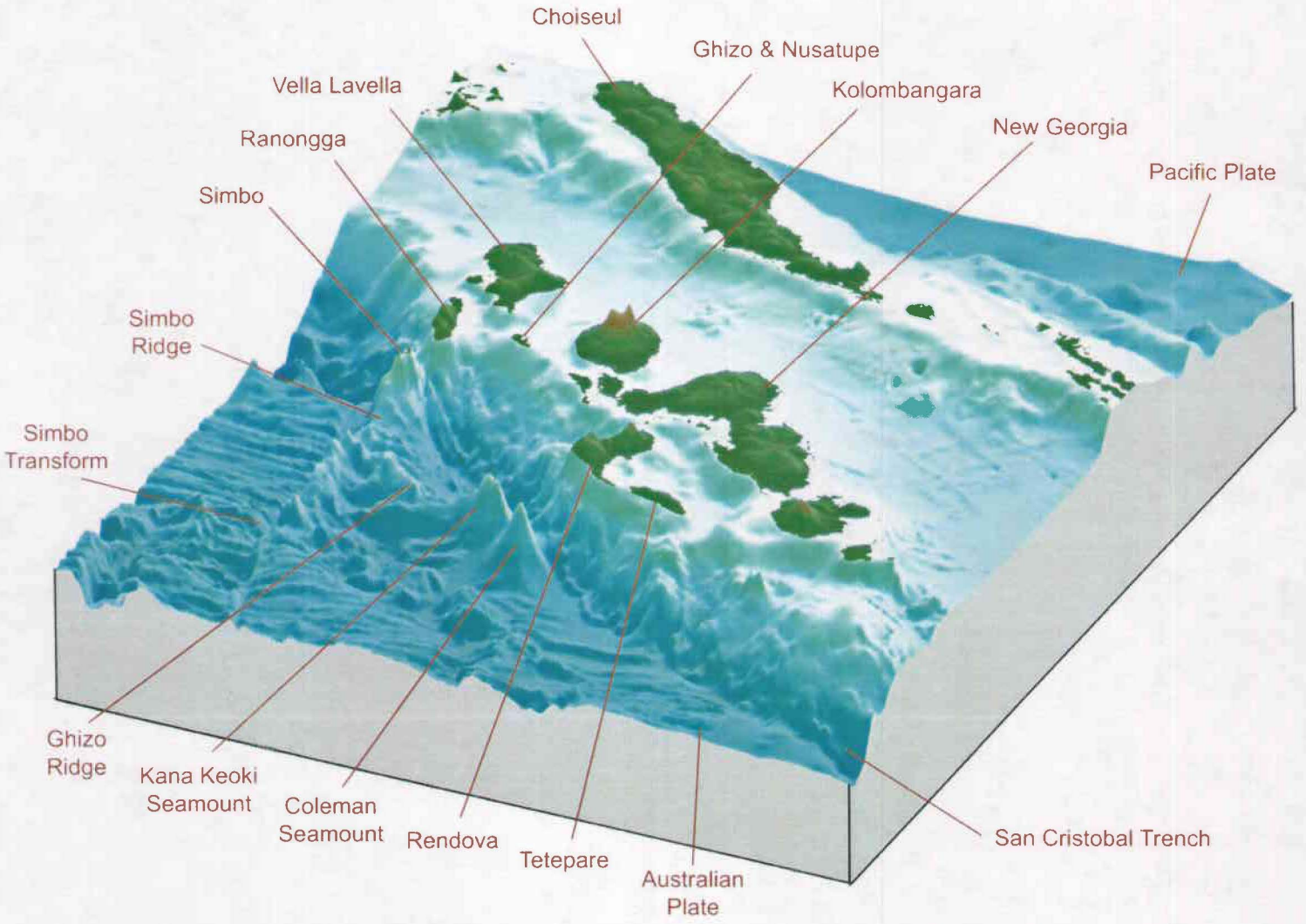
Choiseul
Ghizo & Nusatupe
Vella Lavella
Kolombangara
Ranongga
New Georgia
Simbo
Pacific Plate
Simbo
Ridge
Simbo
Transform
Ghizo
Ridge
Kana Keoki
Seamount
Coleman
Seamount
Rendova
Tetepare
Australian
Plate
San Cristobal Trench

5.3. Data

Crustal motions were determined from a four-year GPS time series. Our Solomon Islands network consists of nine sites: one continuous GPS (CGPS) site and seven campaign or "rover" sites in the New Georgia Group, and one quasi-continuous GPS site on Guadalcanal (Figure 5.3). This network was designed and occupied in accordance with the techniques outlined by the Multimodal Occupation Strategy for GPS surveys (Bevis et al, 1997). All data were collected using Ashtech Z-XII dual-frequency GPS receivers and Dorne-Margolin choke ring antennas.

A CGPS site (GCLC) was installed at Gold Ridge on Guadalcanal in November, 1997. Unfortunately, this site was vandalized soon after conclusion of the 1997 campaign and continued security issues prevented its restoration. GCLC was re-occupied as a rover site using the original monument in March, 1999, but a reoccupation in 2001 was not possible due to a civil war on Guadalcanal. A new CGPS site (NUSA) was established at Nusatupe island in the NGG in March, 1999, and this site has operated continuously since its installation.

Five rover GPS sites (GIZO, MUND, RAVA, SIMB, VELA) were established in the NGG in November, 1997, and were reoccupied in March 1999 and November 2001. Two additional rover sites (HUSU and KONG) were established during the 2001 campaign but additional occupations are required before velocities can be obtained

for these sites. Each rover site was occupied for at least 40 hours during each campaign. All rover occupations were performed using Tech 2000 antenna masts instead of standard survey tripods as the Tech 2000 provides greater stability and a fixed antenna height, which simplifies post-processing.

Additional data were obtained from a regional CGPS reference network comprised of fourteen sites operated by the University of Hawaii, the International GPS Service (IGS), the Institut de Recherches pour le Developpement (IRD) and the Australian National University (ANU).

5.3.1. Data Analysis

GPS data were analyzed using GAMIT, GLOBK, VSTACK and RTVEL software packages (King and Bock, 2002; Herring, 2002; Kendrick et al., 2001) using the methods described in Chapter 2. The resulting velocity field was used to establish geodetic reference frames corresponding to the Australian and Pacific plates. Motion of the Solomons network relative to both reference frames was observed.

5.3.2. Australian-fixed Reference Frame

An Australian-fixed reference frame was generated by minimizing motions at stations known to be situated on the Australian plate. Australian-fixed velocities are reported

in Table 5.1. Velocities at sites located on the Australian plate are on the order of 0-1 mm/yr. Velocities at sites located on the Pacific plate range from 35-121 mm/yr, increasing with distance from the Australia-Pacific Euler pole (61.04° S, 184.19° E, after Beavan et al, 2002). Also reported in Table 5.1 are predicted site velocities based on this Australia-Pacific Euler vector. Predicted velocities compare very well with observed velocities at all sites on the Pacific plate. Site velocities in the Solomon Islands range from 57 to 84 mm/yr. In comparison, predicted velocities for all Solomons sites except SIMB are on the order of 100 mm/yr. Australia-Solomon velocities are plotted in Figure 5.3.

5.3.3. Pacific-fixed Reference Frame

A Pacific-fixed reference frame was generated by minimizing motions at stations known to be situated on the Pacific plate. Site velocities in this Pacific-fixed frame are reported in Table 5.2. Velocities at sites located on the Pacific plate are on the order of 0-2 mm/yr. Velocities at sites located on the Australian plate range from 50-93 mm/yr, increasing with distance from the Australia-Pacific Euler pole (61.04° S, 184.19° E, after Beavan et al, 2002). Also reported in Table 5.2 are predicted site velocities based on this Australia-Pacific Euler vector. Predicted velocities compare very well with observed velocities at all sites on the Australian plate. Site velocities in the Solomon

Table 5.1. Solomon Islands GPS velocities in an Australia-fixed reference frame.

Predicted site velocities are based on the Australia-Pacific Euler vector 61.04° S, 184.19° E, 1.078 deg/Myr, after Beavan et al, 2002.

Location	Site	GPS-Derived Hor. Vel. (mm/yr)	GPS-Derived Azimuth (degrees)	Predicted Hor. Vel. (mm/yr)	Predicted Azimuth (degrees)
		Australian Plate Sites			
New Zealand	AUCK	1.4 ± 0.0	-102.3° ± 1.9°	0	--
Tasmania	HOB2	0.9 ± 0.1	24.7° ± 4.1°	0	--
N. Caledonia	KOUC	0.7 ± 0.0	-120.6°± 3.0°	0	--
Loyalty Is.	LPIL	1.1 ± 0.0	-111.1° ± 1.8°	0	--
N. Caledonia	NOUM	0.4 ± 0.1	-102.9° ± 8.4°	0	--
Australia	TIDB	0.6 ± 0.1	31.5° ± 5.6°	0	--
Australia	TOW2	1.3 ± 0.1	123.3° ± 2.6°	0	--
		Solomon Islands Sites			
Guadalcanal	GCLC	69.6 ± 1.6	-103.4° ± 0.8°	97.7	-104.0
Nusatupe	GIZO	80.2 ± 1.0	-108.0° ± 0.6°	100.3	-105.4
Munda	MUND	79.7 ± 1.0	-104.8° ± 0.4°	100.0	-105.3
Nusatupe	NUSA	82.3 ± 0.2	-106.7° ± 0.1°	100.3	-105.4
Rendova	RAVA	62.6 ± 1.3	-101.5° ± 1.0°	99.5	-105.3
Simbo	SIMB	56.8 ± 0.8	-100.7° ± 0.6°	100.3	-105.6
Vella Lavella	VELA	83.6 ± 1.1	-104.8° ± 0.4°	100.6	-105.5
		Pacific Plate Sites			
Chatham I.	CHAT	34.5 ± 0.0	-88.9° ± 0.1°	35.6	-91.2
Samoa	FALE	89.8 ± 0.1	-87.9° ± 0.0°	88.3	-87.5
Hawaii	KOKB	121.3 ± 0.1	-83.6° ± 0.0°	119.3	-82.2
Marshall Is.	KWJ1	113.4 ± 0.1	-98.8° ± 0.0°	113.4	-98.3
Hawaii	MKEA	121.5 ± 0.1	-81.3° ± 0.0°	119.0	-80.2
Niue	NIUC	81.6 ± 0.1	-85.6° ± 0.0°	80.7	-85.8
Tahiti	THTI	90.5 ± 0.2	-73.2° ± 0.1°	88.3	-73.1

Figure 5.3. New Georgia Group GPS velocities in an Australian-fixed reference frame.

Red arrows show GPS velocities. Gold arrows show predicted Pacific-Australian convergence (Beavan et al., 2002). All points on the Australian plate should have a null velocity in this reference frame yet clearly this is not the case for Simbo island. High resolution bathymetry and tectonic interpretations courtesy of A.M. Goodliffe and B. Taylor.

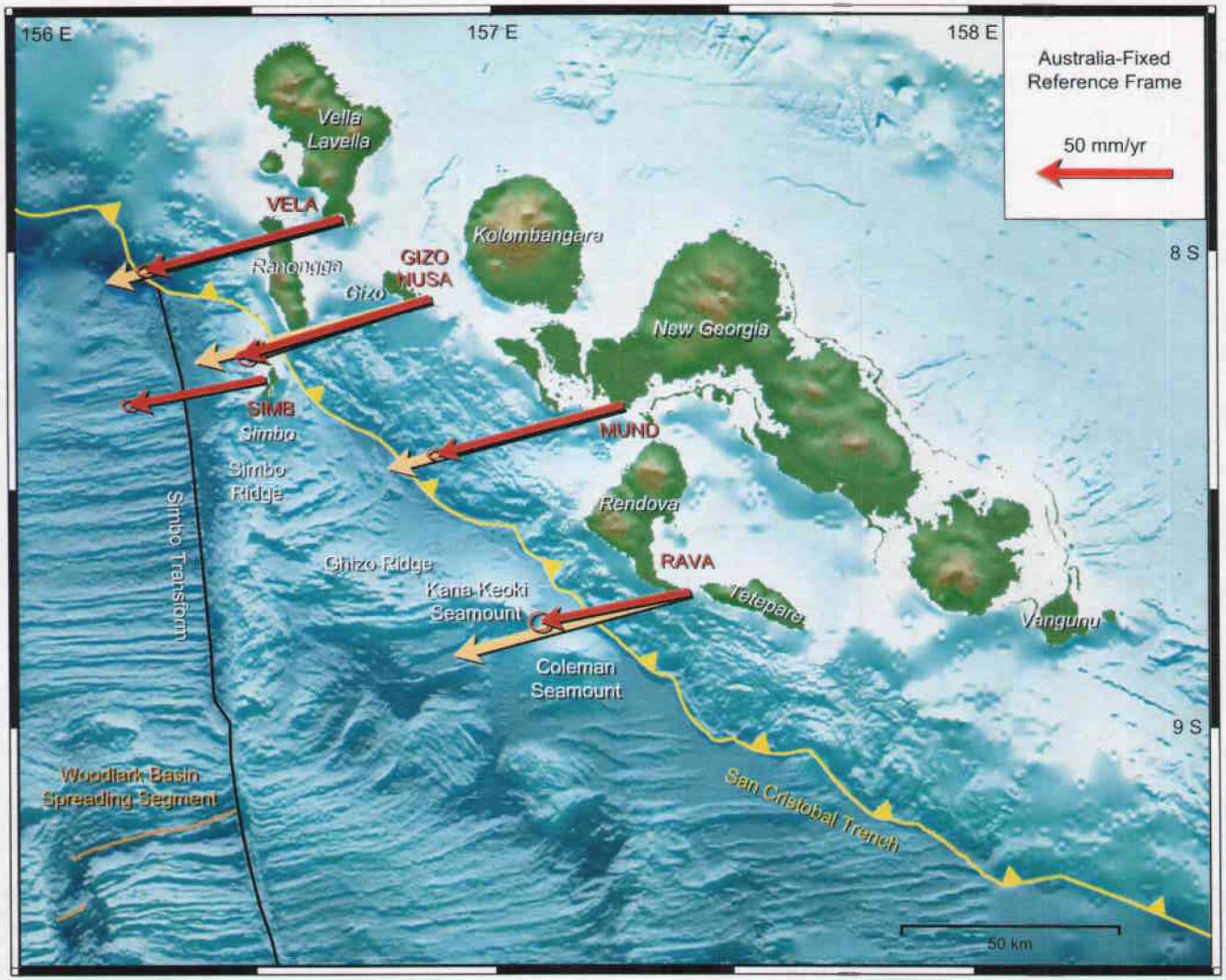
156 E
157 E
158 E
Australia-Fixed
Reference Frame
50 mm/yr
8 S
9 S
Vella
Lavella
VELA
Kolombangara
Ranongga
GIZO
NUSA
Gizo
New Georgia
SIMB
Simbo
Simbo
Ridge
MUND
Rendova
Simbo Transform
Gizo Ridge
RAVA
Kana Keoki
Seamount
Tetepare
Vangunu
Coleman
Seamount
Woodlark Basin
Spreading Segment
San Cristobal Trench
50 km

Table 5.2. Solomon Islands GPS velocities in a Pacific-fixed reference frame.

Predicted site velocities are based on the Australia-Pacific Euler vector 61.04° S, 184.19° E, 1.078 deg/Myr, after Beavan et al, 2002.

Location	Site	GPS-Derived Hor. Vel. (mm/yr)	GPS-Derived Azimuth (degrees)	Predicted Hor. Vel. (mm/yr)	Predicted Azimuth (degrees)
		Australian Plate Sites			
New Zealand	AUCK	50.3 ± 0.0	78.8° ± 0.1°	51.3	79.4
Tasmania	HOB2	59.3 ± 0.1	51.5° ± 0.1°	57.4	52.8
N. Caledonia	KOUC	82.1 ± 0.0	75.6° ± 0.0°	81.7	76.0
Loyalty Is.	LPIL	80.1 ± 0.0	77.5° ± 0.0°	80.2	77.8
N. Caledonia	NOUM	79.0 ± 0.1	76.4° ± 0.0°	78.4	76.9
Australia	TIDB	68.9 ± 0.1	59.3° ± 0.0°	67.3	60.2
Australia	TOW2	93.2 ± 0.1	67.6° ± 0.0°	91.0	67.3
		Solomon Islands Sites			
Guadalcanal	GCLC	29.6 ± 1.6	73.1° ± 2.0°	97.7	76.0
Nusatupe	GIZO	21.8 ± 1.0	82.2° ± 2.0°	100.3	74.6
New Georgia	MUND	21.7 ± 1.0	71.1° ± 1.6°	100.0	74.7
Nusatupe	NUSA	19.5 ± 0.2	78.1° ± 0.3°	100.3	74.6
Rendova	RAVA	38.7 ± 1.3	67.5° ± 1.6°	99.5	74.7
Simbo	SIMB	45.4 ± 0.8	67.3° ± 0.8°	100.3	74.4
Vella Lavella	VELA	18.5 ± 1.1	69.0° ± 2.0°	100.6	74.4
		Pacific Plate Sites			
Chatham I.	CHAT	2.0 ± 0.1	29.3° ± 1.3°	0	--
Samoa	FALE	0.4 ± 0.1	-110.5° ± 6.6°	0	--
Hawaii	KOKB	1.7 ± 0.1	-165.2° ± 3.3°	0	--
Marshall Is.	KWJ1	1.4 ± 0.1	87.5° ± 2.4°	0	--
Hawaii	MKEA	1.3 ± 0.1	-142.2° ± 3.2°	0	--
Niue	NIUC	0.8 ± 0.0	16.0° ± 4.5°	0	--
Tahiti	THTI	0.8 ± 0.2	-66.1° ± 7.3°	0	--

Islands range from 19 to 39 mm/yr. In comparison, the predicted velocity for all Solomons sites except SIMB is 0 mm/yr. Pacific-Solomon velocities are shown in Figure 5.4.

5.4. Discussion

Our GPS results show that most crustal motions in the New Georgia Group are related to subduction at the San Cristobal Trench (SCT). However, our GPS velocities are 20-40% less than predicted Australia-Pacific convergence rates. This discrepancy may be partly due to partitioning of the total convergence rate between the SCT and the North Solomon trench (NST), where marine geophysics surveys indicate that subduction is still active (Phinney et al., 1999). Part of the discrepancy is also likely due to the effects of elastic strain accumulation at both margins. The spatial extent of our existing Solomons network does not allow us to directly measure convergence across the NST. However, it does allow us to investigate potential elastic strain accumulation at the SCT.

5.4.1. Elastic Strain

The lack of shallow interplate seismicity at the SCT has led to the conclusion that convergence is predominantly aseismic and that significant interplate coupling does not occur in this region (e.g., Cooper and Taylor, 1985; Tregoning et al., 1998).

Figure 5.4. New Georgia Group GPS velocities in a Pacific-fixed reference frame.

Red arrows show GPS velocities. Gold arrows show predicted Pacific-Australian convergence (Beavan et al., 2002). All points on the Pacific plate should have a null velocity in this reference frame; observed velocities indicate elastic strain accumulation at the SCT and/or convergence at the NST. The observed velocity at Simbo island differs significantly from predicted Australian plate convergence. High resolution bathymetry and tectonic interpretations courtesy of A.M. Goodliffe and B. Taylor.

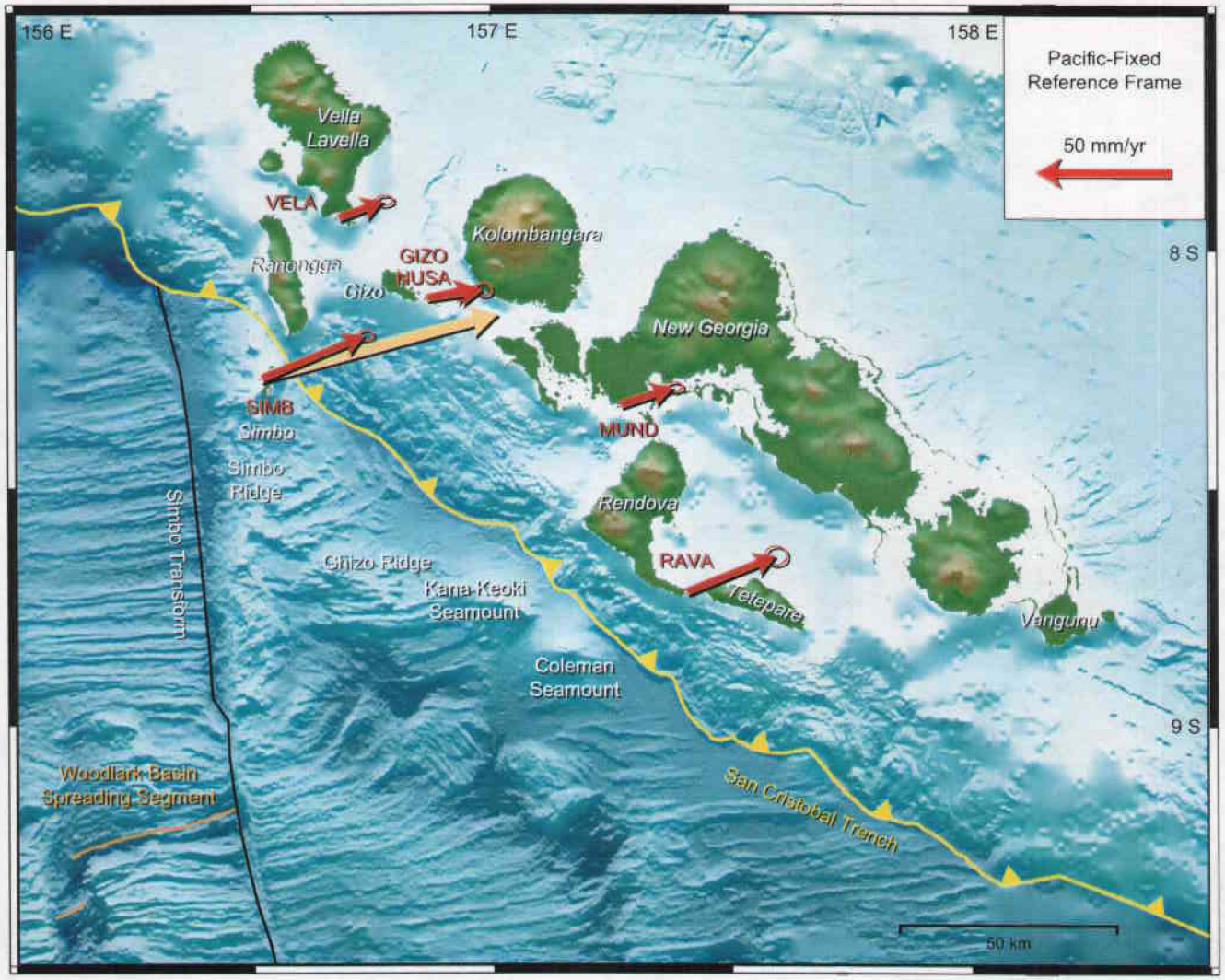
156 E
157 E
158 E
Pacific-Fixed
Reference Frame
50 mm/yr
8 S
9 S
Vella
Lavella
VELA
Kolombangara
Ranongga
GIZO
HUSA
Gizo
New Georgia
SIMB
Simbo
MUND
Simbo
Ridge
Rendova
Gizo Ridge
RAVA
Tetepare
Kana-Keoki
Seamount
Vangunu
Coleman
Seamount
Simbo Transform
Woodlark Basin
Spreading Segment
San Cristobal Trench
50 km

However, the buoyant nature and rugged topography of the subducting Woodlark Basin lithosphere adjacent to the NGG make it likely that some degree of interplate locking and elastic strain accumulation must occur. The occurrence of distinct sub-terraces and notches within Holocene coral reef terraces provides geological evidence that rapid, presumably coseismic, ground displacements have occurred throughout the New Georgia forearc. The great earthquake between the islands of Ranonnga and Vella Lavella in 1959 (Grover, 1965) further demonstrates that significant ruptures, while infrequent, can and do occur. This event, too, produced coastal subsidence and uplift including the emergence of corals on the northern end of Ranongga.

Our GPS measurements show a pattern in which site velocities increase with distance from the SCT, a pattern consistent with elastic strain accumulation at the forearc. To investigate the effects of elastic strain accumulation, we ran a series of two-dimensional dislocation models based on the methods of Savage (1983) and Singh and Rani (1993). Figure 5.5A shows the geometrical framework for our models. The origin of the horizontal distance scale corresponds to the SCT axis. Slab properties such as depth and dip angle are based on Mann et al. (1998) but it should be noted that these properties are poorly constrained. We experimented with a range of locking depths for the SCT and found that models in which locking extends nearly to the surface are in best agreement with our GPS observations.

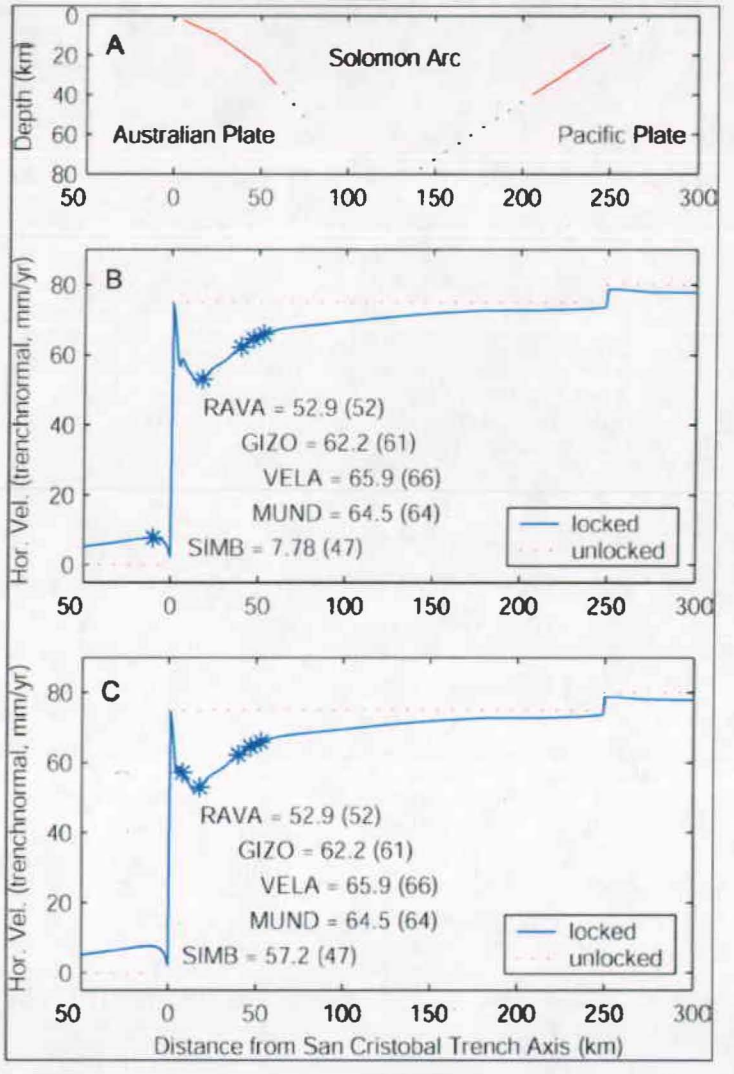

Figure 5.5. Two-dimensional dislocation models of elastic strain accumulation due to subduction zone locking.

5.5-A shows the geometry of the subducting slabs. 5.5-B and -C show trench-normal horizontal velocities with distance from the SCT trench axis for locking depths of 0.5 to 35 km at the SCT and 15 to 80 km at the NST. Modeled trench-normal velocities for GPS sites are explicitly stated with observed values in parentheses.

The Australia-Pacific Euler Pole of Beavan et al. (2000) predicts a total convergence rate of ~100 mm/yr along an azimuth of ~255° throughout the NGG. The trench-normal component of this predicted motion is ~80 mm/yr along an azimuth of ~220°. We explored numerous combinations of convergence rate partitioning between the SCT and NST. Scenarios in which both boundaries were freely slipping (i.e. no locking) were in poor agreement with our GPS measurements. In contrast, scenarios in which the full convergence rate is accommodated at the SCT, and in which the SCT is subject to locking and elastic strain accumulation, are in good agreement with our GPS measurements. However, because there is physical evidence to suggest that some convergence occurs at the NST, the models we present here assume trench-normal convergence rates of 75 mm/yr at the SCT and 5 mm/yr at the NST.

Figures 5.5-B and 5.5-C show trench-normal horizontal convergence rate patterns for locked (solid lines) and unlocked (dotted lines) cases. The parts of the downgoing plates that are free to slip are indicated by a dashed line while the parts that are subject to locking are indicated by a solid line. Both 5.5-B and -C assume that the downgoing Australian plate is locked from 2 to 35 km in depth and that the Pacific plate is locked from 15 to 50 km in depth. Stars on the velocity curve indicate the distances of our GPS sites from the trench axis. The modeled horizontal trench-normal convergence rate for each GPS site is explicitly stated below the stars (observed trench-normal GPS values are stated in parentheses).

The model in 5.5-B assumes that SIMB is situated on the Australian plate, 10 km outboard of the trench axis. The model in 5.5-C assumes that SIMB is part of the Solomon arc, 8 km inboard of the trench axis. Note that placing SIMB inboard of the trench axis also increases the distances of sites VELA, GIZO and possibly MUND from the trench axis and that this model includes these adjusted distances.

5.4.2. Simbo Island

An unexpected result is that Simbo island, thought to be on the Australian plate (e.g., Crook and Taylor, 1993), is observed to be converging with the Australian plate almost as fast as the other islands in the NGG. Moreover, coral reefs on Simbo show that the island has uplifted at a rate of ~1 mm/yr in Holocene time (Mann et al., 1998). These observations suggest that a zone of rapid deformation has developed between Simbo and the rest of the Australian plate. Simbo is situated in a region likely to experience strong interplate coupling, where the Simbo Ridge intersects the SCT. Simbo may be lagging behind the rest of the Australian plate because of compression and deformation of the Simbo fracture zone (SFZ). Indeed, the Woodlark Basin triple junction occurs directly northwest of Simbo where the SFZ, a leaky transform, intersects the SCT (Crook and Taylor, 1994). Convergence of the Solomon Sea (SS) plate occurs more rapidly and along a slightly different azimuth than Australian plate convergence, and this difference is accommodated by slip on the SFZ.

Simbo clearly does not move in unison with the Australian plate. One explanation is that part of the Simbo ridge has detached from the downgoing Australian plate and that Simbo island is part of a tectonic "flake" that has become accreted to the forearc. This explanation is consistent with our observations and elastic strain accumulation models but it requires an active thrust zone south of Simbo island that would, in effect, alter the previously identified plate boundary so that it passes outboard of Simbo. Such a feature has not been observed in previous marine geophysical surveys although it is possible that this is a relatively recent geological development and that no strong surface expression has yet evolved. An alternative explanation proposed by B. Taylor (personal communication) is that Simbo island is situated on a segment of the downgoing plate which undergoes thrusting along the active north-south trending Simbo fracture zone, left lateral shear along an east-west trending fault that passes just north of the Kana Keoki seamount, and subduction along the previously recognized plate boundary.

5.5. Conclusions

This study has produced the first measurements of crustal motion in the western Solomon Islands using a four-year GPS time series. Australian- and Pacific-fixed reference frames were generated using a regional network of continuous GPS sites. Motion of the Solomon island arc is observed relative to both the Australian and Pacific plates. Most interplate motion is related to subduction of the Australian plate

at the San Cristobal trench although our GPS velocities are only 60-80% of predicted Australia-Pacific velocities. 2-D Dislocation models suggest that most of the difference between the observed GPS convergence rates and the predicted Australia-Pacific convergence rates can be attributed to locking of the SCT and elastic strain accumulation in the forearc. It is likely that present day differential motion between the Solomon arc and the Pacific plate contributes to this difference as well. However, we can not yet uniquely apportion the amount of Australian-Pacific convergence accommodated at each plate boundary and the role of elastic strain. The surprising velocity of Simbo island shows that the corner of the Australian plate where the Simbo Ridge enters the SCT is subject to intense deformation and that this part of the Simbo Ridge my have been accreted to the forearc. While future occupations of our existing GPS network will provide further insight into the tectonic behavior of this region, a significantly larger network that includes sites distributed throughout the western Solomon Islands and on the Ontong-Java plateau is required to fully resolve present day convergence rates and elastic strain accumulation behavior at the San Cristobal and North Solomon trench systems.

5.6. Acknowledgements

We would like to thank the citizens of the Solomon Islands for their hospitality. This project was facilitated by Don Tolia, Director of the Solomon Islands Ministry of Natural Resources, and his staff. Data collection was facilitated by Whitlam Saeni

and Wilson Loy. The Guadalcanal GPS site was installed on the property of Ross Mining and we thank them for their support, especially Mr. Eugene Iliescu. The Nusatupe GPS site was installed at the World Fish Center (ICLARM) field station and we thank them for their support, especially Idris Lane. Data analysis was facilitated by Eric Kendrick and James Foster at the Pacific GPS Facility.

References

Altamimi, Z., P. Sillard, and C. Boucher, ITRF2000: A new release of the International Terrestrial Reference Frame for earth science applications, *J.Geophys. Res.*, *107* (B10), 2002.

Auzende, J.M., R.N. Hey, B. Pelletier, D. Rouland, Y. Lafoy, E. Gracia, and P. Huchon, Propagating Rift West of the Fiji Archipelago (North Fiji Basin, Sw Pacific), *J. Geophys. Res.-Solid Earth*, *100* (B9), 17823-17835, 1995.

Beavan, J., P. Tregoning, M. Bevis, T. Kato, and C. Meertens, Motion and rigidity of the Pacific Plate and implications for plate boundary deformation, *J. Geophys. Res.-Solid Earth*, *107* (B10), art. no.-2261, 2002.

Begg, G., and D.R. Gray, Arc dynamics and tectonic history of Fiji based on stress and kinematic analysis of dikes and faults of the Tavua Volcano, Viti Levu Island, Fiji, *Tectonics*, *21* (4), art. no.-1023, 2002.

Bevis, M., Y. Bock, P. Fang, R. Reilinger, T.A. Herring, S. J., and R. Smalley, Jr., Blending Old and New Approaches to Regional GPS Geodesy, *Eos, Transactions, American Geophysical Union*, *78* (6), 61, 64-66, 1997.

Bevis, M., E. Kendrick, R. Smalley, Jr., B. Brooks, R. Allmendinger, and B. Isacks, On the strength of interplate coupling and the rate of back arc convergence in the Central Andes; an analysis of the interseismic velocity field, *Geochemistry, Geophysics, Geosystems - G 3, 2001*, 16 (Paper2001GC000198), 2001.

Bevis, M., E.C. Kendrick, R. Smalley, Jr., T. Herring, J. Godoy, and F. Galban,

Crustal motion north and south of the Arica deflection; comparing recent geodetic results from the Central Andes, *Geochemistry, Geophysics, Geosystems - G 3*, *1*, (5,881 words), 1999.

Bevis, M., F.W. Taylor, B.E. Schutz, J. Recy, B.L. Isacks, S. Helu, R. Singh, E. Kendrick, J. Stowell, B. Taylor, and S. Calmant, Geodetic observations of very rapid convergence and back-arc extension at the Tonga Arc, *Nature (London)*, *374* (6519), 249-251, 1995.

Blewitt, G., From theory to applications, in *GPS for Geodesy*, edited by P. Teunissen, Kleusberg, A., pp. 231-270, Springer-Verlag, New York, 1998.

Blewitt, G., D. Lavallee, P. Clarke, and K. Nurutdinov, A new global mode of Earth deformation; seasonal cycle detected, *Science*, *294* (5550), 2342-2345, 2001.

Bock, Y., S. Wdowinski, P. Fang, J. Zhang, S. Williams, H. Johnson, J. Behr, J. Genrich, J. Dean, M. van Domselaar, D.C. Agnew, F.K. Wyatt, K. Stark, B. Oral, K.W. Hudnut, R.W. King, T.A. Herring, S.J. Dinardo, W. Young, D.D. Jackson, and W. Gurtner, Southern California Permanent GPS Geodetic Array; continuous measurements of regional crustal deformation between the 1992 Landers and 1994 Northridge earthquakes, *Journal of Geophysical Research, B, Solid Earth and Planets*, *102* (8), 18,013-18,033, 1997.

Cabioch, G., K.A. Banks-Cutler, W.J. Beck, G.S. Burr, T. Correge, R.L. Edwards, and F.W. Taylor, Continuous reef growth during the last 23 cal kyr BP in a tectonically active zone (Vanuatu, SouthWest Pacific), *Quaternary Science Reviews*, *22* (15-17), 1771-1786, 2003.

Calmant, S., G. Cabioch, M. Regnier, R. Pillet, and B. Pelletier, Cosismic uplifts and interseismic subsidence recorded in corals at Malekula (Vanuatu, southwest Pacific), *Comptes Rendus Acad. Sci. Ser II-A, 328* (10), 711-716, 1999.

Calmant, S., P. Lebellegard, F. Taylor, M. Bevis, D. Maillard, J. Recy, and J. Bonneau, Geodetic Measurements of Convergence across the New-Hebrides Subduction Zone, *Geophys. Res. Lett., 22* (19), 2573-2576, 1995.

Calmant, S., B. Pelletier, P. Lebellegard, M. Bevis, F.W. Taylor, and D.A. Phillips, New insights on the tectonics along the New Hebrides subduction zone based on GPS results, *J. Geophys. Res.-Solid Earth, 108* (B6), 2003.

Calmant, S., B. Pelletier, R. Pillet, M. Regnier, P. Lebellegard, D. Maillard, F. Taylor, M. Bevis, and J. Recy, Interseismic and coseismic motions in GPS series related to the Ms 7.3 July 13, 1994, Malekula earthquake, central New Hebrides subduction zone, *Geophys. Res. Lett., 24* (23), 3077-3080, 1997.

Calmant, S., J.J. Valette, J.F. Cretaux, and L. Soudarin, Tectonic plate motion and co-seismic steps surveyed by DORIS field beacons: the New Hebrides experiment, *J. Geodesy, 74* (7-8), 512-518, 2000.

Chase, C.G., Tectonic history of the Fiji plateau, *Geological Society of America Bulletin, 82* (11), 3087-3109, 1971.

Chinn, D.S., and B.L. Isacks, Accurate source depths and focal mechanisms of shallow earthquakes in western South America and in the New Hebrides island arc, *Tectonics, 2* (6), 529-563, 1983.

Collot, J.Y., J. Daniel, and R.V. Burne, Recent tectonics associated with the

subduction/collision of the d'Entrecasteaux Zone in the central New Hebrides, *Tectonophysics*, *112* (1-4), 325-356, 1985.

Collot, J.Y., and M.A. Fisher, The collision zone between the North d'Entrecasteaux Ridge and the New Hebrides island arc. 1. Sea beam morphology and shallow structure, *Journal of Geophysical Research*, *96* (B3), 4457-4478, 1991.

Collot, J.-Y., H.G. Greene, L.B. Stokking, K. Akimoto, M.V.S. Ask, P.E. Baker, L. Briqueu, T. Chabernaud, M.G. Collins, M. Coltorti, M.A. Fisher, T. Hasenaka, M.A. Hobart, A. Krammer, J.N. Leonard, J.B. Martin, J.I. Martinez-Rodriguez, S. Menger, M. Meschede, B. Pelletier, R.C.B. Perembo, T.M. Quinn, P. Reid, W.R. Riedel, P. Roperch, T.S. Staerker, F.W. Taylor, X. Zhao, and L.H.e. Dearmont, Site 831: Proceedings of the Ocean Drilling Program, Vanuatu (New Hebrides), covering Leg 134 of the cruises of the drilling vessel JOIDES Resolution, Port of Townsville, Queensland, Australia, to Suva, Republic of Fiji, sites 827-833, 11 October 1990-17 December 1990, *Proceedings of the Ocean Drilling Program, Part A: Initial Reports*, *134*, 317-386, 1992.

Cooper, P.A., and B. Taylor, Polarity reversal in the Solomon Islands arc, *Nature (London)*, *314* (6010), 428-430, 1985.

Crawford, W.C., D.A. Wiens, L.M. Dorman, and S.C. Webb, Tonga Ridge and Lau Basin crustal structure from seismic refraction data, *J. Geophys. Res.-Solid Earth*, *108* (B4), art. no.-2195, 2003.

Crook, K.A.W., and B. Taylor, Structure and Quaternary tectonic history of the

Woodlark triple junction region, Solomon Islands, *Mar. Geophys. Res.*, *16* (1), 65-89, 1994.

Delteil, J., E. Ruellan, I. Wright, and T. Matsumoto, Structure and structural development of the Havre Trough (SW Pacific), *J. Geophys. Res.-Solid Earth*, *107* (B7), art. no.-2143, 2002.

Demets, C., R.G. Gordon, D.F. Argus, and S. Stein, Current Plate Motions, *Geophysical Journal International*, *101* (2), 425-478, 1990.

Demets, C., R.G. Gordon, D.F. Argus, and S. Stein, Effect of Recent Revisions to the Geomagnetic Reversal Time-Scale on Estimates of Current Plate Motions, *Geophys. Res. Lett.*, *21* (20), 2191-2194, 1994.

Dickinson, W.R., Paleoshoreline record of relative Holocene sea levels on Pacific islands, *Earth-Science Reviews*, *55* (3-4), 191-234, 2001.

Duan, J.P., M. Bevis, P. Fang, Y. Bock, S. Chiswell, S. Businger, C. Rocken, F. Solheim, T. vanHove, R. Ware, S. McClusky, T.A. Herring, and R.W. King, GPS meteorology: Direct estimation of the absolute value of precipitable water, *J. Appl. Meteorol.*, *35* (6), 830-838, 1996.

Dubois, J., J. Launay, J. Marshall, and J. Recy, New Hebrides Trench: subduction rate from associated lithospheric bulge, *Canadian Journal of Earth Sciences (Journal Canadien des Sciences de la Terre)*, *14*, 250-255, 1977.

Ebel, J.E., Source processes of the 1965 New Hebrides Islands earthquakes inferred from teleseismic waveforms, *Geophysical Journal, Astronomical Society*, *63* (2), 381-403, 1980.

Eissen, J.P., and others, Rapport de mission de la campagne CALVA, 12-18 Juillet 1996, pp. 34, Centre de Brest, 1997.

Feigl, K.L., D.C. Agnew, Y. Bock, D. Dong, A. Donnellan, B.H. Hager, T.A. Herring, D.D. Jackson, T.H. Jordan, R.W. King, S. Larsen, K.M. Larson, M.H. Murray, Z. Shen, and F.H. Webb, Space geodetic measurement of crustal deformation in Central and Southern California, 1984-1992, *Journal of Geophysical Research, B, Solid Earth and Planets*, *98* (12), 21,677-21,712, 1993.

Fisher, M.A., Tectonic processes at the collision of the d-Entrecasteaux zone and the New Hebrides Island arc, *J.Geophys. Res.*, *91*, 10470-10486, 1986.

Fisher, M.A., J.Y. Collot, and E.L. Geist, The collision zone between the North d'Entrecasteaux Ridge and the New Hebrides island arc. 2. Structure from multichannel seismic data, *Journal of Geophysical Research*, *96* (B3), 4479-4495, 1991a.

Fisher, M.A., J.Y. Collot, and E.L. Geist, Structure of the Collision Zone between Bougainville Guyot and the Accretionary Wedge of the New-Hebrides Island-Arc, Southwest Pacific, *Tectonics*, *10* (5), 887-903, 1991b.

Fisher, M.A., J.Y. Collot, and G.L. Smith, Possible causes for structural variation where the New Hebrides island arc and the D'Entrecasteaux zone collide, *Geology*, *14*, 951-954, 1986.

Fujiwara, T., T. Yamazaki, and M. Joshima, Bathymetry and magnetic anomalies in the Havre Trough and southern Lau Basin: from rifting to spreading in back-

arc basins, *Earth Planet. Sci. Lett.*, *185* (3-4), 253-264, 2001.

Greene, H.G., and J.Y. Collot, Ridge-arc collision: Timing and deformation determined by Leg 134 drilling, central New Hebrides island arc, *Ocean Drilling Program, College Station, TX*, 1994.

Grover, J.C., The great earthquake in the western Solomon Islands on 18 August, 1959 17/2105 GMT, in *The British Solomon Islands Geological Record, v. II (1959-1962)*, pp. 174-182, High Commissioner for the Western Pacific, Honiara, Solomon Islands, 1965.

Hall, R., Cenozoic geological and plate tectonic evolution of SE Asia and the SW Pacific: computer-based reconstructions, model and animations, *Journal of Asian Earth Sciences*, *20* (4), 353-431, 2002.

Hamburger, M.W., *Seismicity of the Fiji Islands and tectonics of the Southwest Pacific*, 332 pp., Cornell University, Ithaca, NY, United States, 1986.

Hamburger, M.W., I.B. Everingham, B.L. Isacks, and M. Barazangi, Active tectonism with the Fiji Platform, Southwest Pacific, *Geology (Boulder)*, *16* (3), 237-241, 1988.

Hamburger, M.W., and B.L. Isacks, Deep Earthquakes in the Southwest Pacific - a Tectonic Interpretation, *Journal of Geophysical Research-Solid Earth and Planets*, *92* (B13), 13841-13854, 1987.

Hamburger, M.W., and B.L. Isacks, Diffuse back-arc deformation in the southwestern Pacific, *Nature (London)*, *332* (6165), 599-604, 1988.

Heflin, M., W. Beriger, G. Blewitt, A.P. Freedman, K. Hurst, S. Lichten, U.J.

Lindqwister, Y. Vigue, F. Webb, T.P. Yunck, and J. Zumberge, Global geodesy using GPS without fiducial sites, *Geophys. Res. Lett.*, *19* (2), 131-134, 1992.

Herring, T.A., *Documentation for the GLOBK Global Kalman filter VLBI and GPS analysis program, Version 10.0*, Mass. Inst. of Technology, Cambridge, 2002.

Hofstetter, A., A. Shapira, K. Bulehite, T. Jones, K. Mafi, A. Malitzky, A. Papabatu, G. Prasad, M. Regnier, G. Shorten, A. Singh, M. Stephen, and L. Vuetibau, Frequency-magnitude relationships for seismic areas around the capital cities of Solomon, Vanuatu, Tonga and Fiji Islands, *J. Seismol.*, *4* (3), 285-296, 2000.

Isacks, B.J.O., and L.R. Sykes, Seismology and the new global tectonics, *J.Geophys. Res.*, *73*, 5855-5899, 1968.

Isacks, B.L., and et al., Seismicity and tectonics of the central New Hebrides island arc, in *Earthquake prediction: an international review*, edited by D.W. Simpson, pp. 93-116, American Geophysical Union, Maurice Ewing Series 4, 1981.

Karig, D.E., Ridges and basins of the Tonga-Kermadec island arc system, *Journal of Geophysical Research*, *75* (2), 239-254, 1970.

Kendrick, E., M. Bevis, R. Smalley, Jr., and B. Brooks, An integrated crustal velocity field for the Central Andes, *Geochemistry, Geophysics, Geosystems - G 3, 2001*, 11 (Paper2001GC000191), 2001.

Kendrick, E.C., M. Bevis, R.F. Smalley, Jr., O. Cifuentes, and F. Galban, Current

rates of convergence across the Central Andes; estimates from continuous GPS observations, *Geophys. Res. Lett.*, *26* (5), 541-544, 1999.

King, R.W., Bock, Y., *Documentation for the GAMIT GPS Analysis Software, Version 10.0*, Mass. Inst. of Technol., Cambridge, 2002.

Lagabrielle, Y., E. Ruellan, M. Tanahashi, J. Bourgois, G. Buffet, G. deAlteriis, J. Dyment, J. Goslin, E. GraciaMont, Y. Iwabushi, P. Jarvis, M. Joshima, A.M. Karpoff, T. Matsumoto, H. Ondreas, B. Pelletier, and O. Sardou, Active oceanic spreading in the northern north Fiji basin: Results of the NOFI cruise of R/V L'Atalante (Newstarmer project), *Mar. Geophys. Res.*, *18* (2-4), 225-247, 1996.

Larson, K.M., J.T. Freymueller, and S. Philipsen, Global plate velocities from the Global Positioning System, *Journal of Geophysical Research, B, Solid Earth and Planets*, *102* (5), 9961-9981, 1997.

Louat, R., and B. Pelletier, Seismotectonics and Present-Day Relative Plate Motions in the New-Hebrides North Fiji Basin Region, *Tectonophysics*, *167* (1), 41-55, 1989.

Mann, P., F.W. Taylor, M.B. Lagoe, A. Quarles, and G. Burr, Accelerating late Quaternary uplift of the New Georgia Island Group (Solomon island arc) in response to subduction of the recently active Woodlark spreading center and Coleman Seamount, *Tectonophysics*, *295* (3-4), 259-306, 1998.

Martinez, F., and B. Taylor, Backarc spreading, rifting, and microplate rotation, between transform faults in the Manus basin, *Mar. Geophys. Res.*, *18* (2-4),

203-224, 1996.

Martinez, F., and B. Taylor, Mantle wedge control on back-arc crustal accretion, *Nature*, *416* (6879), 417-420, 2002.

Martinez, F., B. Taylor, and A.M. Goodliffe, Contrasting styles of seafloor spreading in the Woodlark Basin: Indications of rift-induced secondary mantle convection, *J. Geophys. Res.-Solid Earth*, *104* (B6), 12909-12926, 1999.

Meffre, S., and A.J. Crawford, Collision tectonics in the New Hebrides arc (Vanuatu), *Isl. Arc.*, *10* (1), 33-50, 2001.

Misra, P., and P. Enge, *Global Positioning System: Signals, Measurements and Performance*, 385 pp., Ganga-Jamuna Pr (distrib. by Navtech), 2001.

Monzier, M., J.Y. Collot, and J. Daniel, *Carte bathymetrique des parties centrale et meridionale de l'arc insulaire des Nouvelles-Hebrides*, Bondy, France, 1984.

Monzier, M., L.V. Danyushevsky, A.J. Crawford, H. Bellon, and J. Cotten, High-Mg Andesites from the Southern Termination of the New-Hebrides Island-Arc (Sw Pacific), *Journal of Volcanology and Geothermal Research*, *57* (3-4), 193-217, 1993.

Monzier, M., C. Robin, and J.P. Eissen, Kuwae (1425 A.D.): the forgotten caldera, *Journal of Volcanology & Geothermal Research*, *59* (3), 207-218, 1994.

Musgrave, R.J., and J.V. Firth, Magnitude and timing of New Hebrides Arc rotation: Paleomagnetic evidence from Nendo, Solomon Islands, *J. Geophys. Res.-Solid Earth*, *104* (B2), 2841-2853, 1999.

Neef, G., and M.T. McCulloch, Pliocene-Quaternary history of Futuna Island, South

Vanuatu, southwest Pacific, *Australian Journal of Earth Sciences*, *48* (6), 805-814, 2001.

Okal, E.A., and S.H. Kirby, Deep earthquakes beneath the Fiji Basin, SW Pacific: Earth's most intense deep seismicity in stagnant slabs, *Phys. Earth Planet. Inter.*, *109* (1-2), 25-63, 1998.

Oliver, J., and B. Isacks, Deep earthquake zones, anomalous structures in the upper mantle, and the lithosphere, *Journal of Geophysical Research*, *72* (16), 4259-4275, 1967.

Oral, M.B., *Global Positioning System (GPS) measurements in Turkey (1988-1992); kinematics of the Africa-Arabia-Eurasia plate collision zone*, Massachusetts Institute of Technology, Cambridge, MA, United States, 1994.

Owen, S., P. Segall, J.T. Freymueller, A. Miklius, R.P. Denlinger, T. Arnadottir, M.K. Sako, and R. Buergmann, Rapid deformation of the south flank of Kilauea Volcano, Hawaii, *Science*, *267* (5202), 1328-1332, 1995.

Pacheco, J.F., L.R. Sykes, and C.H. Scholz, Nature of seismic coupling along simple plate boundaries of the subduction type, *Journal of Geophysical Research*, *98* (B8), 14,133-14,159, 1993.

Parson, L.M., and I.C. Wright, The Lau-Havre-Taupo back-arc basin: A southward-propagating, multi-stage evolution from rifting to spreading, *Tectonophysics*, *263* (1-4), 1-22, 1996.

Pascal, G., B.L. Isacks, M. Barazangi, and J. Dubois, Precise relocations of earthquakes and seismotectonics of the New Hebrides island arc, *J.Geophys.*

Res., *83*, 4957-4973, 1978.

Pelletier, B., and J.M. Auzende, Geometry and structure of the Vitiaz trench lineament (SW Pacific), *Mar. Geophys. Res.*, *18* (2-4), 305-335, 1996.

Pelletier, B., S. Calmant, and R. Pillet, Current tectonics of the Tonga New Hebrides region, *Earth Planet. Sci. Lett.*, *164* (1-2), 263-276, 1998.

Pelletier, B., Y. Lagabrielle, M. Benoit, G. Cabioch, S. Calmant, E. Garel, and C. Guivel, Newly identified segments of the Pacific-Australia plate boundary along the North Fiji transform zone, *Earth Planet. Sci. Lett.*, *193* (3-4), 347-358, 2001.

Pelletier, B., M. Regnier, S. Calmant, R. Pillet, G. Cabioch, Y. Lagabrielle, M. Bore, J.P. Caminade, P. Lebellegard, I. Cristopher, and S. Temakon, The Mw 7.5 November 24, 1999, Ambrym-Pentecost (Vanuatu) earthquake: preliminary data on seismicity, associated tsunami and crustal motions, *Comptes Rendus Acad. Sci. Ser II-A*, *331* (1), 21-28, 2000.

Phinney, E.J., P. Mann, M.F. Coffin, and T.H. Shipley, Sequence stratigraphy, structure, and tectonic history of the southwestern Ontong Java Plateau adjacent to the North Solomon Trench and Solomon islands arc, *Journal of Geophysical Research, B, Solid Earth and Planets*, *104* (9), 20,449-20,466, 1999.

Regnier, M., S. Calmant, B. Pelletier, Y. Lagabrielle, and G. Cabioch, The M-w 7.5 1999 Ambrym earthquake, Vanuatu: A back arc intraplate thrust event, *Tectonics*, *22* (4), 2003.

Regnier, M., S. Calmant, B. Pelletier, Y. Lagabrielle, and G. Cabioch, The Mw 7.5 November 26, 199 Ambrym earthquake, a back-arc intraplate thrust event, *Tectonics*, in press.

Robaudo, S., and C.G.A. Harrison, Plate tectonics from SLR and VLBI global data, in *Contributions of Space Geodesy and Geodynamics*, edited by D.E. Smith, and D.L. Turcotte, pp. 51-71, Geodyn. Ser., 1993.

Savage, J.C., A dislocation model of strain accumulation and release at a subduction zone, *JGR. Journal of Geophysical Research. B*, *88* (6), 4984-4996, 1983.

Schellart, W.P., G.S. Lister, and M.W. Jessell, Analogue modeling of arc and backarc deformation in the New Hebrides arc and North Fiji Basin, *Geology*, *30* (4), 311-314, 2002.

Sella, G.F., T.H. Dixon, and A.L. Mao, REVEL: A model for Recent plate velocities from space geodesy, *J. Geophys. Res.-Solid Earth*, *107* (B4), art. no.-2081, 2002.

Singh, S.J., and S. Rani, Crustal deformation associated with two-dimensional thrust faulting, *Journal of Physics of the Earth*, *41* (2), 87-101, 1993.

Smith, D.E., R. Kolenkiewicz, P.J. Dunn, J.W. Robbins, M.H. Torrence, S.M. Klosko, R.G. Williamson, E.C. Pavlis, N.B. Douglas, and S.K. Fricke, Tectonic motion and deformation from satellite laser ranging to Lageos, *Journal of Geophysical Research, B, Solid Earth and Planets*, *95* (13), 22,013-22,041, 1990.

Taylor, B., P. Huchon, P.e. Huchon, B.e. Taylor, A.e. Klaus, S.A.M. Awadallah, C.K.

Brooks, B. Celerier, E.H. DeCarlo, J. Floyd, G.M. Frost, V. Gardien, S. Gerbaudo, A.M. Goodliffe, J.K. Haumu, N. Ishikawa, G.D. Karner, P.M. Kia, A. Kopf, K.S. Lackschewitz, R. Laronga, B. Le Gall, I.D. Mather, B.D. Monteleone, A.H.F. Robertson, R.C.B. Perembo, J.M. Resig, E.J. Screaton, T.R. Sharp, W.G. Siesser, S.C. Stover, K. Takahashi, and P. Wellsbury, Active continental extension in the western Woodlark Basin; a synthesis of Leg 180 results; Proceedings of the Ocean Drilling Program, scientific results, active continental extension in the western Woodlark Basin, Papua New Guinea; covering Leg 180 of the cruises of the drilling vessel JOIDES Resolution; Darwin, Australia, to Sydney, Australia, sites 1108-1118, 7 June-11 August 1998, *Proceedings of the Ocean Drilling Program, Scientific Results (CD-Rom)*, *180*, 1-36, 2002.

Taylor, B., K. Zellmer, F. Martinez, and A. Goodliffe, Sea-floor spreading in the Lau back-arc basin, *Earth Planet. Sci. Lett.*, *144* (1-2), 35-40, 1996.

Taylor, F.W., M.G. Baevis, B.E. Schutz, D. Kuang, J. Recy, S. Calmant, D. Charley, M. Regnier, B. Perin, M. Jackson, and C. Reichenfeld, Geodetic Measurements of Convergence at the New-Hebrides-Island Arc Indicate Arc Fragmentation Caused by an Impinging Aseismic Ridge, *Geology*, *23* (11), 1011-1014, 1995.

Taylor, F.W., M. Bevis, R.L. Edwards, S. Hai Cheng, S. Gray, G. Burr, W.J. Beck, K.B. Cutler, D.A. Phillips, G. Cabioch, J. Recy, and P. Mann, Rapid forearc uplift and subsidence caused by impinging bathymetric features: Examples

from the New Hebrides and Solomon arcs, in press.

Taylor, F.W., R.L. Edwards, G.J. Wasserburg, and C. Frohlich, Seismic recurrence intervals and timing of aseismic subduction inferred from emerged corals and reefs of the central Vanuatu (New Hebrides) frontal arc, *Journal of Geophysical Research, 95* (B1), 393-408, 1990.

Taylor, F.W., C. Frohlich, J. Lecolle, and M. Strecker, Analysis of Partially Emerged Corals and Reef Terraces in the Central Vanuatu Arc - Comparison of Contemporary Coseismic and Nonseismic with Quaternary Vertical Movements, *Journal of Geophysical Research-Solid Earth and Planets, 92* (B6), 4905-4933, 1987.

Taylor, F.W., B.L. Isacks, C. Jouannic, A.L. Bloom, and J. Dubois, Co-Seismic and Quaternary Vertical Tectonic Movements, Santo and Malekula Islands, New-Hebrides Island-Arc, *Journal of Geophysical Research, 85* (NB10), 5367-5381, 1980.

Taylor, F.W., T.M. Quinn, T.M. Gallup, and R.L. Edwards, Quaternary plate convergence rates at the New Hebrides arc from chronostrigraphy of Bougainville Guyot (site 831), *Proceedings of the Ocean Drilling Program, Scientific Results, 134*, 47-57, 1994.

Taylor, G.K., J. Gascoyne, and H. Colley, Rapid rotation of Fiji: Paleomagnetic evidence and tectonic implications, *J. Geophys. Res.-Solid Earth, 105* (B3), 5771-5781, 2000.

Tregoning, P., Plate kinematics in the western Pacific derived from geodetic

observations, *J. Geophys. Res.-Solid Earth, 107* (B1), art. no.-2020, 2002.

Tregoning, P., F. Tan, J. Gilliland, H. McQueen, and K. Lambeck, Present-day crustal motion in the Solomon Islands from GPS observations, *Geophys. Res. Lett., 25* (19), 3627-3630, 1998.

Wessel, P., and L.W. Kroenke, Ontong Java Plateau and late Neogene changes in Pacific plate motion, *J. Geophys. Res.-Solid Earth, 105* (B12), 28255-28277, 2000.

Wessel, P., and W.H.F. Smith, Free software helps map and display data, *Eos, 72* (41), 441,445-446, 1991.

Yan, C.Y., L.W. Kroenke, W.H. Berger, T.R. Janecek, J. Backman, F. Bassinot, R.M. Corfield, M.L. Delaney, R. Hagen, E. Jansen, L.A. Krissek, C. Lange, R.M. Leckie, I.L. Lind, M.W. Lyle, J.J. Mahoney, J.C. Marsters, L. Mayer, D.C. Mosher, R. Musgrave, M.L. Prentice, J.M. Resig, H. Schmidt, R. Stax, M. Storey, K. Takahashi, T. Takayama, J.A. Tarduno, R.H. Wilkens, and G. Wu, A plate tectonic reconstruction of the Southwest Pacific, 0-100 Ma; Proceedings of the Ocean Drilling Program; Ontong Java Plateau, covering Leg 130 of the cruises of the drilling vessel JOIDES Resolution, Apra Harbor, Guam, to Apra Harbor, Guam, Sites 805-807, 18 January-26 March 1990, in *Proceedings of the Ocean Drilling Program, Scientific Results*, edited by E.M. Maddox, pp. 697-709, 1993.

Yang, Y.Q., and M. Liu, Deformation of convergent plates: Evidence from discrepancies between GPS velocities and rigid-plate motions, *Geophys. Res.*

Lett., *29* (10), art. no.-1472, 2002.

Zellmer, K.E., and B. Taylor, A three-plate kinematic model for Lau Basin opening, *Geochem. Geophys. Geosyst.*, *2*, art. no.-2000GC000106, 2001.

Zhang, J., Y. Bock, H. Johnson, P. Fang, S. Williams, J. Genrich, S. Wdowinski, and J. Behr, Southern California Permanent GPS Geodetic Array; error analysis of daily position estimates and site velocities, *Journal of Geophysical Research, B, Solid Earth and Planets*, *102* (8), 18,035-18,055, 1997.